



**GULL LAKE  
SYMPOSIUM**



ON THE



**Two-Body Force in Nuclei**

CONTRIBUTED PAPERS

SEPTEMBER 7-10 1971

MICHIGAN STATE UNIVERSITY

CYCLOTRON LABORATORY  
DEPARTMENT OF PHYSICS

MSUCL-39

THE GULL LAKE SYMPOSIUM ON  
THE TWO-BODY FORCE IN NUCLEI \*

Held at the Gull Lake Conference Center  
September 7-10, 1971

PROGRAM AND CONTRIBUTED PAPERS

Symposium Co-Chairmen  
S. M. Austin  
G. M. Crawley

\* Symposium supported in part by the National Science  
Foundation, The Office of Naval Research and Michigan  
State University

# TABLE OF CONTENTS

PROGRAM . . . . .	Page
CONTRIBUTED PAPERS	1
Topic 2--The Free Two-Nucleon Force	
2.1--Two-Pion-Exchange Nucleon-Nucleon Potential, M. Chemtob, J. W. Durso and D. O. Riska. . . . .	4
2.2--The Two-Pion Exchange Contribution to the Nucleon Nucleon Potential, Geoffrey N. Epstein and Bruce H. J. McKellar . . . . .	10
2.3--On the Definition of a Boson Exchange Potential, C. J. Noble and K. C. Richards . . . . .	16
2.4--Development of a Super Soft Core Potential Model of the Nucleon-Nucleon Interaction, R. de Turreil and D. W. L. Sprung . . . . .	22
Topic 3--Off-Energy-Shell Effects	
3.1--Neutron-Proton Bremsstrahlung Including Gauge-Invariant Terms Arising From the Nuclear Potential, V. R. Brown and J. Franklin . . . . .	28
3.2--Triton Binding Energy Predictions for Phase-Shift Equivalent Potentials, Michael I. Haftel . . . . .	34
3.3--Off-Shell Effects in the $^{18}\text{O}$ and $^{18}\text{F}$ Shell-Model Spectra, H. C. Pradhan, P. U. Sauer and J. P. Vary . . . . .	40
Topic 4--Calculations of the Effective Reaction Matrix in Nuclear Matter and Finite Nuclei	
4.1--Solution of the Bethe-Goldstone Equation in Finite Nuclei from N-N Phase Shift Data, R. J. W. Hodgson . . . . .	46

	Page
Topic 5--Effective Interaction from Empirical Studies of Finite Nuclei	
5.1--Does an Effective E2 Operator have a Two Body Part?, F. Khanna, M. Harvey, D. W. L. Sprung and A. Jopko . . . . .	52
5.2--Comments on the Isospin Dependence of the Two-Body Effective Interaction as Deduced from Nuclear Spectra, W. A. Lanford . . . . .	57
5.3--Experimental Evidence of the Goodness of Seniority in $j=9/2$ Orbits, W. A. Lanford . . . . .	63
5.4--Problems of SD-Shell Calculations for $^{24}\text{Mg}$ , P. Manakos . . . . .	69
5.5--Excitation Structure of Negative Parity States in $^{17}\text{O}$ , A. Müller-Arnke. . . . .	74
5.6--An Improved Prescription for Calculating the Negative Parity Spectrum of Doubly-Closed Shell Nuclei, F. Petrovich, R. Schaeffer and R. Trilling . . . . .	79
5.7--The Coupling of Particle-Hole States to Vibrations, L. Zamick. . . . .	83
5.8--Monopole Polarization with a Surface Delta Interaction, L. Zamick . . . . .	90
Topic 6--The Effective Interaction for Inelastic Scattering and Charge Exchange Reactions	
6.1--The Distribution of Neutrons in the Nuclear Surface from Elastic Alpha-Particle Scattering, Aron M. Bernstein and W. A. Seidler II . . . . .	95
6.2--Strength of Effective Two Body Interaction Obtained from a Study of Inelastic Scattering of 50 MeV Protons by $^6\text{Li}$ , $^9\text{Be}$ , and $^{42}\text{Ca}$ , G. S. Mani . . . . .	101



	Page
6.3--Charge-Exchange and/or Knockout Spectator Poles in the $D(^3\text{He},tp)p$ Reaction, R. E. Warner, G. C. Ball, W. G. Davies, A. J. Ferguson and J. S. Forster . . . . .	111
6.4--The Energy Dependence of the Isospin Part of the Optical Potential, T. J. Woods . . . . .	118
6.5--Renormalized Operators and Collective Particle-Hole Excitations in $\text{Ca}^{40}$ , M. Dworzecka and H. McManus. . . . .	126
PARTICIPANTS . . . . .	130

## GULL LAKE SYMPOSIUM ON THE TWO-BODY FORCE IN NUCLEI

## Session I - Tuesday Morning

Chairman - G. Breit (SUNY, Buffalo)

1. Overview of ConferenceM. H. Macfarlane  
(ANL)2. The Free Two-Nucleon Force2.1 Phase-shift and potential-model  
analysis of experimental infor-  
mation.P. Signell  
(MSU)2.2 Elementary-particle models of the  
two-nucleon force.G. E. Brown  
(Stony Brook  
& Nordita)

2.3 Contributions

## Session II - Tuesday Evening

Chairman - V. Brown (LRL, Livermore)

3. Off-Energy-Shell Effects3.1 Review of experimental information  
on nucleon-nucleon bremsstrahlung.M. L. Halbert  
(ORNL)3.2 The status of the theory of nucleon-  
nucleon bremsstrahlung.L. Heller  
(LASL)3.3 Off-energy-shell effects in many  
nucleon systems.F. Tabakin  
(Pittsburgh)

## Session III - Wednesday Morning

Chairman - S. Moszkowski (UCLA)

4. Calculations of the Effective Reaction Matrix in  
Nuclear Matter and Finite Nuclei4.1 An effective reaction matrix derived  
from nuclear matter calculations.H. A. Bethe  
(Cornell)4.2 The effective two-body interaction  
in finite nuclei and its calculation.B. R. Barrett  
(Arizona)

4.3 Contributions

## Session IV - Wednesday Evening

Chairman - L. Zamick (Rutgers)

5. Effective Interaction from Empirical Studies of Finite Nuclei

5.1 Shell model studies.

J. McGroary  
(ORNL)5.2 The effective two-body force  
derived from nuclear spectra.J. P. Schiffer  
(ANL)

5.3 Contributions

## Session V - Thursday Morning

Chairman - G. T. Garvey (Princeton)

6. The Effective Interaction for Inelastic Scattering and Charge Exchange Reactions6.1 The microscopic description of  
(p,p') and (p,n) reactions.R. Schaeffer  
(Berkeley, Saclay)6.2 Core polarization effects in  
(p,p') reactions.H. McManus  
(MSU)6.3 Empirical values of the effective  
interaction from (p,p') and (p,n)  
reactions.S. M. Austin  
(MSU)

6.4 Contributions

## Session VI - Thursday Evening

Chairman - A. Bernstein (MIT)

6.5 The microscopic description of  
inelastic scattering and charge  
exchange with complex projectiles.V. A. Madsen  
(Oregon State)6.6 Experimental review of the ( $^3\text{He}, ^3\text{He}'$ ),  
( $^3\text{He}, t$ ) and ( $\alpha, \alpha'$ ) reactions.P. G. Roos  
(Maryland)

6.7 Contributions

Session VII - Friday Morning

Chairman - J. S. Blair (Seattle)

6.8 Nuclear spectroscopy with high energy projectiles.

7. Conference Summary

M. H. Macfarlane  
(ANL)

M. Baranger  
(MIT)

TWO-PION-EXCHANGE NUCLEON-NUCLEON POTENTIAL

M. Chemtob

Niels Bohr Institute  
University of Copenhagen, Copenhagen

and

J.W. Durso and D.O. Riska  
NORDITA, Copenhagen

August, 1971



The work reported on here may be regarded as an extension of earlier theoretical derivations (1,2) of the nucleon-nucleon potential with two important modifications. In the first place we include as much information from  $\pi N \rightarrow \pi N$  and  $N\bar{N} \rightarrow \pi\pi$  process as is currently available from theoretical descriptions. The second modification is the use of the Blankenbecker - Sugar - Logunov - Tavkhelidze equation (3,4) to define the potential.

The first modification is illustrative of the advantages of using a dispersion relations approach to calculate the full two-pion-exchange amplitude rather than the field-theoretic approach. (5) In this way, information on  $\pi N$  rescattering effects (nucleon isobars in the intermediate states) as well as on  $N\bar{N} \rightarrow \pi\pi$  helicity amplitudes can be accounted for in a simple way. The price one pays for this is the restriction of the amplitude calculated to on-energy-shell processes.

The second modification is important in several respects. Since the two-particle Green's function in the BSLT equation has the same elastic part as the free, relativistic two-particle Green's function, the resulting amplitude will satisfy a relativistic unitarity condition. (5,6) This means that the elastic unitarity cut of the field - theoretic amplitude will be identical with that of the iterated one-pion-exchange potential for an energy region extending from the  $NN$  elastic threshold to the pion production threshold. Removal of the iterated OPEP then results in a

potential which is extremely energy independent. Furthermore, the iterated OPEP calculated in this way is finite, so that it is unnecessary to introduce infinite subtraction constants in order to calculate the potential.

We have calculated the potentials resulting from several assumed models for  $\pi N \rightarrow \pi N$  and  $N\bar{N} \rightarrow \pi\pi$  processes. (7,8) Some of the results for the model which includes all the information on  $\pi N$  rescattering and  $\pi\pi$  correlation corrections are shown in Figs. 1-2 (curves T'). Basically, the model contains contributions to the  $\pi N$  amplitude from the nucleon and the  $P_{33}$  (1236),  $P_{11}$  (1400) and  $D_{13}$  (1520) isobars. The s-wave  $N\bar{N} \rightarrow \pi\pi$  helicity amplitude is taken from the results of Nielsen, Petersen and Pietarinen (9) and the p-wave  $N\bar{N} \rightarrow \pi\pi$  helicity amplitude is given by nucleon and isobar exchange terms plus the contribution of a finite width  $\rho$ -meson. Three pion effects are taken into account by including  $\omega$ -exchange. The resulting potential is, as stated, very energy independent and quite cut-off insensitive.

In most cases the calculated potential is close to the phenomenological Hamada-Johnston potential, particularly at distances  $\geq 1$  fermi. Significant is the fact that the corrections made by including  $\pi\pi$  correlations via the s- and p-wave  $N\bar{N} \rightarrow \pi\pi$  helicity amplitudes almost invariably improve the agreement. It is hoped that further refinements in the description of  $\pi N$  and  $N\bar{N} \rightarrow \pi\pi$  processes will improve the potential still further.

- (1) J. M. Charap and M. Tausner, *Nuovo Cimento* 18 (1960) 316.
- (2) W. N. Cottingham and R. Vinh Mau, *Phys. Rev.* 130 (1963) 735.
- (3) A. A. Logunov and A. N. Tavkhelidze, *Nuovo Cimento* 29 (1963) 380.
- (4) R. Blankenbecker and R. Sugar, *Phys. Rev.* 142 (1966) 1051.
- (5) M. H. Partovi and E. L. Lomon, *Phys. Rev.* D2 (1970) 1999.
- (6) G. E. Brown, A. D. Jackson, and T. Kuo, *Nucl. Phys.* A133 (1969) 481.
- (7) M. Chemtob and D. O. Riska, *Phys. Letters* 35B (1971) 115.
- (8) G. E. Brown and J. W. Durso, *Phys. Letters* 35B (1971) 120.
- (9) H. Nielsen, J. L. Petersen, and E. Pietarinen, *Nucl. Phys.* B22 (1970) 525.

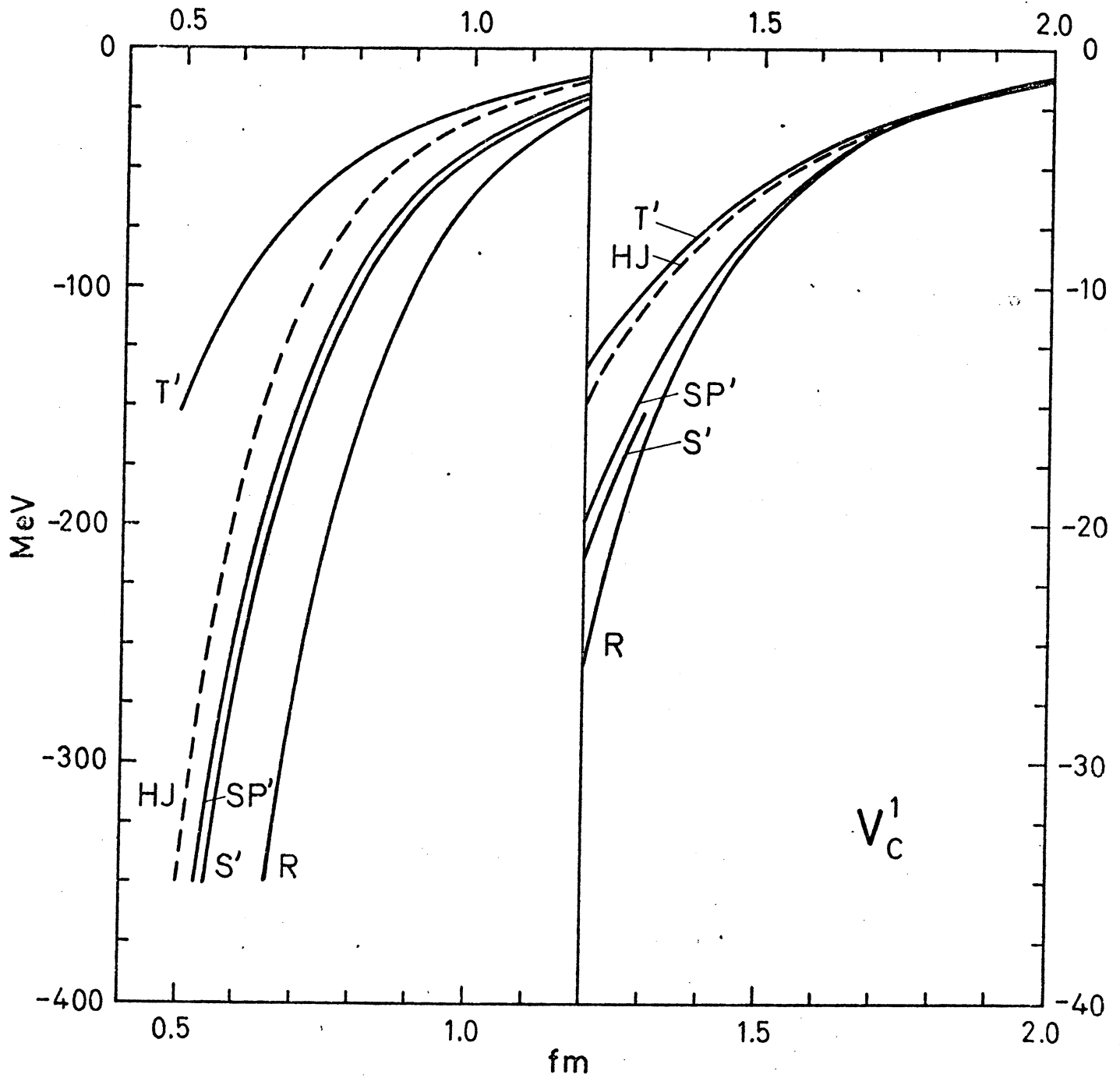


Figure 1

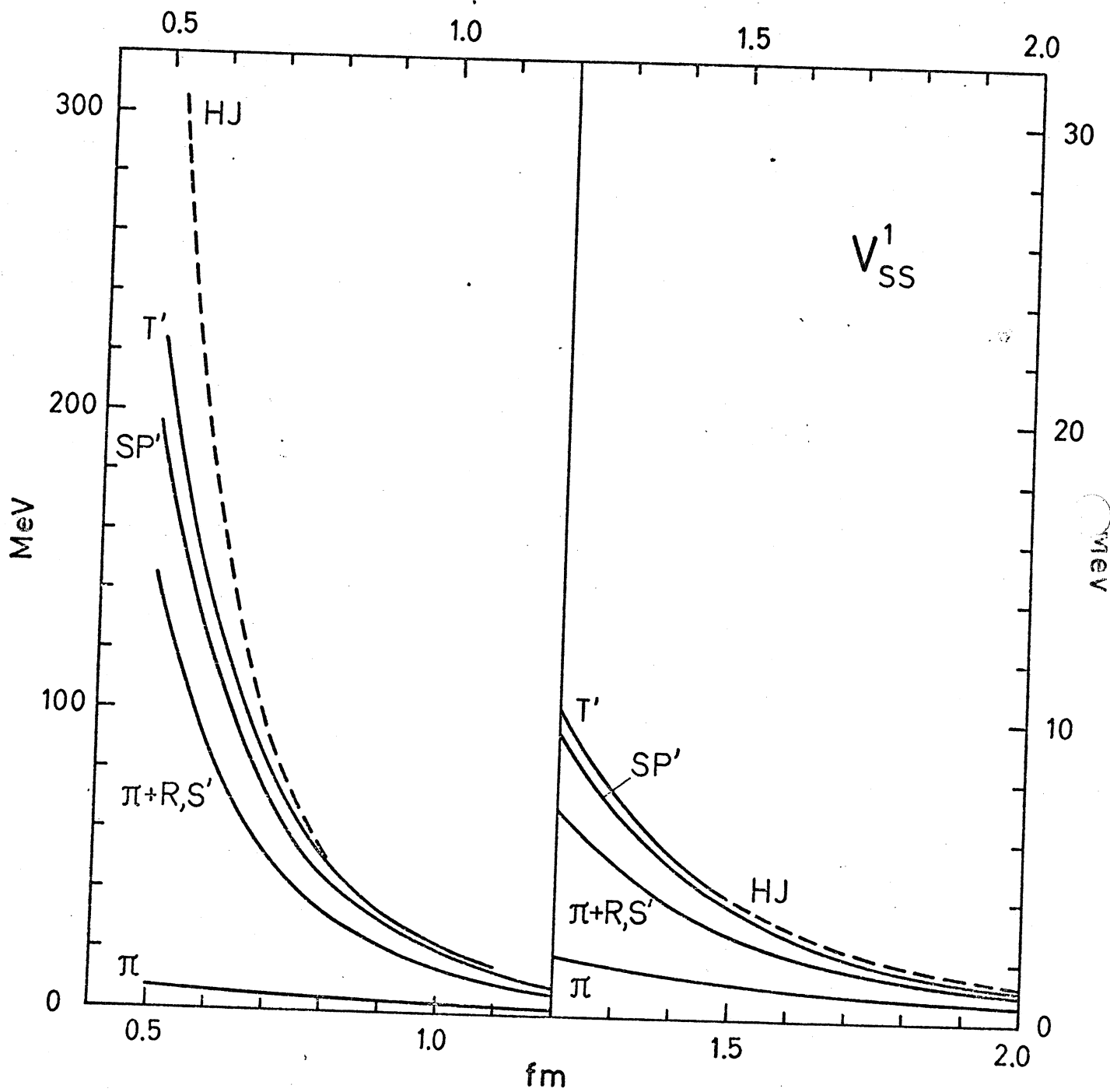


Figure 2



The Two-Pion Exchange Contribution to the  
Nucleon Nucleon Potential.

Geoffrey N. Epstein & Bruce H.J. McKellar

Department of Theoretical Physics, University  
of Sydney, Sydney, N.S.W. 2006. Australia.

The classification of the nucleon-nucleon potential into a long range part ( $r > 1.5\mu^{-1}$ ) due to one pion exchange, and a shorter range part has been most successful. Attempts to calculate the shorter range part from meson theory have been much less successful.

The next obvious step is to try to calculate the two pion exchange potential. The machinery for doing this was set up by Amati, Leader and Vitale<sup>1</sup> some eleven years ago. The basic idea is to calculate the nucleon-nucleon scattering amplitude from a Mandelstam dispersion relation, the discontinuity in the amplitude being calculated from unitarity in the  $\bar{N}N \rightarrow \bar{N}N$  channel. The  $2\pi$  exchange contribution is obtained by restricting the intermediate states in the unitarity relation to  $2\pi$  states.

The idea is sound in principle, but previous attempts at its implementation, notably that of Cottingham and Vinh Mau<sup>2</sup>, ran into difficulties, firstly because of the sensitivity of the calculation to the then available data on the  $\pi N$  scattering amplitude, which enters the calculation when it is analytically continued into the crossed channel to provide the  $\bar{N}N \rightarrow 2\pi$  amplitude, and secondly because of the lack of data at the time on  $\pi\pi$  scattering which also enters into the  $\bar{N}N \rightarrow 2\pi$  amplitude. Because of the improved knowledge of these ingredients, and of the existence of a good recent calculation of the uncorrelated  $2\pi$  exchange potential by Lomon and Partovi<sup>3</sup>, we decided it was reasonable to reattempt the calculation.

Following Cottingham & Vinh Mau, we use the amplitudes for  $\pi N$  scattering constructed by Bowcock, Cottingham and Lurie<sup>4</sup> as the basis of our calculation. A typical such amplitude, neglecting  $\pi\pi$  interactions

is

$$A^+ = G_A \left\{ \frac{1}{S_r - S} + \frac{1}{S_r - u} \right\} + C_A^+ \quad (1)$$

Here the first term represents the effects of the  $\Delta(1236)$ , approximated as a pole.  $G_A$  is determined from the (3,3) phase shift.  $C_A^+$  is introduced to approximate the higher resonances and is adjusted to obtain the correct threshold behaviour.

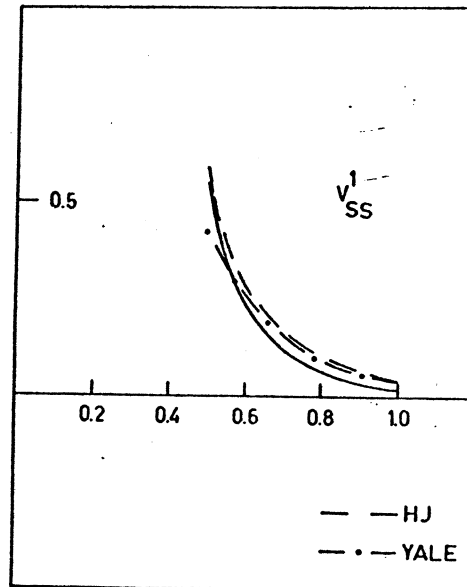
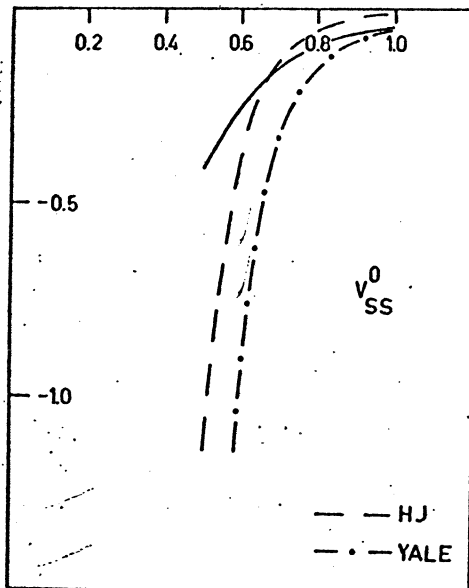
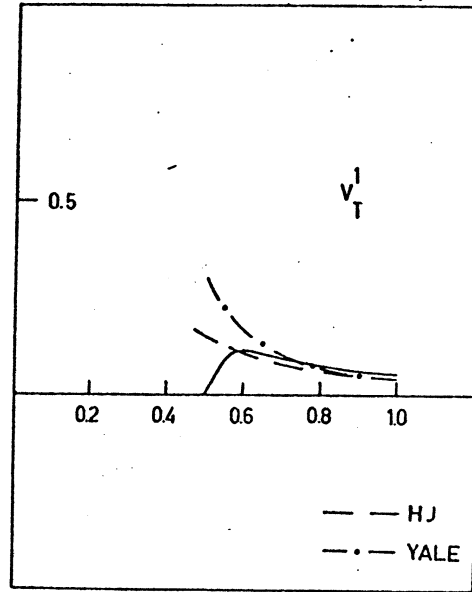
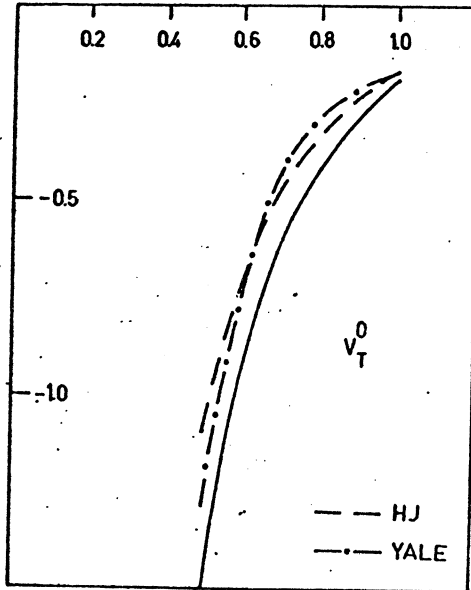
We find, on using the  $\pi N$  phase shifts to compute  $G_A$  and  $C_A^+$ , that  $C_A^+$  is small showing that the (3,3) resonance at 1236 does indeed give the major contribution to the amplitude. (This was not the experience of the earlier calculations).

We also took S and p wave  $\pi\pi$  interactions into account, ~~is on~~. The p wave contribution was assumed to be dominated by the  $\rho$  resonance, which was included as a simple pole. The S wave "resonance" is far too broad to be included in such a way, and we used instead the up down phase shifts of Morgan and Shaw<sup>5</sup>, replacing the S wave contribution of equation (1) by that calculated from the helicity amplitudes.

Our results are shown in figs 1-8, where our potential is compared over the range of interest ( $0.5\mu^{-1} < r < 1.0\mu^{-1}$ ) with the Hamada-Johnson and Yale Potentials. The agreement of the tensor and spin-spin potentials is very good, as is the isotriplet spin orbit. The isosinglet spin-orbit potential and both isotriplet and isosinglet central potentials are rather more attractive than the phenomenological ones. It is well known that the  $\omega$  and  $\phi$  mesons give a large repulsive contribution at short distances to the central potential, but the origin of the additional repulsion in the T=0 spin orbit potential is not at all obvious.

We conclude by mentioning that the  $\Delta(1236)$  gives a very small contribution to the potential in our calculation - it is nowhere larger than 5%, and by emphasising that no parameters not determined by data on  $\pi N$  and  $\pi\pi$  scattering enter our calculation.

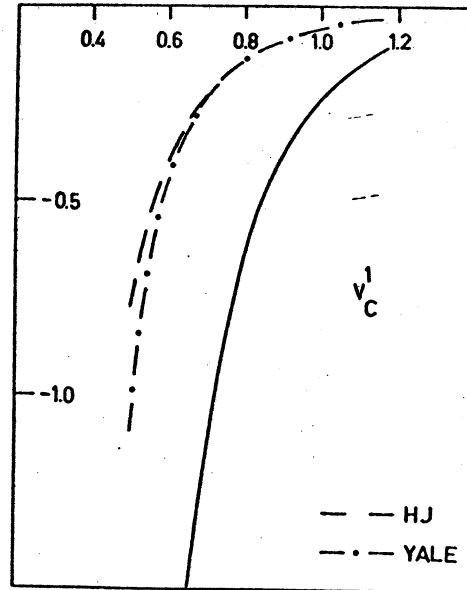
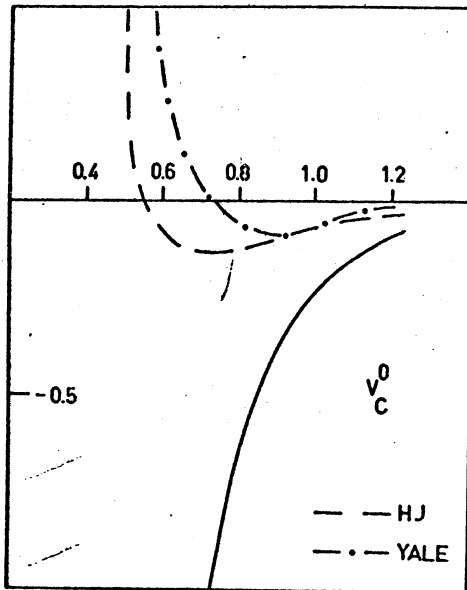
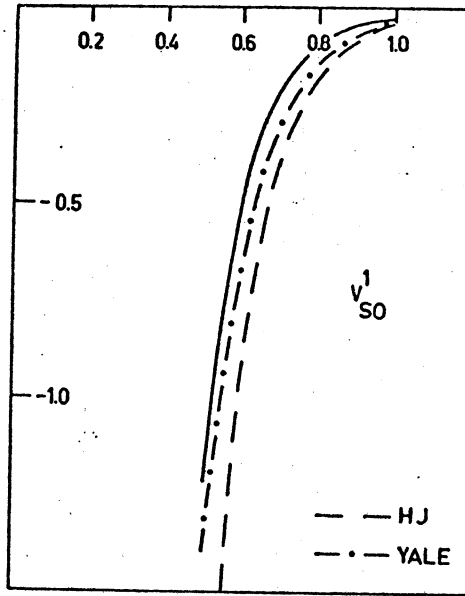
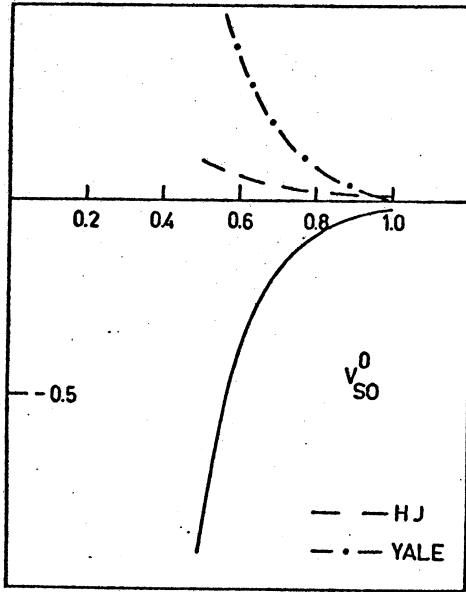
1. D. Amati, E. Leader and B. Vitale, Nuovo Cimento 17, 68 (1960); 18, 409 (1960); 18, 458 (1960); Phys. Rev. 130, 750 (1963).
2. W.N. Cottingham and R. Vinh Mau, Phys. Rev. 130, 735 (1963).
3. E. Lomon and H. Partovi, Phys. Rev. 2D, 1999 (1970).
4. J. Bowcock, W.N. Cottingham and D. Lurie, Nuovo Cimento, 16, 918 (1960); 19, 142 (1961).
5. D. Morgan and G. Shaw, Columbia University Preprint NYO-1932 (2)-160.



### TENSOR AND SPIN-SPIN POTENTIALS

Superscripts 0,1 refer to isospin states 0,1. The solid curves show our calculated potential compared with Hamada-Johnston (HJ) and Yale potentials for  $r > 0.5$  (units  $\hbar = \mu = c = 1$ ).





SPIN-ORBIT AND CENTRAL POTENTIALS

## On the Definition of a Boson Exchange Potential

C.J. Noble and K.C. Richards

Bartol Research Foundation of the Franklin Institute  
Swarthmore, Pennsylvania 19081

Several prescriptions for one-boson-exchange potentials have been discussed in the literature. Some of these have been developed into potentials. Because of a lack of data, some boson coupling constants are used as free parameters. Even with this limitation it has been possible to reproduce the two nucleon scattering phase shifts.

Because of this success, interest has turned to higher order contributions to two nucleon scattering. However, as we demonstrate, the work that has been done does not uniquely determine even the one-pion-exchange phase shifts. This occurs because the details of the various schemes are somewhat different. Items which must be specified to develop a potential are the definition of the potential, the equation which relates the potential to the transition matrix and the relation between the transition matrix and the phase shifts.

To show this, we have calculated one pion exchange phase shifts in uncoupled channels for each of three prescriptions and compared them with the results of a fourth. We have calculated according to the schemes of Scheirholz<sup>1</sup>, Bryan and Scott<sup>2</sup>, and Richards, Haftel and Tabakin<sup>3</sup>. We compare to the calculation of Barker and Haracz<sup>4</sup>.

For reference, we quote the one pion exchange T matrix

given by a pseudoscalar field theory. It is

$$\langle K' | T^{(2)} | K \rangle = \frac{g_p^2}{2\pi^2} \tau_1 \cdot \tau_2 \left( \frac{E+M}{2E} \right) \left( \frac{E'+M}{2E'} \right) \frac{1}{q^2 - \mu^2} \begin{bmatrix} \sigma_1 \cdot K & \sigma_1 \cdot K' \\ \frac{E+M}{E+M} & - \frac{E'+M}{E'+M} \end{bmatrix} \begin{bmatrix} \sigma_2 \cdot K & \sigma_2 \cdot K' \\ \frac{E+M}{E+M} & - \frac{E'+M}{E'+M} \end{bmatrix} \quad (1)$$

This is written in the center of mass system with unprimed quantities referring to the initial state, primed quantities to the final state and  $q$  is the four momentum transfer. The nucleon mass is  $M$  and the pion mass,  $\mu$ .

Bryan and Scott define the potential as  $V=T^{(2)}$  of Eq.(1). In order to generate a potential in configuration space, they approximate  $E = \sqrt{K^2+M^2}$  by  $E = M + \frac{1}{2} \frac{K^2}{M}$ . This procedure gives

$$\langle K' | V | K \rangle = -\frac{g_p^2}{2\pi^2} \frac{1}{4M^2} \tau_1 \cdot \tau_2 \frac{[\sigma_1 \cdot (\underline{K}-\underline{K}')]][\sigma_2 \cdot (\underline{K}-\underline{K}')] }{(\underline{K}-\underline{K}')^2 + \mu^2}$$

They enforce unitarity by using the Schrödinger equation to obtain the phase shifts.

Richards et al. also identify the expression of Eq.(1) as the potential. By solving directly in momentum space, the energy expansion of Bryan and Scott is avoided. The potential matrix elements are decreased on and near the momentum diagonal,  $|K|=|K'|$ . Far off the momentum diagonal, the potential matrix elements are larger than those of Bryan and Scott. Their equation is the Lippman-Schwinger equation in the form

$$R_L^{JST}(K' | K) = V_L^{JST}(K' | K) - \frac{2}{\pi} p \int_0^\infty \bar{K}^2 d\bar{K} \frac{V_L^{JST}(K' | \bar{K}) R_L^{JST}(\bar{K} | K)}{\bar{K}^2 - K^2} \quad (2)$$

with  $\delta_L^{JST}(K_0) = \tan^{-1} [-K_0 R_L^{JST}(K_0 | K_0)]$ .

The Scheirholz potential definition is identical with that of Richards et al. Because he starts with relativistic quantum mechanics, his equation of motion and phase shift relation are different. In terms of the same potential as in Eq. (2), Scheirholz writes

$$R_L^{\text{JST}}(K' | K) = \frac{2}{\pi} \frac{1}{M} V_L^{\text{JST}}(K' | K) - \frac{2}{\pi} P \int_0^\infty \bar{K}^2 d\bar{K} \frac{E(\bar{K}) + E(K)}{2M} \frac{V_L^{\text{JST}}(K' | \bar{K}) R_L^{\text{JST}}(\bar{K} | K)}{\bar{K}^2 - K^2} \quad (3)$$

with  $\delta_L^{\text{JST}}(K_0) = \tan^{-1} \left[ -\frac{\pi}{2} K_0 E(K_0) R_L^{\text{JST}}(K_0 | K_0) \right]$ . The additional energy dependent factor in Eq.(3) provides additional weight to the higher intermediate momenta,  $K$ . Since  $K_0$  is usually in the range  $0 \rightarrow 2 \text{ fm}^{-1}$ , this factor increases the weight of off diagonal potential matrix elements in determining the phase shifts.

Barker and Haracz use a unitary approximation scheme to apply the Schrödinger equation to two particle scattering. An effective interaction operator,  $W$ , is introduced whose contribution in lowest order  $W$  is equivalent to that of the usual interaction operator  $V$ , summed to all orders. To second order in the coupling constant  $\langle f | W_2 | i \rangle = \langle f | V | i \rangle$ . Breit<sup>5</sup> has shown  $W$  is related to the direct part of  $K$  which is related to the  $S$ -matrix by  $S = (1 - \frac{1}{2}iK) / (1 + \frac{1}{2}iK)$ .

An expansion of  $K$  in powers of the coupling constant guarantees a unitary  $S$ -matrix. To second order  $K_2 = iS_2$ . The effective interaction in this approximation is

$$W_2(\underline{K}' - \underline{K}) = \frac{g_p^2 (\tau_1 \cdot \tau_2)}{4[(K' - K)^2 + M^2]} \frac{[\sigma_1 \cdot (K' - K)][\sigma_2 \cdot (K' - K)]}{(K' - K)^2 + \mu^2}$$

This calculation is then carried out to fourth order.

Some results are presented in the table. In all cases  $g_p^2 = 14.00$  and  $\mu = 0.699 \text{ fm}^{-1}$ . Energies are incident laboratory energies in Mev. All phase shifts are in radians.

The correlation between Barker and Haracz and the other three prescriptions is hard to see. Of these other three, the Bryan-Scott scheme generally gives the largest phase shifts while Richards et al. gives the smallest. This holds for all higher uncoupled waves through  $L=8$ . In the  $^1S_0$  wave, this situation is reversed. But here a multiplicative cut-off of the form  $(q^2 + \Lambda^2)^{-1}$  with  $\Lambda = 7.57 \text{ fm}^{-1}$  was used. The other exception is the  $^3D_2$  wave. Here the differences are large. Because the  $^3D_2$  potential is formally identical to the  $^3G_4$ , this result is hard to explain. The  $^3G_4$  result follows the general trend.

The Barker-Haracz result is about the same as the others in the  $^1P_1$ ,  $^1D_2$  and  $^3G_4$  waves. In the  $^3P_1$  it is about fifty percent greater in magnitude. In the  $^3D_2$  it is somewhat smaller. None of the other methods investigated gives the overall behavior of the Barker-Haracz results.

Preliminary calculations of coupled channels show that significant differences persist.

Any one-boson-exchange potential which fits the two-nucleon data does so because of strong cancellations among the contributions of the various bosons used. Because of these



large cancellations, it is important that the contribution of each boson be calculated precisely. As we have shown, under the most favorable circumstances, a spread of ten percent in the one pion exchange phase shifts occurs. If there is to be any hope of using a unique set of coupling constants, a more rigorous attitude toward the definition of a boson exchange potential is indicated. This applies to one-boson-exchange and certainly to higher order contributions.

Since several of these prescriptions have been used to obtain potentials which can be fit to the two nucleon data, further work on nuclear matter and finite nuclei may be needed to determine the most useful choice for a boson exchange potential.

<sup>1</sup> G. Scheirholz, Nucl. Phys. B7, 432 (1968); B7, 483 (1968).

<sup>2</sup> R.A. Bryan and B.L. Scott, Phys. Rev. 177, 1435 (1969).

<sup>3</sup> K.C. Richards, M.I. Haftel and F. Tabakin, Bull. Am. Phys. Soc. 14, 492 (1969) and to be published.

<sup>4</sup> B.M. Barker and R.D. Haracz, Phys. Rev. 186, 1624 (1969).

<sup>5</sup> G. Breit, Ann. Phys. (N.Y.) 16, 346 (1961).

ONE PION EXCHANGE PHASE SHIFTS

$E_{LAB}$  - Incident Laboratory Energy-Mev  
 All phase shifts in radians  
 $g_p^2 = 14.00$      $\mu = 0.699 \text{ fm}^{-1}$   
 1 - Barker and Haracz  
 2 - Scheirholz  
 3 - Bryan and Scott  
 4 - Richards, Haftel and Tabakin

$^1S_0$	$^1P_1$				
	$E_{LAB}$	1	2	3	4
(includes cut-off)	10	-	.0615	.0680	.0509
	50	-	-.0390	-.0270	-.0583
	110	-	-.1436	-.1280	-.1688
	210	-	-.2564	-.2385	-.2862
	310	-	-.3352	-.3171	-.3663
	350	-	-.3614	-.3437	-.3924

$^3P_1$	$^1D_2$				
	$E_{LAB}$	1	2	3	4
	10	-0.488	-.0413	-.0415	-.0414
	50	-.2088	-.1616	-.1635	-.1606
	110	-.3531	-.2567	-.2629	-.2533
	210	-.5094	-.3495	-.3650	-.3407
	310	-.6205	-.4111	-.4376	-.3962
	350	-.6576	-.4302	-.4610	-.4130

$^3D_2$	$^3G_4$				
	$E_{LAB}$	1	2	3	4
	10	.0140	.0152	.0153	.0154
	50	.1326	.1628	.1716	.1740
	110	.2748	.3616	.4194	.4471
	210	.4395	.5484	.7412	.8775
	310	.5582	.6310	.9656	1.2029
	350	.5979	.6481	1.0298	1.2923

DEVELOPMENT OF A SUPER SOFT CORE POTENTIAL MODEL OF THE  
NUCLEON-NUCLEON INTERACTION

R. de Turreil

Institut de Physique Nucleaire, Division de Physique Theorique,  
B.P. No. 1,  
91 - Orsay, France

and

D.W.L. Sprung

Physics Department, McMaster University, Hamilton 16,  
Ontario, Canada

It is by now well known that the elastic scattering data do not require the nucleon-nucleon potential to contain infinite or even strong finite repulsion at short distance. This was shown in the  $^1S_0$  state by Srivastava and Sprung who constructed a number of 'super soft core' potentials whose maximum repulsion ranged from 70 MeV to 260 MeV. A rough criterion for an SSC potential is that in nuclear matter the second order perturbation theory terms are 10 to 20% of the corresponding first order ones. At about the same time, Pires, de Turreil and Gogny (PDG) presented a complete potential, choosing as radial form a sum of gaussians. Their intention was to fit not only the elastic scattering data, but also nuclear matter saturation properties and the radii of finite nuclei in the Hartree Fock approximation. Modest agreement with all three criteria was obtained, but at the expense of a high quality fit to phase shifts, especially in the singlet odd state.

The present work is directed to producing a complete SSC potential which provides an excellent fit to phase shifts and other two body data, and includes the OPEP tail. The forms employed are essentially Yukawas modified by gaussian or similar cut-off functions to keep the potential soft at short distances. The potential is not yet in its final form, but acceptable forces have been found in three of the four spin, isospin (S,T) subspaces and the remaining singlet odd state presents no difficulty. In this note we discuss some characteristics of the potential which are noteworthy. Some preliminary potentials are included to show the type of forms employed.

## 2. Some Considerations in Fitting the Potential.

The potential is fitted to reproduce the single energy phase shift analyses of MacGregor, Arndt and Wright. In addition to the central, tensor and spin orbit components, and  $\tilde{L}^2$  dependent force is used in each (S,T) subspace. This operator is preferable to the so called quadratic spin-orbit force  $\tilde{\sigma}^1 \cdot \tilde{L} \tilde{\sigma}^2 \cdot \tilde{L}$  or equivalently the operator  $L_{12}$  adopted by Hamada and Johnston, on grounds of simplicity and in fitting the phase shifts. In singlet states, any of these more complicated operators reduces to an  $L^2$  force. In triplet states the operator  $L_{12}$  is equivalent to the sum of  $\tilde{L}^2$  and an operator

$$Q_{12} = 3 \tilde{\sigma}^1 \cdot \tilde{L} \tilde{\sigma}^2 \cdot \tilde{L} - \sigma^1 \cdot \sigma^2 L^2$$

which causes a splitting of the three states of different  $J$  for each  $L$ . Although in the triplet even states there is a need for an  $L^2$  force to make the mean D-wave interaction weaker than the S-wave, there appears to be no evidence for an additional splitting of the  $J$ -values beyond that given by the LS and tensor forces. We have not found it necessary to invoke a  $Q_{12}$  force.

Our potential for the singlet even states has the form

$$V_C(r) = p_1 \exp(-r^4/p_2^2) + \left\{ p_3 \frac{\exp(-p_4 x)}{x} + \text{OPEP} \right\} \{1 - \exp(-r^4)\}$$

$$V_{L2}(r) = \left\{ p_5 \exp(-p_6 x) + p_7 \exp(-x) \right\} \left\{ 1 + \frac{3}{x} + \frac{3}{x^2} \right\} \frac{1}{x^3} \{1 - \exp(-r^8)\}$$

$$V = V_C(r) + V_{L2}(r) \underline{L}^2, \quad x = \mu r, \quad \mu = 0.7 \text{ fm}^{-1}$$

$$\text{OPEP} = -10.463 \exp(-x)/x$$

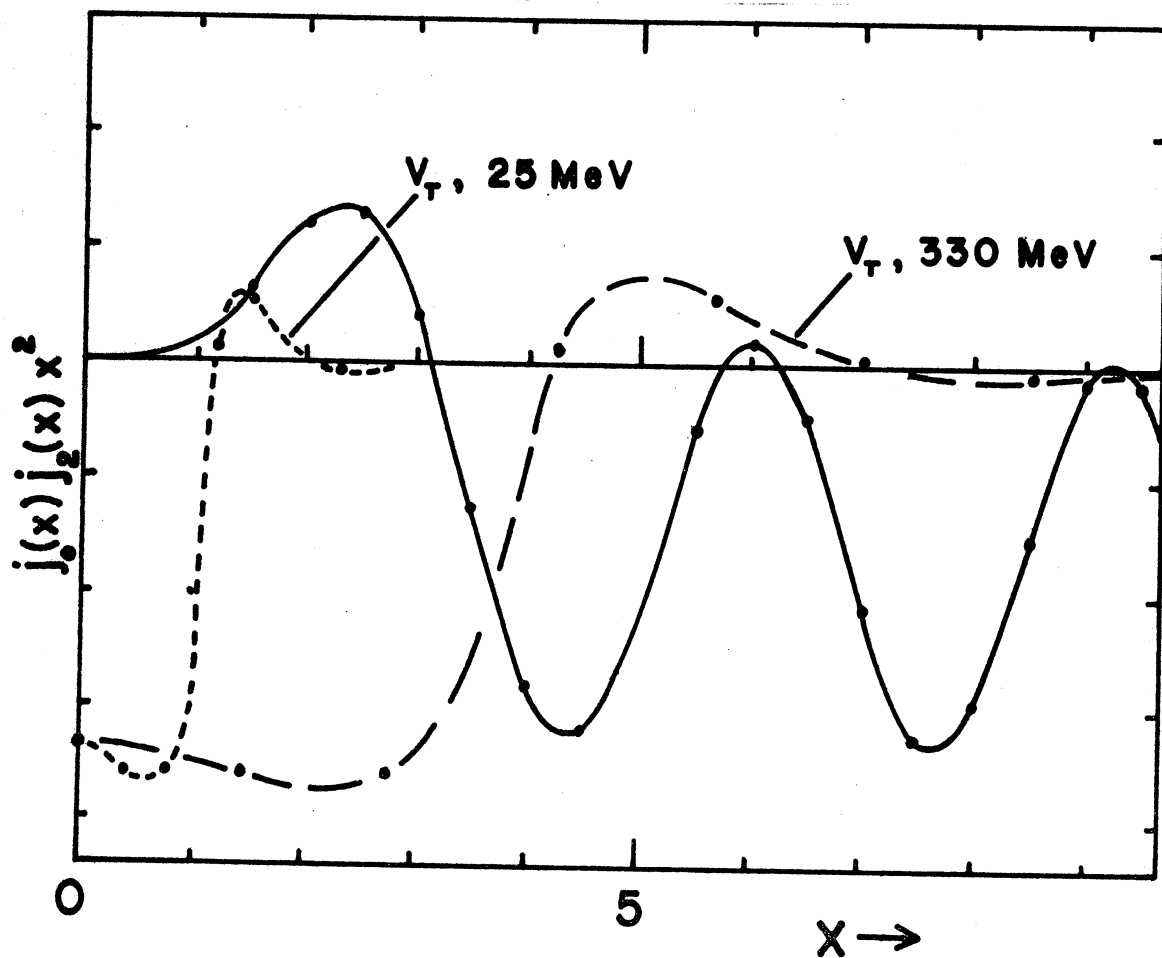
$$p_1 \dots p_7 = 378.4, 0.4792, -1002., 3.599, 2.684, 2.439, -0.03448$$

The forms adopted are highly arbitrary. In particular the  $L^2$  force requires a very high order cut-off to compensate for the singular radial form taken from Hamada and Johnston. Further improvements are planned which will simplify the functional form.

One problem in fitting the triplet even state phase parameters of MAW is to reproduce the steady rise with energy of the coupling constant  $\epsilon^1$ . For a weak potential this can be studied qualitatively in terms of the Born approximation;

$$\epsilon^1 = -\frac{1}{k^2} \frac{m}{k^2} \int_0^\infty j_0(x) j_2(x) V_T(r) x^2 dx, \quad x = kr$$

In the figure we show the Bessel function product  $x^2 j_0(x) j_2(x)$ , and superimposed on it a schematic soft tensor force, the radial scale chosen to correspond to 25 MeV (dashed line) and 330 MeV (long dash line). The oscillations of the Bessel function product are mostly on the negative side of the axis. If the tensor force were always attractive and monotonic, as is the OPEP force, it is clear that as the energy increases, the tail of the tensor force integrated over the first negative loop of the Bessel function product would give a substantial negative contribution to  $\epsilon^1$ , severely reducing its value when  $E=330$  MeV. In the PDG potential one finds as a consequence that  $\epsilon^1$  either heels over or becomes negative at 200 or 300 MeV.



This tendency can be combatted if  $V_T(r)$  takes on severely reduced or even small positive values in the region near 1 fm. An extreme form of such behaviour is illustrated in the sketch. In this case the damage done by the negative loop of the Bessel function product is reduced, or even turned to advantage, and a monotonic increase with energy of  $\epsilon^1$  is obtained. Such a behaviour of the radial form of  $V_T(r)$  may not be completely artificial, since it is found in the potential of Ingber and Potenza where repulsive contributions from the vector mesons combined with the  $\pi$   $\sigma$  and  $\eta$  meson forces give a  $V_T(r)$  which is nearly zero at about 0.5 fm. We agree with Ingber that previous phenomenological potentials did not include such a possibility because they were guided too closely by the OPEP form, supplying only the required regularization of the  $1/x^3$  singularity at the origin.

Because the other components of the force are weak in our potential, even the small  $r$  part of  $V_T$  plays a role in determining  $\epsilon^1$ ; it is not completely masked by a strong repulsion. In order to fit the deuteron quadrupole moment we require an attractive contribution to  $V_T$  of about two pion range.

A triplet even state potential has the form :

$$V = V_C(r) + V_{L^2}(r) L^2 + V_{LS}(r) \vec{L} \cdot \vec{S} + V_T(r) S_{12}$$

$$V_{L^2} = \{P_5 Z(y) + P_6 Z(x)\} \frac{1}{x^3} \{1 - \exp(-r^8)\}$$

$$V_{LS} = -P_8 (1+P_9 x) \exp(-P_9 x) \frac{1}{x^3} \{1 - \exp(-r^6)\}$$

$$V_T = P_{10} \exp\left(\frac{-r^4}{2}\right) + \left\{ P_{12} \frac{Z(y')}{x} - 10.463 \frac{Z(x)}{x} \right\} \{1 - \exp(-r^6)\}$$

$V_C =$  same as singlet even.

$$Z(y) = (1 + 3/y + 3/y^2) \exp(-y)$$

$$y = P_6 \cdot x, \quad x = 0.7r,$$

$$y' = P_{13} \cdot x$$

$P_1 \dots P_{13}$	=	460.0,	0.67,	-1110.0,	3.600,
		10.20,	2.215,	-0.3699,	
		-18.50,	4.20,		
		-178.4,	0.92,	+500.7,	4.352

Deuteron properties :  $E_D = -2.215$  MeV,  $Q = .264$  fm<sup>2</sup>,

$$\mu = .857 \mu_N \quad P_D = 4.55\%$$

low energy properties :  $a = 5.50$  fm,  $r_0 = 1.847$  fm.

In nuclear matter the  $^3S_1$  state gains about 9 MeV potential energy as compared to the Reid force, at normal density. There is not a strong saturating effect due to the tensor force, indicating that it is quite weak. Saturation relies upon odd state repulsion in this case.

Further work is in progress and it is hoped to publish a more detailed report in a few months time.

#### References.

1. D.W.L.Sprung & M.K. Srivastava, Nucl. Phys. A139, 605 (1969).
2. D.Gogny, P. Pires, & R. de Turreil, Phys. Lett. 32B, 591
3. M.H. MaGregor, R.A.Arndt & R.M.Wright, Phys.Rev.182, (1970).  
1714, (1969).
4. T. Hamada & I.D. Johnston Nucl. Phys. 34, 382 (1962).
5. L. Ingber & R.M. Potenza Phys. Rev. C 1, 112 (1970).



Neutron-Proton Bremsstrahlung Including Gauge-Invariant Terms Arising From the Nuclear Potential.\* V. R. Brown, Lawrence Radiation Laboratory, Livermore, California, and J. Franklin, Temple University, Philadelphia, Penn.

In a previous calculation of npy using potentials<sup>1</sup> the coupling of the electromagnetic field to the nucleon currents was obtained in the usual way using the principle of minimal electromagnetic coupling in the kinetic-energy part of the hamiltonian only. This prescription is not fully gauge invariant because of the exchange-nature and momentum-dependence of the two-nucleon potentials. The hamiltonian resulting from this minimal coupling is shown in Eq. (1).

$$H_N + v_{em}^{(1)} = -\frac{v^2}{2\mu} + V_N + a_e \left( e^{-i\vec{k}\cdot\vec{r}/2} - e^{i\vec{k}\cdot\vec{r}/2} \right) i \hat{\epsilon} \cdot \vec{v} \\ + i a_e \left( e^{-i\vec{k}\cdot\vec{r}/2} \mu_1 \vec{\sigma}_1 \cdot \vec{k} \times \hat{\epsilon} + e^{i\vec{k}\cdot\vec{r}/2} \mu_2 \vec{\sigma}_2 \cdot \vec{k} \times \hat{\epsilon} \right), \quad (1)$$

where  $a_e = \frac{e}{m} \sqrt{\frac{2\pi}{K}}$ ,  $\mu_n = -1.913/2$  and  $\mu_p = 2.793/2$

A momentum-dependent one-boson-exchange potential such as that of Bryan and Scott<sup>2</sup> is defined such that when inserted into the Schrodinger equation it yields in Born approximation the same scattering matrix element as the Feynman diagram for one-boson exchange. A potential so

defined is easily written down in momentum space. In a non-relativistic model a method of solution is to Fourier transform everything to configuration space and solve the Schrodinger equation. The correspondence of such a potential with Feynman diagrams suggests a method<sup>3</sup> for introducing minimal coupling.

In the present work the minimal-gauge-invariant interactions are introduced in momentum space in the non-local framework according to the prescription

$$\vec{p} \rightarrow \vec{p} - \frac{e}{c} \vec{A} \quad . \quad (2)$$

For simplicity the present discussion is restricted to the long-wavelength dipole approximation.<sup>4</sup> For np which is a single-photon process only terms linear in  $\vec{A}$  are of interest so that it is sufficient to consider a Taylor expansion in  $\vec{A}$  keeping only the first two terms. The first term is just the nuclear potential, and the second term which involves the gradient of the nuclear potential is the additional electromagnetic potential which we call  $V_{em}^{(2)}$  to distinguish it from  $V_{em}^{(1)}$  of Eq. (1). A transformation of  $V_{em}^{(2)}$  to configuration space and a rearrangement of terms yields

$$V_{em}^{(2)} = \sqrt{\frac{2\pi}{K}} i e \hat{\epsilon} \cdot \left\{ \frac{1}{2} (\vec{r}' - \vec{r}) V_N(r, r') - \vec{r}' V_N^{ex}(r, r') \right\} \quad , \quad (3)$$

where  $V_N^{ex}(r, r')$  is the exchange potential for np scattering still in the non-local representation. The np potential can be written in terms of a direct plus an exchange part as

$$V_N = V_N^d + V_N^{ex} T^{ex} \quad , \quad (4)$$

where  $T^{\text{ex}}$  is the isospin-exchange operator given by

$$T^{\text{ex}} = \frac{1}{2} (1 + \vec{\tau}_1 \cdot \vec{\tau}_2) \quad (5)$$

The first term of  $V_{\text{em}}^{(2)}$ , which consists of direct plus exchange, exists only for non-local or certain momentum-dependent potentials. The second term of  $V_{\text{em}}^{(2)}$ , which involves just the exchange potential arises because of the interchange of a proton and a neutron through the exchange of a charged meson.

The results of n-py including the various contributions are calculated with the Bryan-Scott potential at 200 MeV for coplanar symmetric angles of  $30^\circ$  to compare with the experiment of Brady<sup>5</sup> et al. The terms arising from the explicit momentum dependence of the Bryan-Scott potential are negligible. A comparison of the results for external radiation scattering alone and those including the exchange-bremsstrahlung term in the present approximation is shown in Fig. 1. The cross section integrated over the photon angular distribution is  $35 \mu\text{b}/(\text{sr})^2$  as compared to the experimental result of Brady et al. of  $35 \pm 14 \mu\text{b}/(\text{sr})^2$ .

## References

\*Worked performed under the auspices of the U.S. Atomic Energy Commission.

1. V. R. Brown, Physics Letters 32B, 259 (1970).
2. R. A. Bryan and B. L. Scott, Phys. Rev. 177, 1435 (1969).
3. V. R. Brown and J. Franklin, Bull. Am. Phys. Soc. 16, 560 (1971).  
The present work is an extension of Ref. 3.
4. The minimal prescription applied in the manner described here requires a sequence of approximations in increasing order of difficulty for increasing powers of the photon momentum. Preliminary results indicate that the extreme dipole approximation is correct to within 20%.
5. F. P. Brady, J. C. Young, and C. Badrinathan, Phys. Rev. Letters 20, 750 (1968); F. P. Brady and J. C. Young, Phys. Rev. C 2 1579 (1970).

## FIGURE CAPTIONS

Fig. 1. The coplanar-symmetric npy cross section for  $E = 200$  MeV and  $\theta = 30^\circ$  calculated with the Bryan-Scott potential comparing the results for external-radiation scattering alone with those including the exchange-bremsstrahlung contribution. The latter is calculated in the long-wavelength dipole approximation.

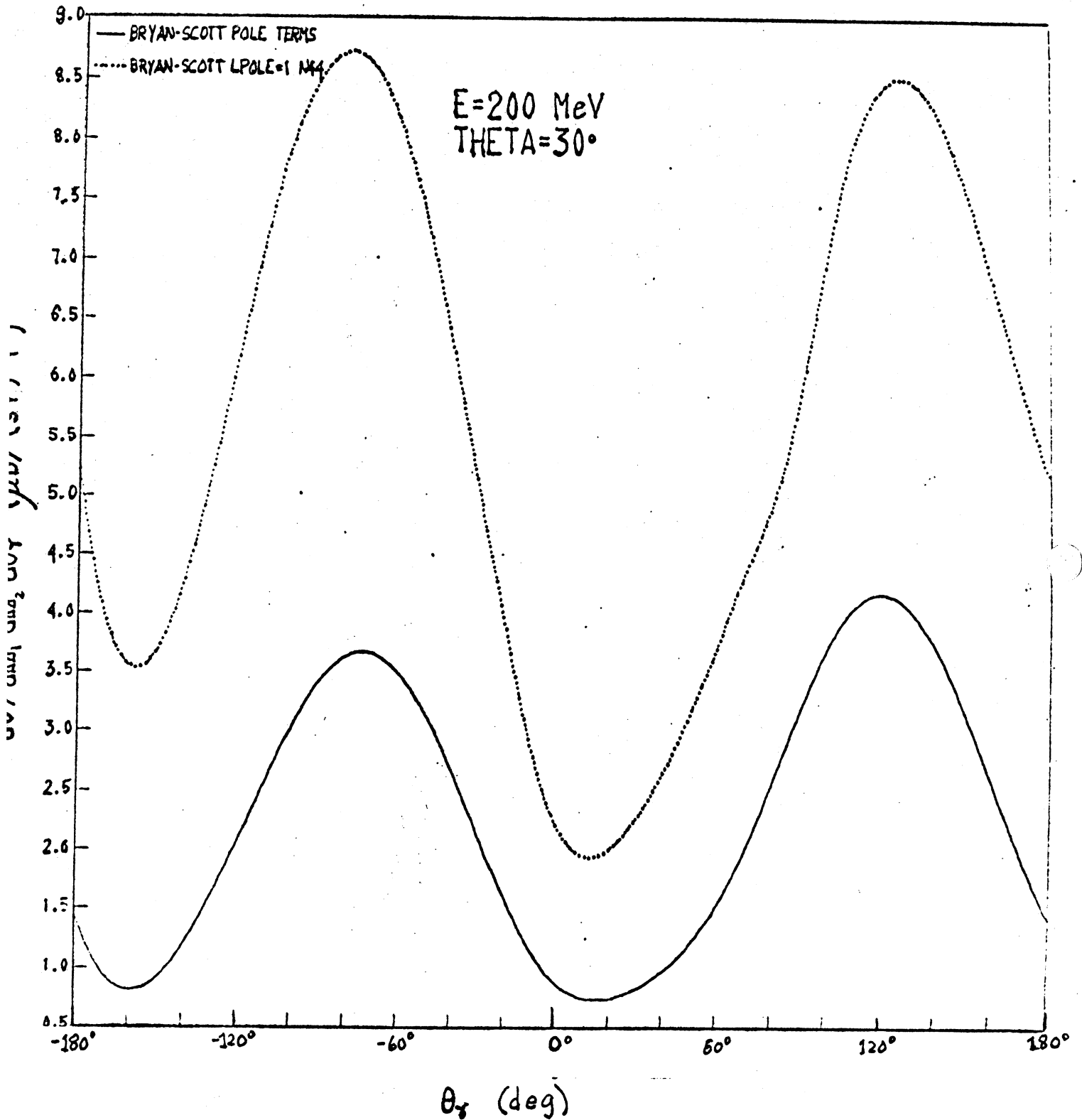


FIG. 1.

## TRITON BINDING ENERGY PREDICTIONS FOR PHASE-SHIFT EQUIVALENT POTENTIALS

Michael I. Haftel<sup>†</sup>

Naval Research Laboratory, Washington, D. C. 20390

## ABSTRACT

We compare theoretical predictions of the triton binding energy for a set of exactly phase-shift equivalent potentials. The potentials are generated through a rank one unitary transformation of the S-wave, spin independent Malfliet-Tjon V potential. We find that potentials that give drastically different (up to 27 MeV) nuclear matter binding energies, but nearly identical deuteron wave functions, give only small (1 MeV) variations in triton binding energy. For the potentials studied, large variations (up to 4.55 MeV) in triton binding energy occur only when there are significant differences in the deuteron wave functions. We find that potentials with enhanced deuteron charge form factors give increased binding in the triton.

Recent studies<sup>1</sup> show that the off-energy-shell properties of the two-nucleon (N-N) interaction play a major role in the prediction of nuclear matter properties. The question arises whether off-energy-shell effects play a major role in the few-nucleon problem. The three-nucleon problem provides an excellent opportunity to learn about the N-N interaction because, unlike the nuclear matter problem, an exact solution is possible in the Faddeev equation framework.<sup>2</sup> Recent advances<sup>3-5</sup> in the numerical solution of the Faddeev equations render the triton problem feasible on most available computers, at least for potentials that act in a small number of partial waves. Furthermore, the three-nucleon binding energy calculations of Malfliet and Tjon,<sup>3</sup> and of Hoenig,<sup>6</sup> indicate some sensitivity of triton binding energy results to off-shell properties.

---

<sup>†</sup>NRC-NRL Postdoctoral Resident Research Associate

This paper investigates the sensitivity of triton binding energy predictions to the off-shell properties of the N-N interaction with exactly phase-shift-equivalent potentials. We compare the triton binding energy results with the nuclear matter and deuteron properties for the potentials under consideration.

We generate the potentials employed in our study by applying a set of rank one unitary transformations<sup>1</sup> to the Malfliet-Tjon V (MTV) potential.<sup>3</sup> The unitary transformations U have the form

$$\langle \vec{r} | U | \vec{r}' \rangle = \delta(\vec{r} - \vec{r}') - 2g(r) g(r') P_0, \quad (1)$$

where  $P_0$  is a projection operator onto the  $L = 0$  partial wave, and  $g(r)$  is normalized to ensure unitarity. The unitarity of U assures that the "untransformed" two-body Hamiltonian  $H \equiv T + V$  ( $V$  is the MTV potential in our case) and the "transformed" two-body Hamiltonian  $\tilde{H} = UHU^\dagger$  give the same two-body spectrum. In other words, if  $H\psi_n = E_n\psi_n$ , then  $\tilde{H}\tilde{\psi}_n = E_n\tilde{\psi}_n$  where  $\tilde{\psi}_n = U\psi_n$ . Furthermore, since U is short ranged, i.e.,  $\psi_n(\vec{r}) \xrightarrow{r \rightarrow \infty} \tilde{\psi}_n(\vec{r})$ , H and  $\tilde{H}$  give the same two-body scattering cross-sections and phase-shifts. The two-body potentials  $V$  and  $\hat{V} \equiv \tilde{H} - T$  predict the same spectrum and scattering in the two-body problem; however, the insertion of two-body interactions  $V_{ij}$  and  $\hat{V}_{ij}$  in the many-body Hamiltonian does not correspond to a unitary transformation of the many-nucleon wave function. Therefore, the two-body potentials  $V$  and  $\hat{V}$  may yield different spectra in the many-nucleon system.

Using the matrix elements of  $\hat{V} - \langle k | \hat{V} | k' \rangle$  as input, we solve for the off-shell T-matrix,  $\langle k | \hat{T}(\omega) | k' \rangle$ , by the direct inversion of the Lippmann-Schwinger equation. The off shell T matrix provides the input for the Faddeev equations.

Since the MTV potential and its transforms are pure S-wave, spin independent interactions, the Faddeev equations, for  $J = 0$ ,  $S = 1/2$ ,  $I = 1/2$ , reduce to one uncoupled integral equation in two continuous variables. This integral



equation is, in the notation of Malfliet and Tjon,<sup>3</sup>

$$\psi(p,q) = \varphi(p,q) + \frac{4}{\sqrt{3}} \int_0^\infty q' dq' \int_0^{\frac{1}{\sqrt{3}}(2q+q')} \frac{1}{\sqrt{3}} |2q-q'| p' dp' \frac{\langle p | \hat{T}(\omega-q^2) | \bar{p} \rangle \psi(p',q')}{\omega - q'^2 - p'^2} \quad (2)$$

where  $\bar{p} = p'^2 + q'^2 - q^2$ . In Eq. (2)  $\psi(p,q)$  is essentially the particle 1 component of the Faddeev three-body T matrix,  $\varphi(p,q)$  an inhomogenous term determined by the two-body T matrix, and  $\hat{T}$  is the two-body T matrix. The momentum  $p$  represents the relative momentum of particles 2 and 3, and  $q$  represents the momentum of particle 1 relative to the center of mass of 2 and 3. A bound state occurs whenever the energy ( $\omega$ ) is such that  $\psi(p,q)$  has a pole.

We solve Eq. (2) by the method of Padé approximants. The details of this method appears in references 3 and 4. Since the Padé approximant method requires the iteration of Eq. (2), we must evaluate a large number of double integrals. We evaluate these integrals by employing a 16 point Gaussian quadrature in the  $q'$  variable and a variable mesh, up to 20 points, in the  $p'$  variable. We find that the Padé approximants to  $\psi(p,q)$  converge rapidly even when the Born series of Eq. (2) diverges. The binding energies were also stable (to within .2 MeV) with varying number of mesh points.

In our calculations we parameterize the transformation function  $g(r)$  by

$$g(r) = C_0 e^{-\alpha_0 r} (\beta_0 + \beta_1 r + \beta_2 r^2) \quad (3)$$

where  $C_0$  is a normalization constant. In Table I we present the transformation parameters, nuclear matter properties, and triton binding energies for the MTV potential and five transformed potentials. The quantity  $\langle g | \psi_B \rangle$  in Table I is the overlap between  $g(r)$  and the MTV deuteron wave function. This overlap is a measure of the difference between the untransformed and transformed deuteron wave functions.

TABLE I

Transformation Parameters, Nuclear Matter and Triton  
Binding Energies for the Transformed Potentials

Force	MTV	1	2	3	4	5
$\alpha_0$	--	2.40	1.80	2.40	2.80	2.40
$\beta_0$		1.00	1.00	1.00	0.00	1.00
$\beta_1$	--	-.8392	-.681	-.960	1.00	-.800
$\beta_2$		0.00	0.00	0.00	-.640	0.00
E/A-Nuclear Matter (MeV)	-33.0	-15.5	-6.4	-2.7	-3.4	-13.9
$k_F$ -Nuclear Matter ( $F^{-1}$ )	2.0	1.32	1.00	0.80	0.75	1.20
$\langle g   \psi_B \rangle$	--	.00028	.00038	-.0642	.0986	.0194
$E_T$ (MeV)	-7.65	-7.03	-6.59	-8.21	-3.66	-6.25

The triton binding energies of MTV and potentials 1 and 2, which have almost identical deuteron wave functions, vary by only about 1 MeV despite a very large variation in nuclear matter properties. In figure 1 we plot the saturation curves of these three forces for  $4F^{-1} \leq k_F < 1.50F^{-1}$ . We observe that the variations in triton binding energies ( $E_T$ ) are smaller, but in the same direction, as the variations in nuclear matter binding energies ( $E/A$ ). In fact, the variations in  $E_T$  are comparable to the variations in  $E/A$  calculated at densities of  $k_F \sim .6F^{-1}$  to  $1.0F^{-1}$ , which are well below the empirical nuclear matter density. These results indicate that, since the triton is a less dense system than nuclear matter, triton binding energy predictions are much less sensitive to far off-shell matrix elements than are nuclear matter properties.

If we relax the restriction of nearly identical deuteron wave function,<sup>5</sup> much larger variations in  $E_T$  occur. Despite the fact that forces 3 and 4 give

similar nuclear matter properties, a 4.55 MeV variation in triton binding energy occurs. Evidentially the triton binding energy is mainly sensitive to the deuteron wave function. What properties of the deuteron largely determine  $E_T$ ?

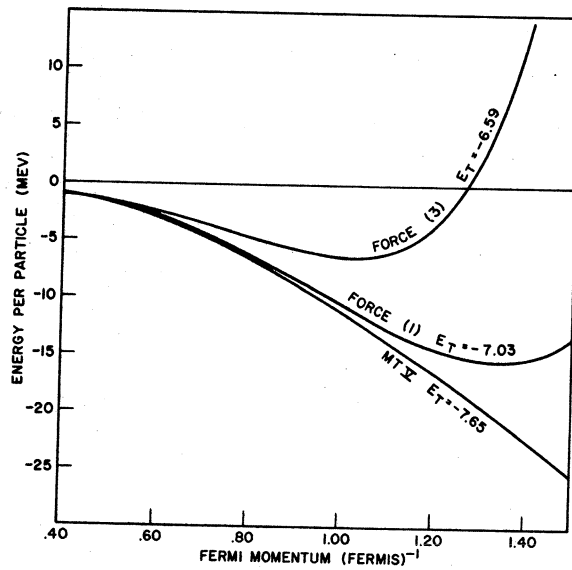
In comparing the variations of  $E_T$  with various deuteron properties, we found a close connection between  $E_T$  and the charge form factor of the deuteron ( $F_{ch}^2(q^2)$ ). In figure 2 we plot  $F_{ch}^2(q^2)$  for forces 1, 3, 4 and 5 (forces 1 and 5 also have similar nuclear matter properties). Examination of this figure yields a consistent pattern--potentials with enhanced charge form factors at low and moderate  $q^2$  give larger triton binding energies. Also, potentials with diffraction minima occurring at larger  $q^2$  give greater triton binding energies.

The above results demonstrate the importance of pole dominance in the two-body T matrix for the three-nucleon bound state problem. Once we fix the deuteron electric form factor, the triton binding energy seems pretty well determined, at least to within 1 MeV or so. This statement holds even for potentials whose far off-shell properties differ enough to cause large differences (up to 27 MeV) in nuclear matter binding energies.

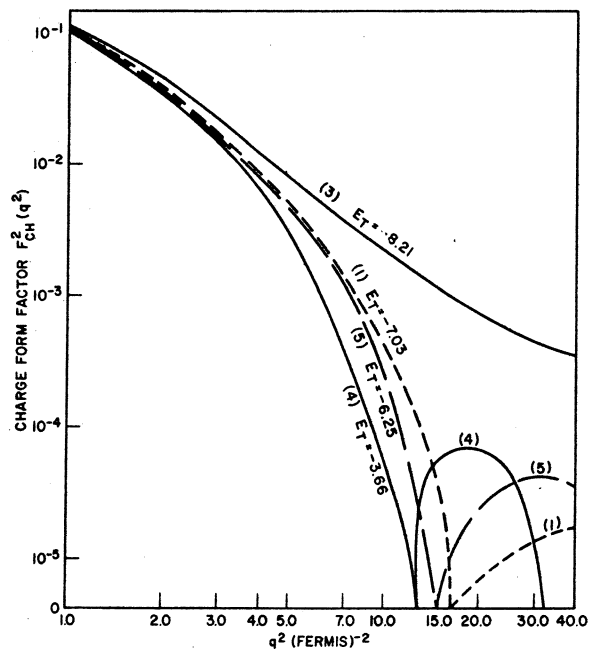
Although we have neglected the spin dependent and tensor properties of the N-N interaction, this investigation does suggest a close relation between electron-deuteron scattering experiments and the predictions of three-nucleon properties. Future three-body calculations should help clarify the role of these experiments.

#### REFERENCES

1. F. Coester, S. Cohen, B. Day and C.M. Vincent, Phys. Rev. C1, 769 (1970); M.I. Haftel and F. Tabakin, Phys. Rev. C3, 921 (1971).
2. L.D. Faddeev, Sov. Phys.-JETP 12, 1014 (1961).
3. R.A. Malfliet and J.A. Tjon, Nucl. Phys. A127, 161 (1969).
4. J.A. Tjon, Phys. Rev. D1, 2109 (1970).
5. D.D. Brayshaw, Phys. Rev. 182, 1658 (1969); J.W. Humberston, R.L. Hall, and T.A. Osborn, Phys. Letters 27B, 195 (1968).
6. M.M. Hoenig, Phys. Rev. C3, 1118 (1971).



1. Nuclear matter saturation curves of the MTV potential and potentials 1 and 2 for  $.4F^{-1} \leq k_F \leq 1.5F^{-1}$ . Triton binding energies ( $E_T$ ) are indicated.



2. The deuteron charge form factor ( $F_{ch}^2(q^2)$ ) for potentials 1, 3, 4 and 5. Triton binding energies are indicated.

Off-Shell Effects in the  $^{18}\text{O}$  and  $^{18}\text{F}$  Shell-Model Spectra<sup>†</sup>

H.C. Pradhan, P.U. Sauer and J.P. Vary  
 Center for Theoretical Physics  
 Massachusetts Institute of Technology

ABSTRACT

The two-particle shell-model spectra of  $^{18}\text{O}$  and  $^{18}\text{F}$  are studied using effective interactions obtained from phase-shift-equivalent nucleon-nucleon potentials. The spectra depend significantly on the off-shell behavior of the potentials.

I. INTRODUCTION

Adequate knowledge of the two-nucleon interaction, both on-shell and off-shell, and a proper many-body theory to employ that knowledge are the ingredients for a microscopic description of nuclear phenomena. At present, neither of these essentials is reliably established. The effective interaction in a finite, numerically manageable, model space remains the central problem of a shell-model calculation. However, this problem is beyond the scope of this study. We retreat to the crude and even questionable<sup>1)</sup> but common assumption that the effective interaction can be approximated by the sum of the bare reaction matrix  $G$  and the three-particle one-hole ( $3p$ - $1h$ ) core-polarization correction. Within this limited model we want to examine the degree of sensitivity which the low-lying shell-model spectrum exhibits to changes in the off-shell behavior of the free two-nucleon interaction. Is there reason to expect sensitivity?

Using phase-shifts only Elliott et. al.<sup>2)</sup> obtained nuclear structure matrix elements in an oscillator basis which are quite suitable for shell-model calculations. For the most part the diagonal elements compare satisfactorily with those of the bare effective shell-model interaction based on realistic potentials. This fact might suggest that the spectra of nuclei are rather stable under off-shell changes in the nucleon-nucleon interaction. Indeed, Lynch and Kuo<sup>3)</sup> found only minor variations in the  $^{18}\text{O}$  and  $^{18}\text{F}$  spectra when using different potentials. However, they employed only local potentials, i.e. potentials of a similar type. In contrast, the  $^{18}\text{F}$  spectra computed from the non-local Tabakin<sup>4)</sup> and the local Hamada Johnston potential<sup>5)</sup> differ in the low-lying  $1^+$  states substantially<sup>6)</sup> when the same core-excitation corrections are included in the effective interaction. On the other hand, comparing the results of these two potentials is meaningless for the purpose of revealing off-shell effects since the Tabakin potential does not fit the  $^3S_1$ - $^3D_1$  two-body data<sup>7)</sup>. Thus, previous shell-model calculations do not enlighten us about the importance of the off-shell part in the nucleon-nucleon interaction for nuclear spectra.

In this study we perform shell-model calculations for  $^{18}\text{O}$  and  $^{18}\text{F}$  using a variety of non-local potentials which are exactly phase-equivalent with the soft-core Reid potential<sup>8)</sup>. These nonlocal potentials were obtained by Haftel and Tabakin<sup>9)</sup> from the Reid potential by a short-range unitary transformation and have been applied in calculations of nuclear matter<sup>9)</sup> and  $^{16}\text{O}$ <sup>10)</sup>. We select for our calculations from ref. 9) transformations 1 and 6 which act in the  $^1S_0$  partial wave and transformations 8, 10 and 11 which change the  $^3S_1$ - $^3D_1$  partial wave. All untransformed partial waves remain identical with the Reid potential. Those particular transformations were selected because they dramatically alter the off-shell behavior of the Reid potential, though it is very unlikely that the particular non-localities generated by the unitary transformations have any theoretical basis. All calculations were performed with the same

approximations for the effective interaction and with the same computational techniques.

## II. CALCULATIONAL TECHNIQUE

In computing the spectra of  $^{18}\text{O}$  and  $^{18}\text{F}$  we restrict the model space to oscillator states with  $0s_{1/2}$ ,  $0p_{3/2}$  and  $0p_{1/2}$  shells filled and two particles distributed among the valence levels  $0d_{5/2}$ ,  $1s_{1/2}$  and  $0d_{3/2}$ . The experimental single-particle energies are given in Table 1. The residual shell-model interaction is taken to be the reaction matrix  $G(\omega)$  corrected by the  $3p$ - $1h$  core-polarization contribution. Relative-center of mass (RCM) matrix elements of  $G(\omega)$  are calculated according to the method of ref. 11) which is especially suited for non-local potentials. An "angle-averaged" Pauli operator appropriate for shell-model calculations is used. All intermediate states, even the valence states when allowed by the shell-model Pauli operator are taken to be purely kinetic. For the oscillator energy we take  $\hbar\Omega = 14.02\text{MeV}$ . The available energy  $\omega$  in the bare reaction matrix is  $-10\text{MeV}$ . The RCM matrix elements characteristic for the phase-equivalent potentials employed here are listed in Table 2. Untabulated matrix elements for the other partial waves are those of the Reid potential<sup>11)</sup>. For the c.m. variables only a dependence on the combination  $2N+L$  of the oscillator quantum numbers is maintained.

In the core-polarization correction of the effective interaction excitations to the  $3p$ ,  $2f$ , and  $1h$  oscillator orbitals are permitted so that the contributions of all intermediate particle-hole states through  $6\hbar\Omega$  excitation energy are included. These states are assumed to be pure oscillator states in contrast to the purely-kinetic intermediate states used for the reaction matrix. This is not believed to be serious in comparison with the general convergence problems concerning the effective interaction<sup>1)</sup>.

In the reaction matrices needed for core-polarization correction the starting energy has to be shifted by  $1\hbar\Omega$  ( $\omega = -25\text{MeV}$ ) or  $2\hbar\Omega$  ( $\omega = -40\text{MeV}$ ) depending on whether a  $0p$  state core particle or a  $0s$  state core particle is excited. This is done for all results of Section 3 and, as seen in Figure 1, it amounts to a sizeable effect when compared with a calculation of common practice which uses the same starting energy in  $G$  for all higher-order diagrams. In the present study this is significant for two reasons. First, for those partial waves ( $^3S_1$ - $^3D_1$  and  $^1S_0$ ) in which off-shell variations are generated the reaction matrix is strongly  $\omega$ -dependent. The unitary transformations can dramatically change<sup>10)</sup> the wound  $\langle \chi(\omega), n\ell | \chi(\omega), n\ell \rangle = -\langle n\ell | \frac{\partial G(\omega)}{\partial \omega} | n\ell \rangle$  in an oscillator state  $|n\ell\rangle$  of relative motion. We therefore anticipate alterations in this  $\omega$ -dependence. Second, the core-polarization correction of the  $^{18}\text{O}$  ground state is especially sensitive to the  $^3S_1$ - $^3S_1$  matrix elements which usually exhibit the strongest  $\omega$ -dependence. This is shown in Table 3. Interactions with the same  $^3S_1$ - $^3S_1$  matrix elements as the Reid potential but substantial differences in other partial waves yield comparable shifts. Force 8 has less attractive  $^3S_1$ - $^3S_1$  matrix elements than Reid while those for Tabakin are more attractive and this pattern correlates well with the  $^{18}\text{O}$  ground state shift due to core-polarization.

## III. RESULTS AND DISCUSSION

We shall present the results on three levels. First, we discuss the changes of important RCM reaction matrix elements due to unitary transformations. Second, we describe the resulting  $^{18}\text{O}$  and  $^{18}\text{F}$  spectra and third, we discuss the results and compare them with parallel calculations of  $^{16}\text{O}$ .

The unitary transformations yield sizeable changes in the RCM matrix elements as demonstrated in Table 2. Variations are much stronger than believed possible in view of the calculations of Lynch and Kuo<sup>3)</sup> and of Elliott et. al<sup>2)</sup>. We are unable to relate these variations to the para-

meters of the transformations in a transparent way. However, the variations of diagonal elements are accompanied by changes in the corresponding defect wave functions of  $^{16}\text{O}$ . Diminished attraction or augmented repulsion related to a larger wound integral.

A strong state dependence of the changes is to be noted; e.g. transformation 1 removes attraction from the diagonal  $n=0$  and  $n=1$   $^1\text{So}$  matrix elements and adds some to  $n=2$ . A somewhat contrary trend occurs with transformation 6 which induces an especially strong repulsive shift from Reid in the  $n=2$   $^1\text{So}$  element. In the  $^3\text{S}_1 - ^3\text{D}_1$  partial wave transformation 8(10 and 11) only changes the  $\ell_1=0$  ( $\ell_1=2$ ) components of the deuteron and of the two-nucleon scattering wave functions,  $\langle r\ell_1 | \psi^+(k) | \ell_2 \rangle$ , where  $k$  is the momentum of relative motion. As a consequence only the  $\ell_1=0$  ( $\ell_1=2$ ) half-shell elements  $\langle k_1\ell_1 | T(k_2^2 + i0) | k_2\ell_2 \rangle$  of the free-nucleon transition matrix  $T(\omega)$  are changed. According to the dispersion integral<sup>12)</sup>, which connects the off-shell  $T(\omega)$  to its half-shell elements and to the bound-state pole, the  $^3\text{D}_1 - ^3\text{D}_1$  ( $^3\text{S}_1 - ^3\text{S}_1$ ) part of  $T(\omega)$  remains unaltered. Since the reaction matrix differs from  $T(\omega)$  by the Pauli correction only, the negligible shifts in its  $^3\text{D}_1 - ^3\text{D}_1$  ( $^3\text{S}_1 - ^3\text{S}_1$ ) elements arise solely through the propagator modification in the Pauli correction. However, the changes found in the other matrix elements can be quite dramatic. The trend of the variations are the same for the G matrices with starting energies  $\omega = -25$  and  $-40\text{MeV}$ .

Figures 2 and 3 display the calculated  $T=1$  spectra of  $^{18}\text{O}$  and the  $T=0$  spectra of  $^{18}\text{F}$  respectively. The results of force 10 are not presented. They are similar to those of force 11 in that all low-lying levels deviate by no more than  $0.15\text{MeV}$  with three exceptions. For force 10 the first excited  $0^+$  state of  $^{18}\text{O}$  is more bound by  $0.28\text{MeV}$  and the second and third  $1^+$  states of  $^{19}\text{F}$  are more bound by  $0.72$  and  $1.90\text{MeV}$  respectively than for force 11. For comparison we present the experimental spectra and the spectra resulting from the Tabakin potential. We note in passing that the spectra for the Reid and the Tabakin potentials show even larger discrepancies than those mentioned in Section 1 for the Hamada-Johnston and the Tabakin potentials.

For  $^{18}\text{O}$  the differences between the spectra resulting from the untransformed Reid (force 0) and those resulting from forces 8, 10, and 11 are generated solely through core-polarization. The changes are small. The particular strong differences in the RCM matrix elements between forces 8 and 11 do not significantly alter the  $^{18}\text{O}$  spectra. For  $^{18}\text{F}$  forces 1 and 6 affect the spectra only via core-polarization. Except for the third  $1^+$  state in the results of force 1 the level shifts encountered are comparable to those obtained in  $^{18}\text{O}$  with forces 11 and 8.

Transformations 1 and 6 (8 and 11) affect both the bare and the core-polarization contribution to the effective interaction for  $^{18}\text{O}$  ( $^{18}\text{F}$ ). The resulting spectra appear with significant shifts usually beyond those obtained with those forces that affect core-polarization alone. When the transformations are combined to yield the forces labelled 1 + 11 and 6 + 8, the spectra are further shifted from the Reid spectra. We especially note, that the combined force 6 + 8 makes the ground state and the first excited state of  $^{18}\text{O}$  degenerate. For the Reid potential these levels are  $1.40\text{MeV}$  apart. In  $^{18}\text{F}$  force 6 + 8 makes the first  $1^+$  state and the first  $2^+$  state almost degenerate which were separated by  $2.06\text{MeV}$  for the Reid potential. In  $^{18}\text{F}$  forces 1, 11 and 1 + 11 shift the third  $1^+$  level over a range of  $4\text{MeV}$  while leaving the lowest  $1^+$  relatively unchanged. On the other hand, forces 6, 8 and 6 + 8 shift the lowest  $1^+$  over a range of  $2\text{MeV}$  while leaving the third  $1^+$  relatively unchanged. The other states display varying degrees of sensitivity.

Since we use a limited model<sup>1)</sup> for the effective interaction, agreement with experiment would mean little and should not be expected. In fact, the agreement is poor for the Reid potential, especially in  $^{18}\text{F}$ . Furthermore, the off-shell changes studied here push the low-lying levels up in energy, i.e. normally further away from their experimental positions, in both  $^{18}\text{O}$  and  $^{18}\text{F}$ . Increased repulsion is also a consequence of these transformed potentials in nuclear matter<sup>9)</sup> and  $^{16}\text{O}$ <sup>10)</sup>. However the detailed trends have little else in common. A comparison of our results with those for the binding energy of  $^{16}\text{O}$  serves as an example: The loss of energy per particle in  $^{16}\text{O}$  is minor for the forces 6, 8 and 6 + 8 (0.31MeV, 0.06MeV and 0.38MeV respectively). The loss is dramatic for the forces 1, 11 and 1 + 11 (2.00 MeV, 0.98 MeV and 2.76 MeV respectively). In contrast, the  $^{18}\text{O}$  and  $^{18}\text{F}$  spectra are severely affected by the transformations 6, 8 and 6 + 8, but are rather stable under 1, 11 and 1 + 11. The reason is: The changes in the reaction matrix are strongly state-dependent, and the  $^{16}\text{O}$  ground-state and the shell-model states are sensitive to different parts of the reaction matrix;  $^{16}\text{O}$  especially to  $n=0$ ,  $^{18}\text{O}$  and  $^{18}\text{F}$  especially to  $n=1$  and 2 elements. In addition, even the different shell-model states tend to exploit the components of the effective interaction with varying weights. Thus, off-shell effects in the spectra do not simply show up as a displacement of a whole group of levels. The shifts of levels occurs selectively. E.g. the violent changes in the  $^3\text{D}_1$ - $^3\text{D}_1$  matrix elements for forces 10 and 11 are almost unfelt in the low-lying spectra, whereas the comparatively smaller changes in the S waves of forces 6 and 8 have a devastating effect on the same levels. We conclude strong sensitivity of the low-lying  $^{18}\text{O}$  and  $^{18}\text{F}$  spectra with respect to the off-shell behavior of the nucleon-nucleon interaction in the relative S waves. This conclusion contrasts the implications of the works by Lynch and Kuo<sup>3)</sup> and Elliott et. al.<sup>2)</sup>

#### Figure Captions

- Fig. 1 T=1 spectra of  $^{18}\text{O}$  and T=0 spectra of  $^{18}\text{F}$ , The spectra are calculated with the Reid potential using different prescriptions for the starting energy in the reaction matrices for core-polarization. The results are compared with the experimental spectra.
- Fig. 2 T=1 spectra for  $^{18}\text{O}$ . Results for the Reid potential (force 0) and various non-local potentials (labelled as in ref. 9) phase-equivalent with the Reid potential are presented. Also shown are the experimental spectrum and that of the Tabakin potential.
- Fig. 3 T=0 spectra for  $^{18}\text{F}$ . See caption to Fig. 2.

#### Table Captions

- Table 1 Single particle energies of the valence states
- Table 2 RCM G matrix elements in MeV. Matrix elements of the Reid potential are compared as well as those of the Tabakin potential.  $\hbar\Omega = 14.02\text{MeV}$  and  $\omega = -10\text{MeV}$
- Table 3 The shift in calculated ground-state energy of  $^{18}\text{O}$  due to the inclusion of core-polarization in the effective interaction.

#### References

<sup>†</sup>This work supported by funds provided by the Atomic Energy Commission under contract AT(30-1)-2098

1. M. W. Kirson, preprint and references therein.
2. J. P. Elliott, A. D. Jackson, H. A. Mavromatis, E. A. Sanderson and B. Singh, Nucl. Phys. A121 (1968) 241.
3. R. P. Lynch and T. T. S. Kuo, Nucl. Phys. A95(1967)561.



4. D. M. Clement and E. U. Baranger, Nucl. Phys. A108 (1968)27.
5. T. T. S. Kuo, Nucl. Phys. A103(1967)71.
6. E.U. Baranger, Proc. Int. School of Physics Enrico Fermi (1967) Course 40, p.643.
7. P. Signell, Phys. Rev. C2 (1970), 1171.
8. R. V. Reid, Ann. of Phys. 50(1968)411.
9. M.I. Haftel and F. Tabakin, Phys. Rev. C3(1971)921.
10. M. I. Haftel, E. Lambert, F. Tabakin and P. U. Sauer, to be published.
11. P. U. Sauer, Nucl. Phys. A150(1970)467.
12. P. U. Sauer, Nucl. Phys. A170(1971) 497.

		<u>Force</u>	<u>18<sub>0</sub></u>
$\epsilon(0d_{5/2})$	0.0	Reid	-0.82
		1	-0.71
$\epsilon(1s_{1/2})$	0.87	6	-0.87
		8	-0.35
		10	-0.78
$\epsilon(0d_{3/2})$	5.08	11	-0.73
		1+11	-0.62
		6+8	-0.48

Table 1

Table 3

<u>T=0</u>	$\ell$	$\ell'$	n	n'	N	L	Reid	1	6	8	10	11	Tabakin
$^3S_1$	0	0	0	0	2	0	-9.52			-9.52	-9.52	-9.47	-10.43
			1	1	1	0	-6.73			-4.46	-6.70	-6.58	- 8.15
			2	2	0	0	-3.32			2.47	-3.27	-3.07	- 6.20
$^3(S-D)_1$	0	2	1	0	1	0	-2.91			-2.92	-3.24	-4.46	- 2.26
			2	1	0	0	-3.31			-3.43	-4.00	-5.76	- 2.34
$^3D_1$	2	2	0	0	1	0	1.31			1.30	3.63	9.77	3.95
			1	1	0	0	1.46			1.42	5.91	12.91	3.69
<u>T=1</u>													
$^1S_0$	0	0	0	0	2	0	-6.76	-4.92	-6.52				- 7.05
			1	1	1	0	-4.55	-4.47	-3.25				- 4.62
			2	2	0	0	-2.05	-2.82	0.84				- 2.52

Table 2.

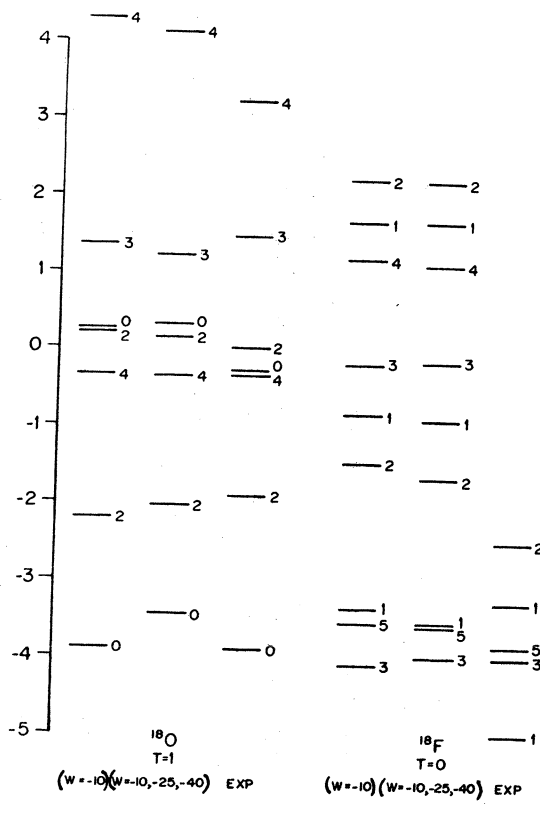


FIG. 1

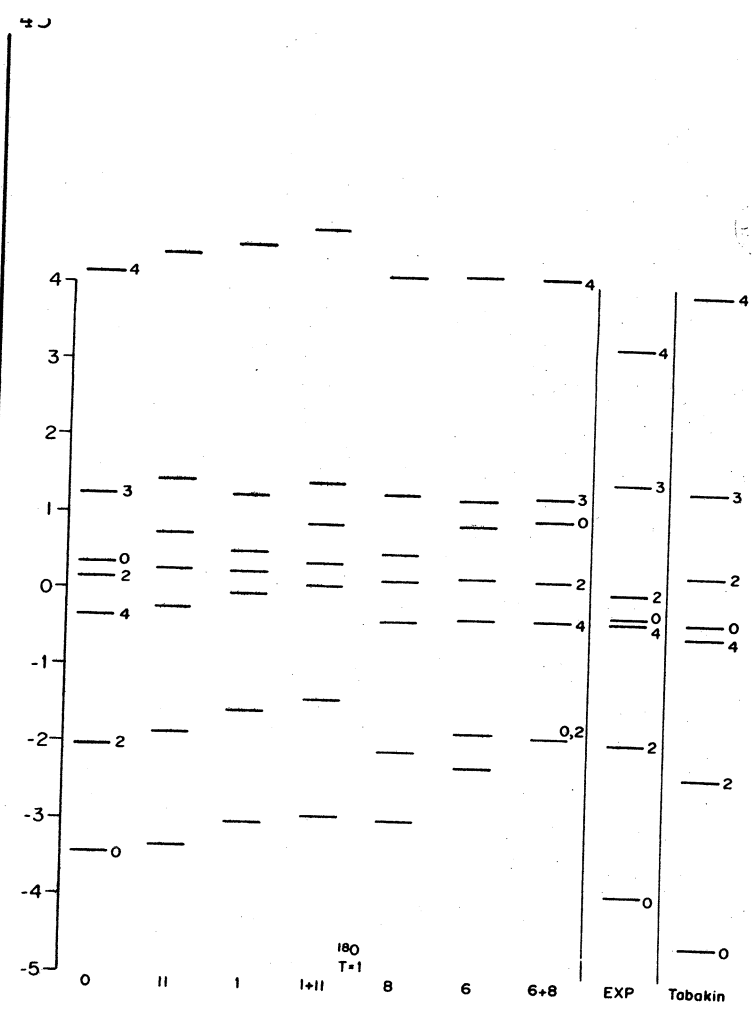


FIG. 2

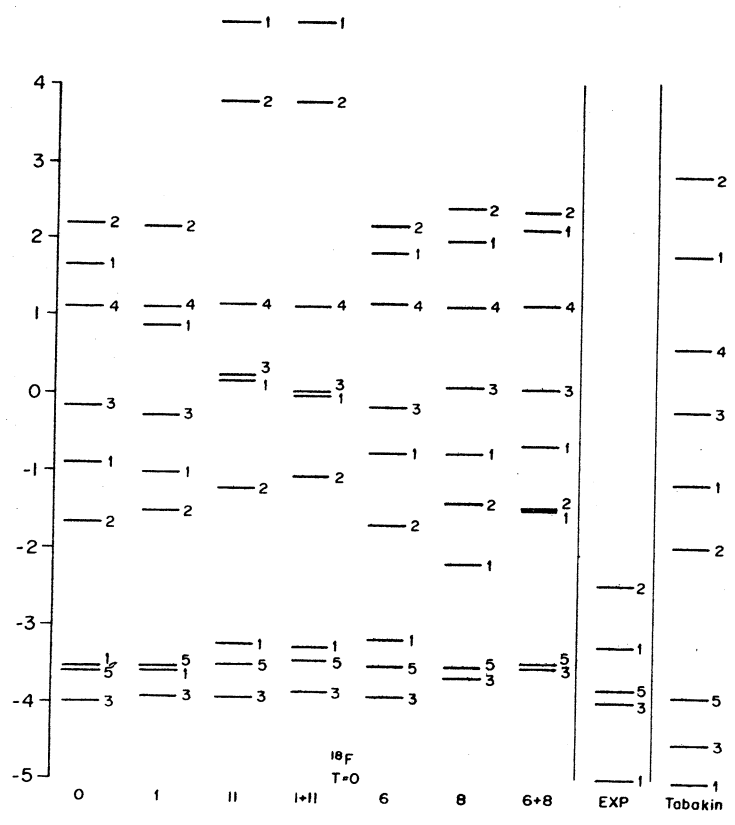


FIG. 3

SOLUTION OF THE BETHE-GOLDSTONE EQUATION  
IN FINITE NUCLEI FROM N-N PHASE  
SHIFT DATA\*.

R.J.W. HODGSON  
Department of Physics  
University of Ottawa  
Ottawa, Canada

Recently, considerable interest has centered around nuclear structure calculations which work directly from the observed free N-N phase shift data, rather than from an intermediate potential model [1, 2, 3, 4]. One of the advantages of this new approach is that it offers a method enabling one to perform some structure calculations without introducing an arbitrary off-energy-shell behaviour. This, together with some recent developments in techniques for performing finite nuclei calculations [5, 6], results in a fresh new approach to the problem which is fast and flexible

We present here an outline of the method used to calculate the reaction matrix in finite nuclei which employs harmonic-oscillator matrix elements which have been determined from the free N-N phase shift data [1, 2]. The technique employed follows from a suggestion of S.T. Butler et al. [5] and the work of Barrett, Hewitt and McCarthy [6].

\* Work supported in part by the National Research Council.

It allows for the exact treatment of the Pauli operator, and for a simple and rapid way of studying the effect of a variation of the intermediate-state energy.

The starting point for our calculation is the dispersion relation for the partial-wave scattering amplitude  $A_\ell(E)$ :

$$A_\ell(E) = b_\ell(E) + \frac{1}{\pi} \int_0^\infty \frac{\text{Im} A_\ell(E')}{E' - E - i\epsilon} dE' + \frac{1}{\pi} \int_{-\infty}^{-\mu^2} \frac{\text{Im}[A_\ell(E') - b_\ell(E')]}{E' - E} dE' + \frac{\Gamma_{\ell 0}^\delta}{E - E_B} \quad (1)$$

Assuming that  $A_\ell(E)$  is known for  $E > 0$  from the experimental results, and making the approximation

$$\text{Im} b_\ell(E) = \text{Im} A_\ell(E), \quad E < -\mu^2 \quad (2)$$

enables one to express the Born approximation term  $b_\ell(E)$  as a function of the phase shift  $\eta_\ell(E)$ . Here  $\mu$  is the pion rest mass.

$$b_\ell(E) \approx \frac{\cos \eta_\ell(E) \sin \eta_\ell(E)}{\sqrt{E}} - \frac{p}{\pi} \int_0^\infty \frac{\sin^2 \eta_\ell(E') dE'}{\sqrt{E'} (E' - E)} \quad (3)$$

Thus, from a knowledge of the phase shifts  $\eta_\ell$ , the Born term can be computed.

Two problems require some further investigation before these results can be used. Experimentally, the phase shifts have only been measured for  $E < 400$  MeV, so that in order to evaluate the integral in (3), some extrapolation must be employed

We have found that the harmonic-oscillator matrix elements are not strongly sensitive to the behaviour of  $\eta_\ell$  at high energies [7], and for the present work, have chosen to set  $\eta = 0$  for  $E > 500$  MeV. In addition, special consideration must be given to the treatment of the bound state [8].

Once  $b_\ell(E)$  has been computed, it is a fairly straight forward procedure to determine the harmonic-oscillator matrix element

$$\langle n\ell | V | n'\ell' \rangle = \int_0^\infty R_{n\ell}(r) V(r) R_{n'\ell'}(r) r^2 dr \quad (4)$$

from a series of recurrence relations [7].

The final step is to employ the matrix elements in (4) to solve the Bethe-Goldstone wave equation

$$\Psi_\alpha^{BG}(\omega) = \phi_\alpha + \sum_\mu \frac{Q_\mu \phi_\mu \langle \phi_\mu | V | \Psi_\alpha^{BG}(\omega) \rangle}{\omega - \epsilon_\mu} \quad (5)$$

where the  $\phi_\alpha$  are eigenfunctions of the two-body harmonic-oscillator Hamiltonian  $H_0$ ,

$$H_0 \phi_\alpha = \epsilon_\alpha \phi_\alpha \quad (6)$$

and  $Q_\mu$  is the eigenvalue of the Pauli projection operator.

Following the suggestion of Butler et al. [5], the BG wavefunction is expanded in terms of the eigenfunctions of the complete two-body Hamiltonian  $H_0 + V$ , so that short range correlations are already incorporated.

That is, we consider

$$\Psi_\alpha^{BG} = \sum_i a_{i\alpha}(\omega) \psi_i \quad (7)$$

where

$$(H_0 + v) \psi_i = E_i \psi_i. \quad (8)$$

Then, as has been shown by Barret et al. [6], the reaction matrix

$$G_{\beta\alpha}(\omega) = \langle \phi_\beta | v | \psi_\alpha^{BG}(\omega) \rangle \quad (9)$$

can be expressed as

$$G_{\beta\alpha}(\omega) = G_{\beta\alpha}^R(\omega) - \sum_{\mu}^{\infty} G_{\beta\alpha}^R(\omega) \frac{1-Q_{\mu}}{\omega-\epsilon_{\mu}} G_{\mu\alpha}(\omega) \quad (10)$$

where

$$G_{\beta\alpha}^R(\omega) = (\epsilon_{\alpha} - \omega) \left[ \delta_{\alpha\beta} - (\epsilon_{\beta} - \omega) \sum_i \frac{b_{i\alpha} b_{i\beta}}{E_i - \omega} \right] \quad (11)$$

Here  $b_{i\alpha}$  is an overlap function defined by

$$b_{i\alpha} = \langle \psi_i | \phi_{\alpha} \rangle \quad (12)$$

Equations (10) and (11) form the basis of our calculation.

The values of  $b_{i\alpha}$  and  $E_i$  are first computed by diagonalizing the matrix

$$\begin{aligned} \langle \phi_{\alpha} | H_0 + V | \phi_{\alpha'} \rangle &= \epsilon_{\alpha} \delta_{\alpha\alpha'} \\ &+ \sum C_{\alpha} [n\ell S\bar{J}N\bar{L};JT] C_{\alpha'} [n'\ell' S\bar{J}N\bar{L};JT] \\ &\times \langle n\ell | V | n'\ell' \rangle \end{aligned} \quad (13)$$

where the  $C_{\alpha} [n\ell S\bar{J}N\bar{L};JT]$  are recoupling coefficients [6].

In addition to using the harmonic-oscillator matrix elements derived from the dispersion relation approach outlined above, we have also used those obtained by the Sussex group [1] who employ a cut-off oscillator potential.

The results have been applied to a calculation of the spectra of the  $A = 18$  nuclei, using the shell model with an inert  $^{16}\text{O}$  core.

Fig. 1 shows the spectra for  $^{18}\text{O}$ , and Fig. 2 that for  $^{18}\text{F}$ .

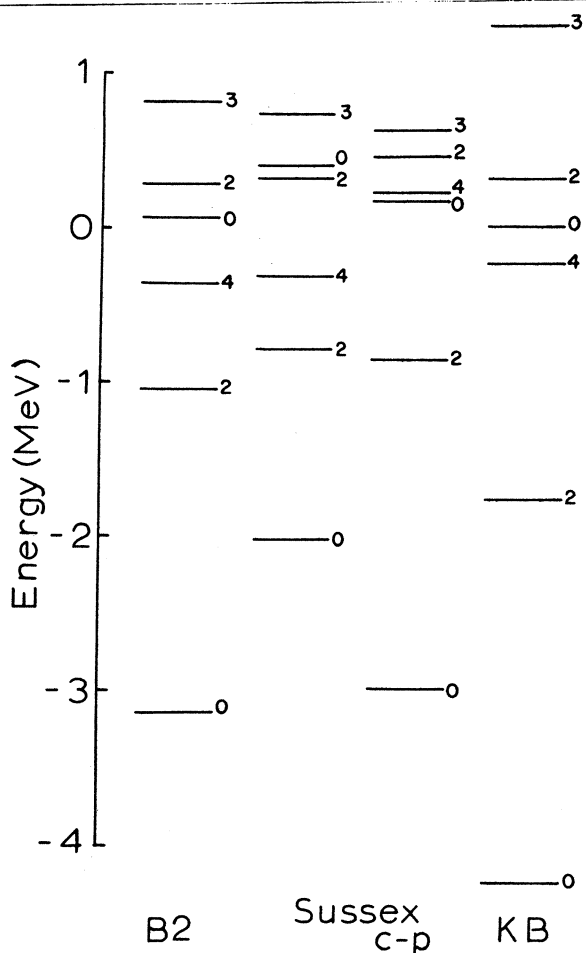


Fig. 1

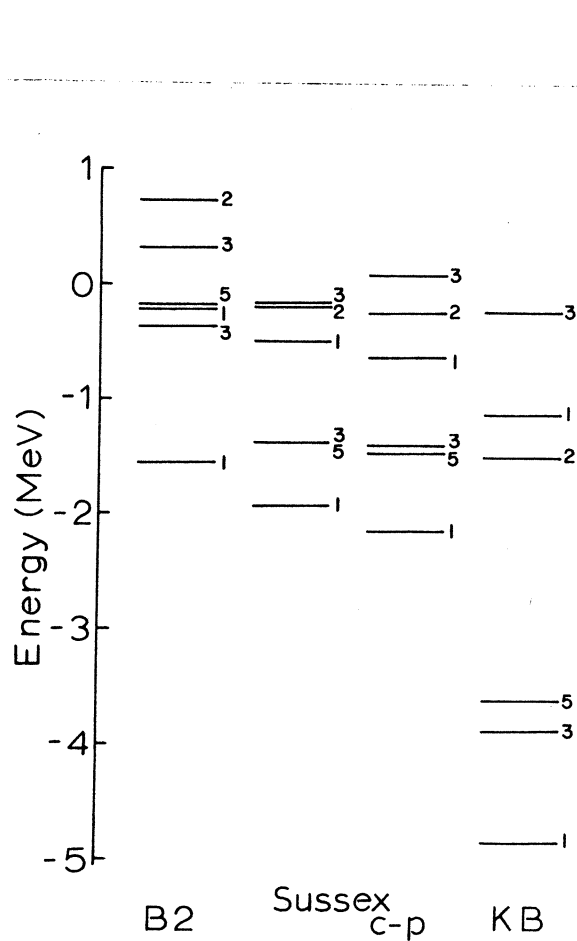


Fig. 2

The calculations were done with  $\omega = 98.0$  MeV, which is approximately self-consistent [6]. The results obtained using the dispersion approximation (3) are labelled B2, and all spectra are compared with the results of Kuo and Brown [9]. The latter include the effects of the core polarization term  $G_{3p1h}$ . We have applied this same correction to the Sussex spectra, and the results are included in both diagrams (c-p).

The results for  $^{18}\text{O}$  are reasonably good, and we intend to examine the effect on the B2 spectra of including  $G_{3p1h}$  shortly. However, the lowest levels of  $^{18}\text{F}$  are underbound by about 3 MeV. This appears to be due to the effective interaction in the  $^3\text{S} - ^3\text{D}$  states, which is quite different than that obtained from realistic potential models [7]. This seems to be caused by a sensitive dependence of the Born term  $b(E)$  on the form of the phase shift near 500 MeV, which is not known experimentally. More work must be done in this area.

#### REFERENCES

1. J.P. Elliott, A.D. Jackson, H.A. Mavromatis, E.A. Sanderson, and B. Singh, Nucl. Phys. A121 (1968), 241.
2. M. Razavy and R.J.W. Hodgson, Nucl. Phys. A149 (1970) 65.
3. E. Ley Koo, M. de Llano, D.V. Grillot, and H. McManus, Nucl. Phys. A133 (1969) 610.
4. P. Ripa and E. Maqueda, Nucl. Phys. A166 (1971) 534.
5. S.T. Butler, R.G.L. Hewitt, B.H.J. McKellar, I.R. Nicholls, and J.S. Truelove, Phys. Rev. 186 (1969) 963.
6. B.R. Barrett, R.G.L. Hewitt, and R.J. Mc Carthy, Phys. Rev. C3, (1971) 1137.
7. R.J.W. Hodgson, Can. J. Phys. 49 (1971) 1401.
8. R.J.W. Hodgson; to be published.
9. T.T.S. Kuo and G.E. Brown, Nucl. Phys. 85 (1966) 40.



## DOES AN EFFECTIVE E2 OPERATOR HAVE A TWO BODY PART?

*F. Khanna & M. Harvey, Chalk River Nuclear Labs, Chalk River, Ont.  
D.W.L. Sprung & A. Jopko, McMaster University, Hamilton, Ontario*

The question of calculating the effective charge for E2 transitions has been quite annoying to the theoretical physicists. In recent years a general theory for the effective transition operators as needed in the nuclear shell model has been formulated. (*Brandow, Rev. Mod. Phys.* 39(1967)771; *Harvey & Khanna, Nucl. Phys.* A152(1970)588; *Nucl. Phys.* A155(1970)337, & *Khanna, Lee & Harvey, Nucl. Phys.* A164(1971)612; the last ref. contains a complete list of references). Several calculations have been done to estimate the effective charge for one-particle or one-hole nuclei near a closed shell. There has only been some mild success in getting quantitative results for E2 transitions in A=17 and A=15 systems. Using realistic nuclear forces and a partial summation to include RPA diagrams has led to a fair agreement with experiments. However in the region of  $^{40}\text{Ca}$ , the RPA calculations have shown some instabilities which are discussed in the paper by Khanna et al.

In this communication we would like to ask whether the transition rates in A=18 system can be quantitatively estimated by including only the effective charge calculated for A=17 system with small corrections due to Pauli exclusion principle. Benson & Flowers (*Nucl. Phys.* A126(1969)332) have observed that in calculating the E2 transition rates in A=18

system with Saxon-Woods functions, the transitions between  $T=1$  states require an effective charge of 0.5 - 0.7 while the transition rates between  $T=0$  states require no effective charge. This observation suggests some special property about the core polarisation effects for  $T=1$  and  $T=0$  states. To understand the nature of this property we have calculated the two-body part ( $\tilde{t}_2$ ) of the E2 operator to look for features that will lead to a cancellation for  $T=0$  states but will give enhancement for  $T=1$  states. We have used two separate approaches for this study.

a) We have parametrised the coupling operator ( $v_{21}$ ) as

$$v_{21} = -\kappa Q_2 \cdot Q_2 [A^{31}, A^{13}, A^{33}, A^{11}], \quad Q_2 = 4 \sqrt{\pi/5} r^2 Y^2$$

and  $A^{2T+1, 2S+1}$  are exchange parameters. Estimating these parameters from the effective charge in  $^{17}\text{O}$ ,  $^{17}\text{F}$ ,  $^{15}\text{O}$  and  $^{15}\text{N}$ , we found that the matrix elements of  $\tilde{t}_2$  were as large as  $\sim 40\%$  of the matrix elements for the one-body part ( $\tilde{t}_1$ ) of the effective E2 operator. There are three relevant observations: (i) for  $T=1$  states the contributions from  $\tilde{t}_1$  and  $\tilde{t}_2$  are in phase; (ii) for  $T=0$  states  $\tilde{t}_1$  and  $\tilde{t}_2$  give contributions that are in-phase or out-of-phase depending on the details of the structure of the states and (iii) for  $T=1$  states  $\tilde{t}_2$  gave large enough contributions to bring  $B(E2; 2^+ \rightarrow 0^+)$  in  $^{18}\text{O}$  and  $^{18}\text{Ne}$  into fair agreement with experiment ( $^{18}\text{O}: 825 (8.8) e^2 \text{fm}^4$ ,  $^{18}\text{Ne}: 69 \pm 16 (65) e^2 \text{fm}^4$ , the bracketed numbers are calculated).

b) The large magnitude of the two-body effect with a simple parametrisation of  $v_{21}$  suggested that a detailed

calculation with realistic interactions is needed to establish the presence of  $\tilde{t}_2$  in the E2 transition rates. We have constructed the reaction matrix for a non-local separable potential (Kahana, Lee & Scott, *Phys. Rev.* 180(1969)956) and for a phase equivalent potential (Sprung). Then we have renormalised the reaction matrix elements by including (i) one bubble, (ii) TDA series and (iii) RPA series. Using these three different sets of reaction matrix elements we have calculated the matrix elements of  $\tilde{t}_2$ . The following observations can be made with regard to the two body part of the E2 operator:

- i) For transitions between T=1 states, the matrix elements of  $\tilde{t}_1$  and  $\tilde{t}_2$  are generally in phase and E2 transitions for low lying states are enhanced by 10-15%. However for some matrix elements the two body part is quite large (and even of opposite sign), for example
 
$$\langle 2S_{1/2} \ 1d_{3/2} \ J=1 \ || \tilde{t}_2 || 2S_{1/2} \ 1d_{5/2} \ J=3 \rangle$$

$$= -1.285 \langle 2S_{1/2} \ 1d_{3/2} \ J=1 \ || \tilde{t}_1 || 2S_{1/2} \ 1d_{5/2} \ J=3 \rangle$$
 with RPA renormalised G-matrix elements. The net result is that the B(E2) will be reduced by a factor of  $\sim 12$ .
- ii) For transitions between T=0 states, the matrix elements of  $\tilde{t}_1$  and  $\tilde{t}_2$  are out of phase in general.
- iii) In the calculation of the effective charge it was observed that in going from one-bubble to TDA to RPA renormalised G-matrix elements, the effective charge increased steadily. But for the matrix elements of  $\tilde{t}_2$  no such regularity has been observed. Actually many of

the matrix elements of  $\tilde{t}_2$  have smaller magnitude (and even opposite signs) for RPA than for one-bubble re-normalised reaction matrix elements. This indicates that the off-diagonal matrix elements of  $v_{21}$  are substantially different from the bare reaction matrix elements and this will have implications with regard to the exchange character of the effective interaction.

- iv) the magnitudes of the matrix elements of  $\tilde{t}_2$  are quite similar for the two different potentials.

From the study of the effective operators with realistic interactions, it appears that the two body part of the effective E2 operator can be quite large as compared to the one body part of effective E2 operator. It can perhaps give some dramatic effects like the sharp decrease in the effective charge needed for  $^{18}\text{F}$ . This really brings us to the important question as to the behaviour of the effective charge as we move away from the closed shell nuclei. In s-d shell an interesting case will be a study of the E2 transitions in  $^{20}\text{Ne}$  which we are undertaking presently.

Recently Forster, Davies & Ball at Chalk River have measured  $B(\text{E}2; 2^+ \rightarrow 0^+)$  in  $^{42}\text{Ti}$  and its magnitude is  $\sim 200 e^2 \text{fm}^4$ . This cannot be reconciled with a corresponding  $B(\text{E}2)$  of  $81 e^2 \text{fm}^4$  in  $^{42}\text{Ca}$ . As in the  $A=18$  system, there is a strong suggestion that the two body part of the E2 operator is large. There are complications in this region due to the presence of deformed 4p-2h components (*Flowers & Skouras, Nucl. Phys.*

A136(1969)353). We are presently doing calculations with renormalised realistic reaction matrix elements to compare the contributions of the two-body and the one-body part of the effective E2 operator.

Comments on the Isospin Dependence of the Two-Body  
Effective Interaction as Deduced from Nuclear Spectra\*

W. A. Lanford

Nuclear Structure Research Laboratory  
University of Rochester  
Rochester, New York 14627

A multipole expansion of the two-body effective interaction in the  $h_{9/2} \times 2f_{7/2}$  and  $h_{9/2} \times i_{13/2}$  shell model configurations has been made using recent data on the proton-proton and proton-neutron (hole) multiplets in  $^{210}\text{Po}$  and  $^{208}\text{Bi}$ . The experimental multipoles have been compared with the multipoles of charge independent scalar interactions. It is seen that an interaction of the form  $V_{12} = V_0(1 + 1/10\sigma_1 \cdot \sigma_2) \exp[-r/r_0]^2 - V_0^\tau 1/2(1 + \tau_1 \tau_2)$  gives good agreement with the data.

Recent studies of stripping<sup>1)</sup> and pickup<sup>2)</sup> reactions on  $^{209}\text{Bi}$  have identified two particle weak coupling multiplets corresponding to  $\pi h_{9/2} \times \pi 2f_{7/2}$ ,  $\pi h_{9/2} \times \pi i_{13/2}$ ,  $\pi h_{9/2} \times (\nu 2f_{7/2})^{-1}$ , and  $\pi h_{9/2} \times (\nu i_{13/2})^{-1}$  shell model configurations. From the excitation energies of members of these multiplets, the matrix elements of the effective nucleon-nucleon interaction ( $V_{12}$ ) in the  $h_{9/2} \times 2f_{7/2}$  and  $h_{9/2} \times i_{13/2}$  configurations can be extracted using perturbation theory. The zero and one body energy contributions can be subtracted using the binding and single particle energies of the adjacent nuclei, and the Coulomb energy contributions can be removed by calculation.

The isospin of the pair of nucleons in the two proton configurations is  $T=1$ . The proton (particle)-neutron (hole) pairs have mixed isospin in that their particle-particle matrix ele-

\*Work supported by National Science Foundation.

ments obey:

$$E(j_1, j_2, J) = 1/2(E(j_1, j_2, J, T=0) + E(j_1, j_2, J, T=1)) \quad (j_1 \neq j_2) \quad (1)$$

where  $E(j_1, j_2, J)$  is the p-n matrix element of  $V_{12}$  and  $E(j_1, j_2, J, T)$  is the matrix element with definite isospin.

Shown in Fig. 1 are the experimentally observed matrix elements of  $V_{12}$  in these configurations. The  $T=0$  matrix elements are obtained from the p-n and the  $T=1$  matrix elements by using Eq. (1). Note that the  $T=0$  matrix elements are large and negative (attractive) while the  $T=1$  are small and, on the average, positive. The dispersion of the  $T=1$  matrix elements is also much less than the dispersion of the  $T=0$ . Also note that both the  $T=0$  and  $T=1$  matrix elements have the same general dependence on  $J$ . In fact, their dependence on  $J$  is similar to that of the p-n matrix elements studied by Moinester et al.<sup>3)</sup> and Schiffer<sup>4)</sup>.

In order to understand what sorts of simple interactions are consistent with these data, it is convenient to make a multipole expansion on  $V_{12}$  in Racah unit tensors in the product space of angular momentum and isospin. Following the work of Moinester et al.<sup>3)</sup>, we expand

$$V_{12} = \sum_{k\tau} [j_1 j_2 k]^{1/2} [\tau] \alpha^{k\tau} (u^{k\tau}(1) \cdot u^{k\tau}(2)) \quad (2)$$

where  $u^{k\tau}$  is the unit tensor in the direct product space of  $j$  and  $t$ . One can evaluate matrix elements of  $V_{12}$  to get an expression for  $E(j_1, j_2, J, T)$  in terms of the  $\alpha^{k\tau}$ . This expression can be inverted to give  $\alpha^{k\tau}$  in terms of the  $E(j_1, j_2, J, T)$ . (See Ref. 3.) Hence, one has the means of evaluating the multipole moments of

the effective interaction from the experimental matrix elements or some calculated matrix elements. To compare multipoles of  $V_{12}$  from different configurations, it is convenient to normalize these multipoles by dividing all the  $\alpha^{k\tau}$  by one of the larger multipoles. (We will use  $\alpha^{20}$ .) By doing this, one obtains a set of normalized multipole coefficients which is approximately independent of the particular two particle configuration.

This multipole analysis has been carried out for the  $h_{9/2} \times 2f_{7/2}$  and  $h_{9/2} \times i_{13/2}$  configurations, and the results were compared with the multipoles of charge independent scalar interactions of the form:  $V_{12}=V_0 \exp[-(r/r_0)^2]$ ,  $V_{12}=V_0 \tau_1 \cdot \tau_2 \exp[-(r/r_0)^2]$ ,  $V_{12}=V_0 \sigma_1 \cdot \sigma_2 \exp[-(r/r_0)^2]$  and  $V_{12}=V_0 \sigma_1 \cdot \sigma_2 \tau_1 \cdot \tau_2 \exp[-(r/r_0)^2]$  with  $r_0=0.8f$ . The results of this analysis are shown in Fig. 2. The averaged normalized multipoles are plotted as dots with error bars representing the differences in the normalized multipoles from the two configurations as well as some uncertainties in the spin assignments in the spectrum of  $^{210}\text{Po}$ . The curves are the calculated multipoles, which are representative of both the  $h_{9/2} \times 2f_{7/2}$  and  $h_{9/2} \times i_{13/2}$  configurations since the differences are small. Note that the pure Wigner interaction gives rather good agreement with the data. This interaction qualitatively reproduces the trends in the experimental multipoles, but misses some of the low order multipoles.

The most general charge independent scalar interaction can be any linear combination of these four interactions. Also shown



in Fig. 2 are some particular combinations:  $V^{\text{Rosenfeld}} = 1/3 V_0 (\tau_1 \cdot \tau_2) (0.3 + 0.7 (\sigma_1 \cdot \sigma_2)) V(r)$ ,  $V^{\text{Serber}} = V_0 (1 - 1/4 (1 + \tau_1 \tau_2) (1 + \sigma_1 \cdot \sigma_2)) V(r)$ , and one combination suggested by this data  $V_{12} = V_0 (1 + 1/10 \sigma_1 \cdot \sigma_2) V(r)$ , where again  $V(r) = \exp[-(r/r_0)^2]$  with  $r_0 = 0.8f$ . Note that both the Rosenfeld and Serber interactions give only qualitative agreement; neither agrees better than a pure Wigner. However, the interaction  $V_{12} = V_0 (1 + 1/10 \sigma_1 \cdot \sigma_2) \exp[-(r/r_0)^2]$  gives good agreement, except for the monopole moments ( $\alpha^{\circ\tau}$ ). This discrepancy in the  $\alpha^{\circ\tau}$  can be removed by adding a long ranged, isospin dependent interaction  $V_{12} = -V_0^{\tau} 1/2 (1 + \tau_1 \cdot \tau_2)$ , which will affect the  $\alpha^{\circ\tau}$  but none of the higher order coefficients. Hence, one interaction which reproduces the experimental results is of the form

$$V_{12} = V_0 (1 + 1/10 \sigma_1 \cdot \sigma_2) \exp[-(r/r_0)^2] - V_0^{\tau} 1/2 (1 + \tau_1 \cdot \tau_2) \quad (3)$$

with  $r_0 = 0.8f$ . This particular admixture is not necessarily the only combination which will give agreement, but it is one obvious admixture which follows from the results in Fig. 2, almost by inspection.

It should be pointed out that, while all these calculations were carried out with  $r_0 = 0.8f$ , the general features of the calculated multipoles are not very sensitive to the exact value. This particular range is the one which gives best agreement with this data for an effective interaction of the form of Eq. (3).

There is one other case where a complete set of matrix elements (both  $T=0$  and  $T=1$ ) is available from nuclear spectra, and that is the  $d_{3/2}^{-1} \times f_{7/2}$  particle-hole spectrum of  $^{40}\text{Ca}^{51}$ . It

was pointed out by Moinester et al.<sup>3)</sup> that this spectrum is fit reasonably well with a short range Wigner interaction with a small spin dependent term, except that the monopole moments are not given correctly. But the long ranged, isospin dependent term of Eq. (3) is just what is necessary to correct for this discrepancy with  $V_0^\tau \approx 1$  MeV.

An interaction of the form of Eq. (3) has a number of interesting features. For example, the parameters  $V_0$  and  $V_0^\tau$  appear to be approximately constant for a given nuclear well. If one fixes  $V_0$  by fitting the  $h_{9/2} \times (2f_{7/2})^{-1}$  multiplet in  $^{208}\text{Bi}$  and then calculates the spectrum of  $^{210}\text{Po}$ , one gets a r.m.s. deviation between experiment and theory of less than 50 keV for the 20 lowest known levels. (The zero and one-body energies were taken from the binding and single particle energies of neighboring nuclei and  $V_0^\tau$  was set at 225 keV.) Also, an interaction of this form agrees with all the known p-n weak coupling spectra<sup>3,4)</sup>; the isospin dependent term has no effect on the p-n matrix elements, and the value of  $r_0 = 0.8f$  gives as good agreement as does the value of  $r_0 = 0.0f$  used in Refs. 3 and 4.

---

#### References

1. W.A. Lanford, W.P. Alford and H.W. Fulbright (to be published).
2. W.P. Alford, J.P. Schiffer and J.J. Schwartz, Phys. Rev. C3 (1971) 860.
3. M. Moinester, J.P. Schiffer and W.P. Alford, Phys. Rev. 179 (1969) 984.
4. J.P. Schiffer, Preprint for the de-Shalit memorial issue of Annals of Physics (1970).
5. J.R. Erskine, Phys. Rev. 135 (1964) B110.

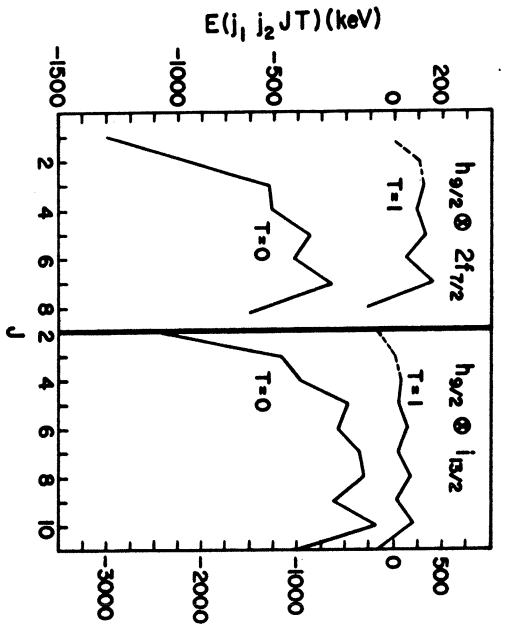
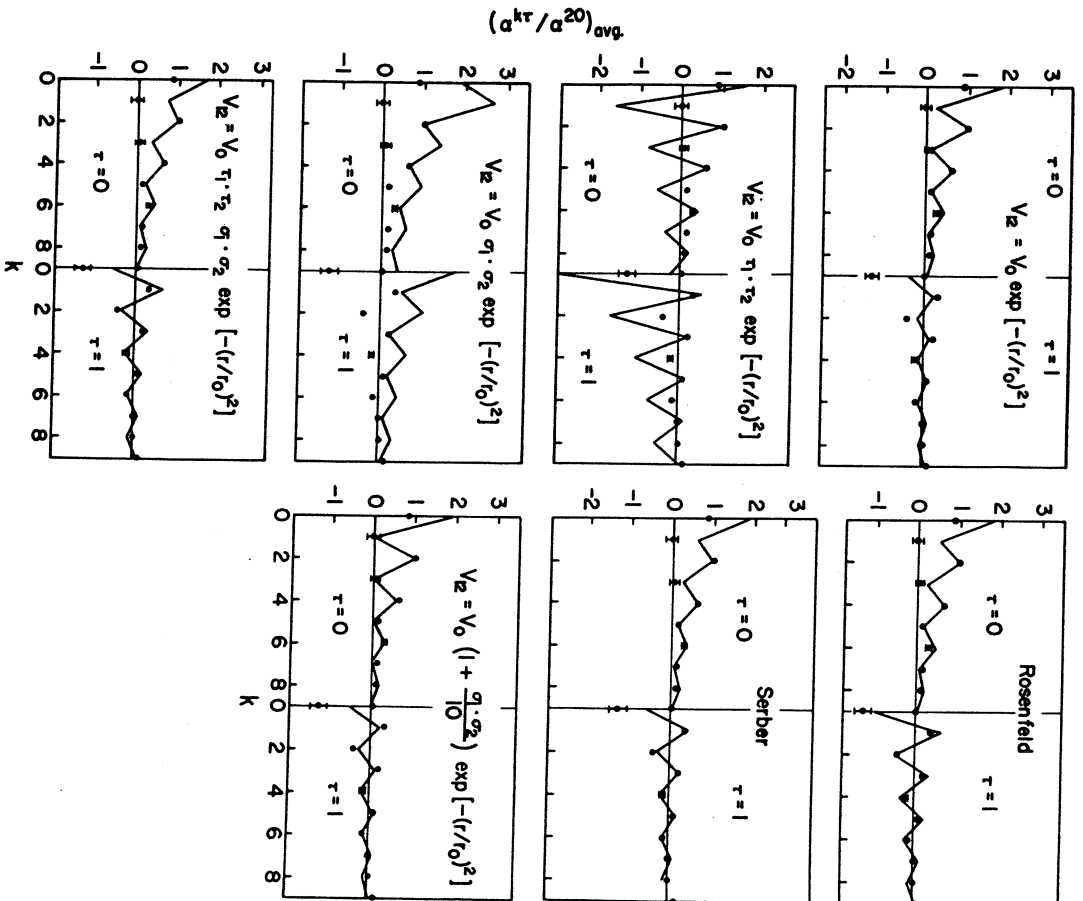


Fig. 1 The experimentally observed matrix elements  $E(j_1, j_2, J, T)$  vs.  $J$ . The dotted lines are possible assignments.

Fig. 2 The average experimental multipoles  $(\alpha^{kr}/\alpha^{20})_{avg}$  plotted as dots. The curves are the multipoles of the interactions indicated.



# Experimental Evidence of the Goodness of Seniority in $j=9/2$ Orbits\*

W. A. Lanford

Nuclear Structure Research Laboratory  
University of Rochester, Rochester, New York 14627

The goodness of the seniority quantum number in the  $g_{9/2}$ ,  $h_{9/2}$ , and  $2g_{9/2}$  shell model orbits has been investigated by checking the mixing of the  $(9/2)^3 J=9/2 v=1$  and the  $(9/2)^3 J=9/2 v=3$  states. This mixing is calculated to be less than 1/10 of one percent. An upper limit of 3% on this mixing in the  $g_{9/2}$  orbit has been set by  $^{92}\text{Mo}(^4\text{He}, t)^{93}\text{Tc}$  and  $^{92}\text{Mo}(^3\text{He}, d)^{93}\text{Tc}$  reactions. A residual interaction which exactly preserves seniority is seen to give two-body matrix elements which have a r.m.s. deviation from the experimental spectra of less than 16 keV for the present cases.

The relevant theoretical information concerning the goodness of seniority is conveniently summarized by the following theorem<sup>1)</sup>:

If seniority is preserved in the  $(j)^3$  configuration and if the Hamiltonian is at most a two-body operator, then seniority is preserved in  $(j)^n$  configurations.

From this theorem it follows that seniority is automatically good for arbitrary two-body interaction in  $(j \leq 7/2)^n$  since for  $(j \leq 7/2)^3$  configurations there are no two states with the same total angular momentum but different seniorities. The fact that seniority is preserved in  $(j \leq 7/2)^n$  has been known for some time; we introduce the subject in this way because the above theorem can be generalized and used to investigate other group symmetries.

Hence, the question of the goodness of seniority first becomes interesting for  $j=9/2$  orbits. For the  $(9/2)^3$  configuration there are two states with the same total angular momentum

---

\*Work supported by the National Science Foundation.

but different seniorities:  $|(9/2)^3 J=9/2 v=1\rangle$  and  $|(9/2)^3 J=9/2 v=3\rangle$  where  $J$  is the total angular momentum and  $v$  is the seniority. A useful corollary to the above theorem is<sup>4)</sup>:

If the Hamiltonian is at most a two-body operator, then in  $(9/2)^n$  all the off-diagonal matrix elements (in seniority) are proportional to  $\langle (9/2)^3 J=9/2 v=1 | H | (9/2)^3 J=9/2 v=3 \rangle$ .

In order to have a reasonable measure of the goodness of the seniority, we define the following "seniority admixing" parameter:

$$\Delta^2 = \left\{ \frac{\langle (9/2)^3 J=9/2 v=1 | H | (9/2)^3 J=9/2 v=3 \rangle}{E((9/2)^3 J=9/2 v=1) - E((9/2)^3 J=9/2 v=3)} \right\}^2$$

where  $E((j)^n_J v) = \langle (j)^n_J v | H | (j)^n_J v \rangle$ . This quantity is dimensionless, it is zero when seniority is exactly preserved in a shell, and it is of order unity when seniority is badly mixed. For small admixtures one sees from perturbation theory that  $\Delta^2 =$  the intensity of admixture of the  $|(9/2)^3 J=9/2 v=1\rangle$  and  $|(9/2)^3 J=9/2 v=3\rangle$  states.

One procedure we used to evaluate  $\Delta^2$  was to find  $(9/2)^2$  spectra in nuclei and to use the fractional parentage expansion to evaluate  $\Delta^2$ . The low-lying states of  $^{90}\text{Zr}$ <sup>5)</sup> and  $^{92}\text{Mo}$ <sup>6)</sup> are believed to be predominantly  $(1g_{9/2})^2$  proton states. There is evidence that the  $0^+$  states are not pure  $(1g_{9/2})^2$ , but this is of little consequence since  $\langle (9/2)^3 J=9/2 v=1 | H | (9/2)^3 J=9/2 v=3 \rangle$  does not depend on the energy of any  $0^+$  state. The low-lying spectra of two identical particles outside  $^{208}\text{Pb}$  are also  $(9/2)^2$  spectra:  $(1h_{9/2})^2$  for protons<sup>7)</sup> and  $(2g_{9/2})^2$  for neutrons.<sup>8)</sup> The results of a calculation of  $\Delta^2$  using these spectra are shown in Table I. Note that in all cases the seniority is very good;

the intensity of admixture is less than about 1/10 of one percent in all cases.

A second way to look at the same data is to see how much the experimental spectra deviate from those  $(9/2)^2$  spectra which would imply exact seniority conservation. To answer this, the minimum root-mean-squared deviation between the experimental spectra and the spectra produced by an interaction which exactly preserves seniority was calculated. The results of this calculation are also shown in Table I. In all cases the experimental spectra deviate only a few keV from seniority preserving ones.

These results indicate that seniority is a very good quantum number. However, they rely on observing  $(9/2)^2$  spectra and calculating the mixing of seniority in  $(9/2)^3$ . It seems worthwhile to try to make a more direct measurement of  $\Delta^2$ , one which does not rely sensitively on calculated matrix elements. One way to do this is to study a stripping reaction on a  $(9/2)^2$   $J=0$   $v=0$  target and to measure the ratio of the cross sections to the two  $(9/2)^3$   $J=9/2$  states. (Even if there are admixtures in the ground state, the  $(9/2)^2$  component will have  $v=0$ , and all the results still follow.) If seniority is not preserved in the shell, the wave functions of these two states can be written, with  $\Delta \neq 0$ :

$$\begin{aligned} |a\rangle &= |(9/2)^3 J=9/2 v=1\rangle + \Delta |(9/2)^3 J=9/2 v=3\rangle \\ |b\rangle &= |(9/2)^3 J=9/2 v=3\rangle - \Delta |(9/2)^3 J=9/2 v=1\rangle \end{aligned}$$

Since a direct reaction must obey the seniority selection rule  $\Delta v = \pm 1$ , only the  $v=1$  components of the  $(9/2)^3$  configuration can be populated. Hence, the direct reaction cross-sections to states

$|a\rangle$  and  $|b\rangle$  are:  $(\frac{d\sigma}{d\Omega})_a = N' (\sigma)_{DW}^L$  and  $(\frac{d\sigma}{d\Omega})_b = \Delta^2 N' (\sigma)_{DW}^L$  where  $N'$  is a constant and  $(\sigma)_{DW}^L$  is the distorted wave cross-section. So by measuring the ratio of the cross-sections to states  $|a\rangle$  and  $|b\rangle$ , one has a method of determining  $\Delta^2$  which depends only on some limited DWBA assumptions and does not rely on calculated matrix elements.

In order to make such a measurement, the  $^{92}\text{Mo}(\alpha, t)^{93}\text{Tc}$  and  $^{92}\text{Mo}(^3\text{He}, d)^{93}\text{Tc}$  experiments were performed with  $E_\alpha = 30$  MeV and  $E_{^3\text{He}} = 20$  MeV.<sup>11)</sup> As mentioned above, the  $^{92}\text{Mo}$  ground state is believed to be largely  $(1g_{9/2})^2_{J=0} v=0$ . The ground state of  $^{93}\text{Tc}$  is known to be  $9/2^+$ , but the excited  $9/2^+$  level has not been identified. Ideally, one would like to locate the excited  $9/2^+$  state, then use the  $^{92}\text{Mo}(\alpha, t)^{93}\text{Tc}$  or  $^{92}\text{Mo}(^3\text{He}, d)^{93}\text{Tc}$  reaction to find the  $L=4$  strength of the transition to that level, then calculate  $\Delta^2$ . In the present case that procedure was not followed. Instead, the position of the  $v=3$  state was estimated by means of a shell model calculation<sup>12)</sup> believed reliable to within a few hundred keV. (This calculation gives  $E(J=9/2 v=3) = 1.94$  MeV.) Then the strongest of all transitions possibly with  $L_{\text{Trans}}=4$  observed forming any state within one MeV of the predicted level was used as a basis for calculating  $\Delta^2$ . Thus, an upper limit was obtained. The analysis of the  $^{92}\text{Mo}(\alpha, t)^{93}\text{Tc}$  and  $^{92}\text{Mo}(^3\text{He}, d)^{93}\text{Tc}$  spectra identifies the transition to a state at 2.14 MeV as the strongest transition which possibly has  $L=4$  to any state below 3 MeV, except the ground state. Using the ratio of the cross-section

to this state at 2.14 MeV to the ground state cross-section and the DWBA calculation of  $(\sigma)_{DW}^{L=4}(E=0)/(\sigma)_{DW}^{L=4}(E=2.14)$ , one gets an upper limit on the intensity of admixing of the  $v=1$  and  $v=3$  states of  $\Delta^2 \leq 0.03$ .

Finally, we would like to make a few remarks about what the conservation of seniority implies. For an arbitrary two-body interaction in  $(9/2)^n$  configurations, there is no simple relation between the  $(9/2)^m$  and  $(9/2)^{m+2}$  spectra. In general, one must construct the wave functions, calculate the Hamiltonian matrix in terms of the two-body matrix element, and diagonalize. However, if seniority is good, the states of the same seniority in  $(9/2)^m$  and  $(9/2)^{m+2}$  have the same spectra since, by assumption, there are no off diagonal matrix elements in seniority. A good experimental example of this effect is the comparison of the  $(9/2)_{v=0,2}^2$  spectrum of  ${}_{42}^{92}\text{Mo}_{50}$  and the low-lying states of  ${}_{44}^{94}\text{Ru}_{50}$ , which should be  $(9/2)^4$  states. If seniority is good, there should be the same  $v=0$  and 2 spectra in both nuclei. As can be seen in Fig. 1, the low-lying spectra of these nuclei are almost identical.

#### References

1. J. B. French (private communication).
2. B. H. Flowers, Proc. Roy. Soc. A212 (1952) 248.
3. C. Schwartz and A. de-Shalit, Phys. Rev. 94 (1954) 1257.
4. J. B. French, Nucl. Phys. 15 (1960) 393.
5. C. M. Lederer, J. M. Hollander and I. Perlman, Table of Isotopes, Sixth Ed. (Wiley, New York, 1967).
6. J. K. Dickens, E. Eichler, R. J. Silva and I. R. Williams, Phys. Letters, 21 (1966) 657.



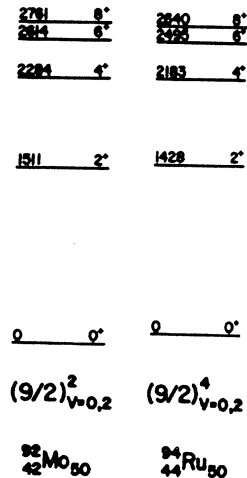
7. W. A. Lanford, W. P. Alford and H. W. Fulbright (to be published).
8. J. H. Bjerregaard, O. Hansen, O. Nathan, L. Vistisen, R. Champan and S. Hinds, Nucl. Phys. A113 (1968) 484.
9. I. Talmi and I. Unna, Nucl. Phys. 19 (1960) 225.
10. W. A. Lanford, Phys. Letters, 30B (1969) 213.
11. W. A. Lanford and H. W. Fulbright (to be published).
12. N. Auerbach and I. Talmi, Nucl. Phys. 64 (1965) 458.
13. J. M. Jaklevic, C. M. Lederer, and J. M. Hollander, Phys. Letters 29B (1969) 179.

Table I

Nucleus	Orbit	$\langle V=1 H V=3 \rangle$	$\Delta^2 \text{ } \frac{a}{8}$	$\sigma_{\text{rms}}^a$
$^{90}\text{Zr}$	$1g_{9/2}$	- 30 keV	.03	12 keV
$^{92}\text{Mo}$	$1g_{9/2}$	-23	.02	9
$^{210}\text{Po}$	$1h_{9/2}$	40	.10	16
$^{210}\text{Pb}$	$2g_{9/2}$	18	.04	7

a) Some of these results have been previously reported; see references 9 and 10.

Fig. 1 Comparison of the low lying  $0^+$ ,  $2^+$ ,  $4^+$ ,  $6^+$ ,  $8^+$  states of  $^{92}\text{Mo}$  and  $^{94}\text{Ru}$ .  
From reference 13.



PROBLEMS OF SD-SHELL CALCULATIONS FOR  $^{24}\text{Mg}$ 

P. Manakos

Institut für Theoretische Kernphysik  
der Technischen Hochschule Darmstadt, Germany

One is encountered with some difficulties when attempting to reproduce the low energy spectrum of  $^{24}\text{Mg}$  by means of sd-shell configuration mixing calculations. We discuss these problems here in some detail especially in conjunction with the supermultiplet and SU(3) classification scheme. We concentrate our attention on two problems: the truncation of vector space and the SU(3) purity of the calculated state vectors.

First we look for a useful truncation recipe in the framework of the above mentioned SU(6)-SU(3) classification scheme. Previous calculations including states of orbital symmetry  $[44]^{1)}$  or  $[44]$  and  $[431]^{2)}$  do not reproduce the density of the spectrum. Therefore one has to examine whether a different truncation can possibly modify the spectrum. In the reported work we have used essentially the diagonal matrix elements of the interaction in the SU(6)-SU(3) classified basis as a criterion for the states to be included in the calculation. The precise prescription is as follows. Eight-nucleon configurations in the sd-shell are classified with the help of quantum numbers  $[\lambda]$ ,  $(\lambda, \mu)$ , L, S, T, J (i.e. symmetry class, SU(3) representation, orbital angular

momentum, spin, isotopic spin and total angular momentum). If there is only one state with a given set of quantum numbers we calculate the expectation value of the Hamilton operator in this state. If there are more than one state we diagonalize the Hamilton operator in the "small" vector space, the states of which carry all the same set of quantum numbers  $[\lambda], (\lambda, \mu), L, S, T, J$ . The so calculated energies are now used as a criterion for the states to be included or truncated. Fig. 1 shows the relative

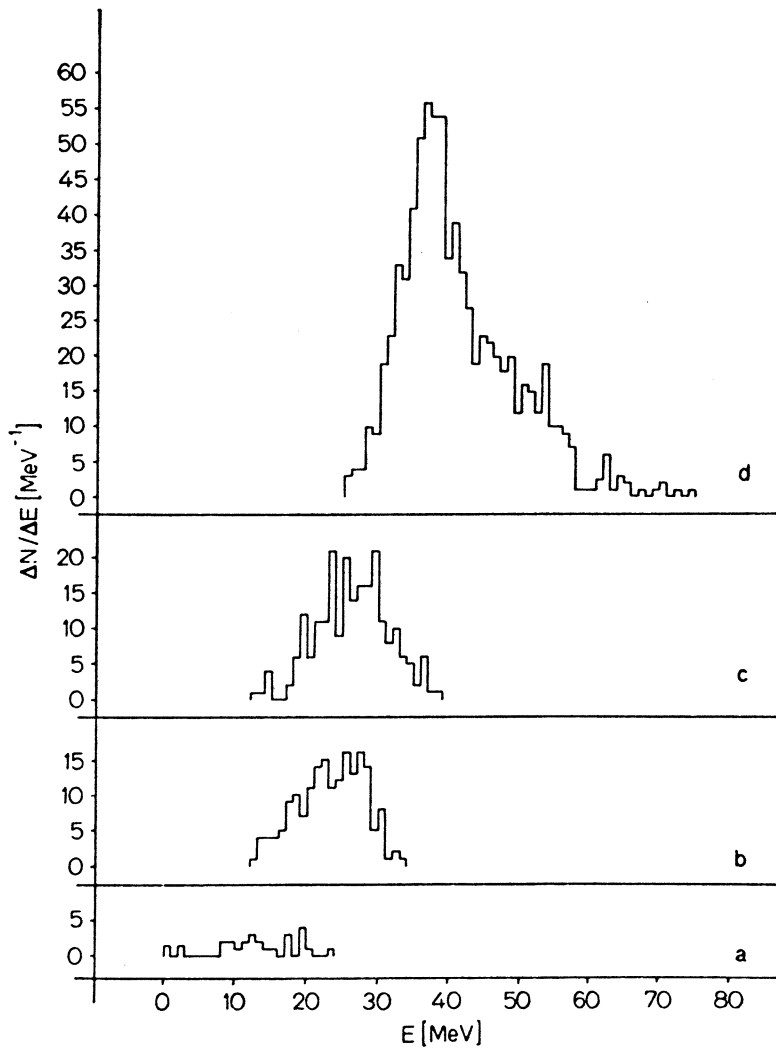


Fig. 1: Density of  $J = 2, T = 0$  levels.  
 (a) symmetry  $[44]$ ; (b) symmetry  $[431]$ ; (c) symmetry  $[422]$ ; (d) other symmetries

energetic position of  $J = 2$  ( $T = 0$ ) states calculated in this way (The two body interaction is a Yukawa-Rosenfeld force). All states not belonging to the symmetry classes  $[44]$   $[431]$   $[422]$  lie more than 25 MeV above the lowest state. This is a nice illustration of the usefulness of the supermultiplet classification scheme. The spectra of fig. 1 indicate further that some states of orbital symmetry  $[422]$  lie low enough so that they should be treated on the same footing as  $[431]$ -symmetry states. More specifically the low lying  $[422]$  states are  $S = 2$  states which are depressed by the long range part of the spin-exchange force. The truncation is performed by setting an arbitrary cutoff energy limit. Our calculations have indicated that a value of 17 MeV for the cutoff energy is reasonable. To check the influence of the cutoff limit one should compare spectra obtained for various truncations. The calculations have shown that for central two-body interactions (Yukawa-Rosenfeld) the calculated spectrum up to 7 MeV is not modified strongly by the admixture of  $[431]$  and  $[422]$  states.

We performed configuration mixing calculations in the truncated space which includes states of symmetry  $[44]$   $[431]$   $[422]$ . We used a central two body interaction with Rosenfeld exchange mixture and Yukawa radial shape of 1.37 f range (Fig. 2). The calculation reproduces essentially the density of levels up to 10 MeV excitation energy. This agreement is attained at the cost of  $SU(3)$  purity. The ground state has only a 48 % component of the leading  $SU(3)$  representation  $(8,4)$ . This departure from  $SU(3)$  symmetry which seems necessary for a reasonable overall agreement with experiment has serious consequences for the lowest states. The ground state rotational band is distorted the lowest  $2^+$  state being pushed up by a half MeV above the experimental value. The branching ratio  $\Gamma(2_2^+ \rightarrow 0) : \Gamma(2_2^+ \rightarrow 2_1^+)$  obtained from the calculated wave functions is 14 : 86, in heavy disagreement with the experimental value 75 : 25. It should be noted that the extreme  $SU(3)$  model (where only the leading representation  $(8,4)$  is taken into account)

reproduces the experimental value!

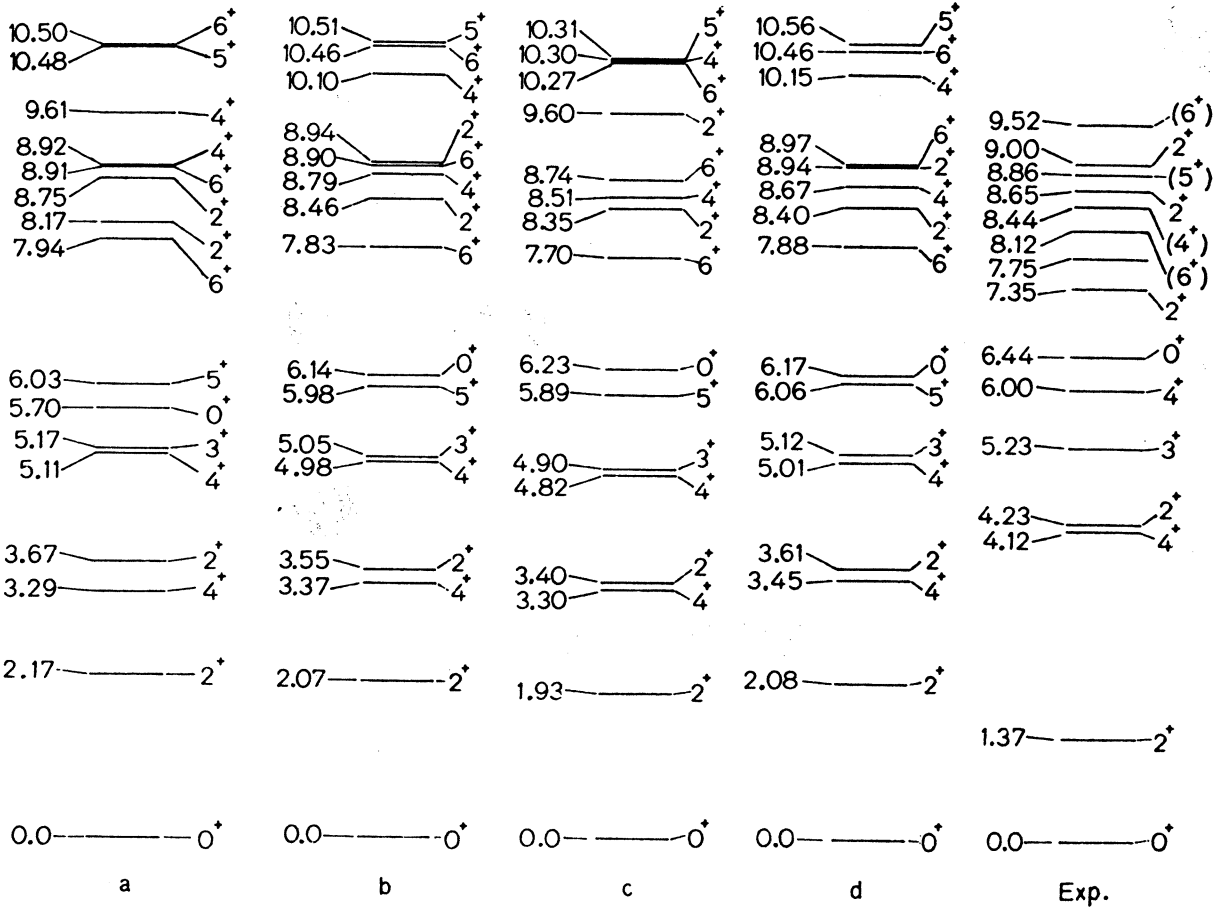


Fig. 2: Spectrum for various truncations

- (a)  $[44]$  states;
- (b)  $[44]$  states and some  $[431]$  states;
- (c) states of symmetries  $[44][431][422]$
- (d) same as (c) with higher cutoff limit

Obviously there are two extreme alternatives:

Either  $SU(3)$  purity combined with a too compressed spectrum or a reproduction of the experimental density of levels accompanied by distortion of the ground state band.

Due to the low lying  $S = 2$  states of symmetry  $[422]$  it might seem promising to investigate whether tensor-forces can change the

above described situation. Preliminary calculations, which are in progress now, indicate that there is no drastic influence of the tensor force.

#### REFERENCES

1. C. Wathne and T. Engeland, Nucl. Phys. A 94 (1967) 129
2. Y. Akiyama, A. Arima and T. Sebe, Nucl. Phys. A 138 (1969) 273

EXCITATION STRUCTURE OF NEGATIVE PARITY STATES IN  $^{17}\text{O}$ .

A. Müller-Arnke

Institut für Theoretische Kernphysik  
der Technischen Hochschule Darmstadt, Germany

There has been a considerable discussion during the last years concerning the excitation structure of the lowest negative parity states of  $^{17}\text{O}$ . It is a tempting idea to try to find out a similarity of these states to the lowest rotational band of  $^{16}\text{O}$  thus considering them in a shell model frame as  $4p3h$  configurations. This picture which could show up some sort of preferred  $\alpha$  particle formation in the  $sd$  shell seems to get experimental support from various  $\alpha$ -transfer reactions (1),(2). Alternatively these lowest negative parity states may consist of  $1h\omega$  excitations. This has been the result of various shell model studies (3),(4), but also a strong mixing was obtained (5),(6).

In the present paper we make in a conventional oscillator shell model approach the attempt to decide if anyone of these two pictures can be ruled out. For the purpose of physical interpretation of the states we start with a basis of nonspurious  $1h\omega$  and  $3h\omega$  excitations which are classified according to orbital and  $SU(3)$  symmetry. This basis is constructed by diagonalizing a linear combination of the c.m. operator, the second order Casimir operator of  $SU(3)$ , and the Casimir operator of  $SU(4)$  in the space

consisting of configurations of the three classes  $(2p1f)$ ,  $(2s1d)^2(1p)^{-1}$ , and  $(2s1d)^4(1p)^{-3}$ , where in the last class we restrict ourselves to the coupling of three orbital symmetric holes to four orbital symmetric particles. This restriction should for the question posed above not be a serious one. Thereby just the configurations which result from coupling a  $(1p)$  particle to the  $4p4h$  class of maximum orbital symmetry are retained, and this in turn is known to form the lower rotational band of  $^{16}_0$  ( $\mathbb{7}$ ). Table 1 shows the nonspurious basis in terms of  $SU(3)$  representations, where the orbital angular momentum multiplicities are obtained by the familiar prescription of Elliott.

f	$(2s1d)^2(1p)^{-1}, (2p1f)$	$(2s1d)^4(1p)^{-3}$
	$(\lambda, \mu)$	$(\lambda, \mu)$
[4441]	(4,1), (2,2), (3,0), (3,0), (0,3), (1,1)	(8,3), (4,5), (0,7)
[4432]	(4,1), (3,0), (0,3), (1,1)	
[44311]	(2,2), (3,0), (1,1)	

Table 1: List of nonspurious irreducible  $SU(3)$  representations retained in this calculation.

Although it is believed that there exist fairly well defined one particle and one hole states relative to the  $^{16}_0$  vacuum there is a considerable ambiguity of the particle hole energy  $\epsilon_{ph}$  if multiparticle excitations are considered. If one decides to parameterize the problem in a way as to choose phenomenological single particle energies and diagonalize some conventional residual two body force with omission of Hartree-Fock parts there is no a priori reason for taking the same value of  $\epsilon_{ph}$  for both  $1h\omega$  and  $3h\omega$  excitations. If we write the one particle Hamiltonian in the form



$$H_0 = \sum_i \left( \frac{\vec{p}_i^2}{2m} + \frac{m\omega^2}{2} \vec{r}_i^2 - \alpha_i \vec{l}_i \cdot \vec{s}_i + \beta_i \vec{l}_i^2 \right)$$

its matrix elements being taken in the three active major shells we may take the spin orbit coupling parameters  $\alpha_i$  and the s-d shell shift parameter  $\beta_d$  from the adjacent nuclei of  $^{16}\text{O}$ , still being left with the major shell distance.

The residual interaction is the sum of five terms

$$V = V_{pppp} + V_{hhhh} + V_{phph} + V_{ppph}$$

where the first two terms act in only one shell, the third and fourth term connect p and sd shell and the fifth term connects all three active shells. For the two body force we take a Yukawa potential with Rosenfeld exchange mixture and a range to oscillator parameter ratio  $\mu = 0.86$ .

The principal result of the diagonalization is the following:

(I) With a force strength of -48 MeV and a major shell distance of about 16.5 MeV the four lowest  $\pi = -$  levels are in correct order and position to within 0.3 MeV being almost pure 2p1h configurations.

(II) The lowest levels with dominant 4p3h part exhibit a reversed ordering of  $3/2^-$  and  $5/2^-$  as compared to experiment irrespective of the  $\epsilon_{ph}$  value. We conclude that in calculations which favour 4p3h structure of the lowest  $\pi = -$  levels these are pushed down by the inappropriate  $\epsilon_{ph}$  choice which is taken from a  $^{12}\text{C}$  core description.

(III) By choosing  $\epsilon_{ph}$  for 4p3h configurations about 2.5 MeV less than that for 2p1h configurations we attain fairly good agreement of the level density above 6 MeV without disturbing the order of the lowest multiplet. In particular we ascertain thereby an upper

limit of 10 %  $4p3h$  admixture to the lowest  $1/2^-$  state.

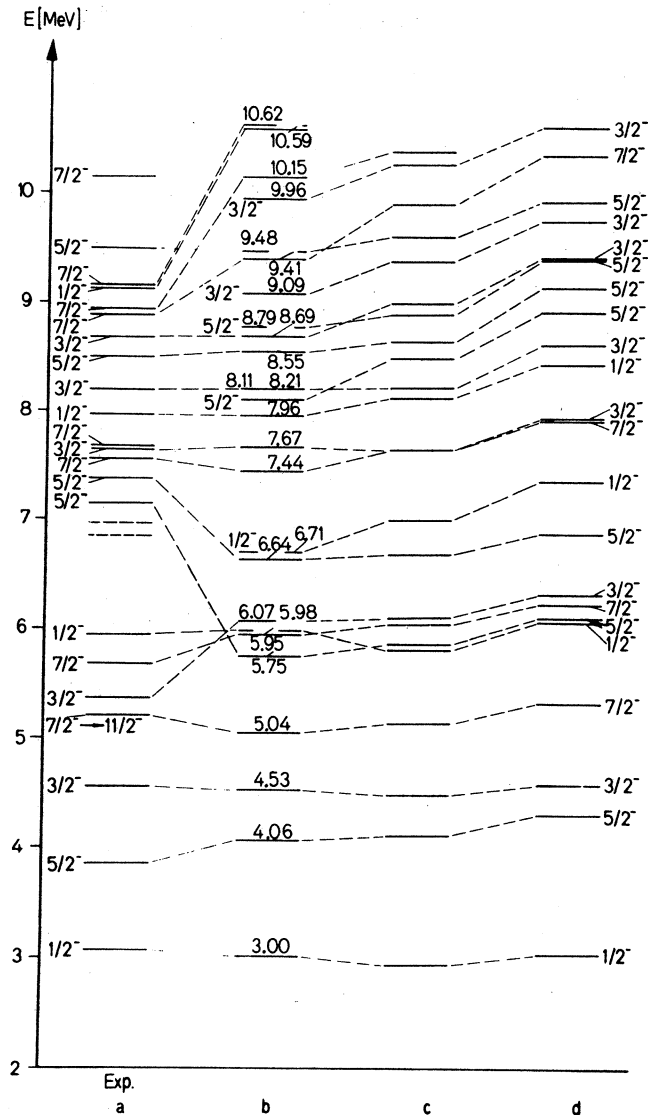


Fig. 1: Various choices of the ph energy for  $1h\omega$  excitations and  $4p3h$  states separately.

a. experimental spectrum (8)

b.  $(\epsilon_{ph})_{2p1h} = 15.0$  MeV,  $(\epsilon_{ph})_{4p3h} = 12.3$  MeV,  $V_0 = -40$  MeV

c.  $(\epsilon_{ph})_{2p1h} = 15.8$  MeV,  $(\epsilon_{ph})_{4p3h} = 13.3$  MeV,  $V_0 = -44$  MeV

d.  $(\epsilon_{ph})_{2p1h} = 16.54$  MeV,  $(\epsilon_{ph})_{4p3h} = 14.2$  MeV,  $V_0 = -47$  MeV

The resultant spectrum is shown in fig. 1 for various values of

$\epsilon_{ph}$  different for  $4p3h$  and  $2p1h$ . We note the following qualitative features of the wave functions. In nearly all states a supermultiplet structure is exhibited by concentration of 85-90 % of the wave function in only one orbital symmetry class. On the other hand broad  $SU(3)$  mixing occurs except in the second  $1/2^-$  and the third and fourth  $3/2^-$  where the  $(8,3)$  representation and thereby  $4p3h$  structure dominates.

There remains the challenging question of a new interpretation of the  $\alpha$ -transfer reactions which populate the lowest  $\pi = -$  states.

#### REFERENCES

- 1) K. Bethge, D.J. Pullen, and R. Middleton, Phys. Rev. C 2 (1970) 395.
- 2) V.Z. Goldberg, V.V. Davydov, A.A. Ogloblin, S.B. Sakuta, and V.I. Chuev, Sov. J. Nucl. Phys. 12 (1970) 16.
- 3) B. Margolis and N. de Takacsy, Can. J. Phys. 44 (1966) 1431.
- 4) M. Hirata, Prog. Theor. Phys. 43 (1970) 1526.
- 5) J. Bobker, Phys. Rev. 185 (1969) 1294.
- 6) P.J. Ellis and T. Engeland, Nucl. Phys. A 144 (1970) 161.
- 7) G. Kluge and P. Manakos, Phys. Letters 29 B (1969) 277.
- 8) F. Ajzenberg-Selove, Nucl. Phys. A 166 (1971) 1.

AN IMPROVED PRESCRIPTION FOR CALCULATING  
THE NEGATIVE PARITY SPECTRUM OF DOUBLY-  
CLOSED SHELL NUCLEI

F. Petrovich, R. Schaeffer, and R. Trilling

The negative parity states in doubly closed shell nuclei have been studied theoretically in some detail, e.g. reference 1. The basic theoretical tools used in these studies are the Tamm-Dancoff Approximation (T.D.A.) and the Random Phase Approximation (R.P.A.) which lead to a description of these states in terms of particle-hole excitations of the closed shell. For doubly-closed shell nuclei with  $N=Z$  these calculations typically underestimate, by several MeV, the splitting between the  $T=0$  and  $T=1$  states belonging to given multiplet. One consequence of this is that estimates of the Coulomb mixing of  $T=0$  and  $T=1$  states tend to be quite large, i.e. upwards to 40%.

Recently it has been pointed out that the monopole components of particle-hole matrix elements can be fixed from the known properties of the single particle potential in nuclei.<sup>2</sup> The symmetry term in this potential gives rise to an iso-spin dependence in the monopole components of these matrix elements which is in reasonable agreement with the experimentally observed splitting between  $T=0$  and  $T=1$  states. It was proposed that T.D.A.

and R.P.A. studies be carried out according to the above prescription. The only modification which is required in the calculations is a shift in the single particle energies, as the monopole components only enter in diagonal matrix elements.

We present here some preliminary results of such calculations. Figure 1 illustrates the effect for the states in  $^{40}\text{Ca}$  which belong essentially to the  $f_{7/2}d_{3/2}^{-1}$  particle-hole multiplet. This is a T.D.A. result obtained with the K-K force. The improvement in the spectrum resulting from inclusion of the shift is apparent. The results for  $^{16}\text{O}$  are somewhat more dramatic as the strength of the symmetry potential, hence the size of the shift, varies as  $1/A$ .

One might draw exception to the results shown for two reasons. The first is the fact that the  $T=1$  states are predicted to be somewhat too low after inclusion of the shift. The second is that the  $T=0$  states, particularly the  $3^-$  and  $5^-$  levels, are at about the right energy although the calculation does not take into account the effect of ground state correlations which will lead to a further depression of these levels.

In answer to the first objection we point out that it is not clear from the results for other levels in  $^{40}\text{Ca}$  and in other nuclei that a depression of  $T=1$  levels is a universal result of these calculations in which the monopole components of the matrix elements are fixed in a configuration independent manner. In regard to the second objection we observe that the K-K force is somewhat stronger than most estimates of the interaction between bound nucleons and that screening effects are likely to be important in particle-hole calculations.<sup>3,4</sup> R.P.A. results

obtained using the Sussex matrix elements with lowest order screening corrections included are quite similar to those shown in Figure 1. The inclusion of the shift is still essential.

It is found that the configuration mixing due to the nuclear interaction is rather insensitive to the inclusion of the shift; however, a large reduction in Coulomb mixing is obtained. Estimates of the Coulomb mixing of T=0 and T=1 states in  $^{40}\text{Ca}$  are of the order of 25% and 5% with and without inclusion of the shift, respectively. Experimental estimates of the amount of Coulomb mixing are of interest. Possible sources of such information are  $\gamma$ -transition rates, spectroscopic factors from the  $(\text{He}^3, d)$  reaction, and energy differences between the members of the T=1 iso-spin triplet. Present data,<sup>5</sup> such as it is, is consistent with little or no mixing.

#### References

1. V. Gillet and N. Vinh Mau, Nucl. Phys. 54(1964)321.
2. R. Schaeffer and F. Petrovich, Phys. Rev. Letts. 26  
(1971)1380.
3. J. Blomqvist and T. T. S. Kuo, Phys. Lett. 29B(1969)544.
4. M. Weigel, L. Garside, and P. K. Haug, UCRL-19940, to be published.
5. K. K. Seth, et al., Phys. Rev. 164(1967)1450.

$^{40}\text{Ca}$

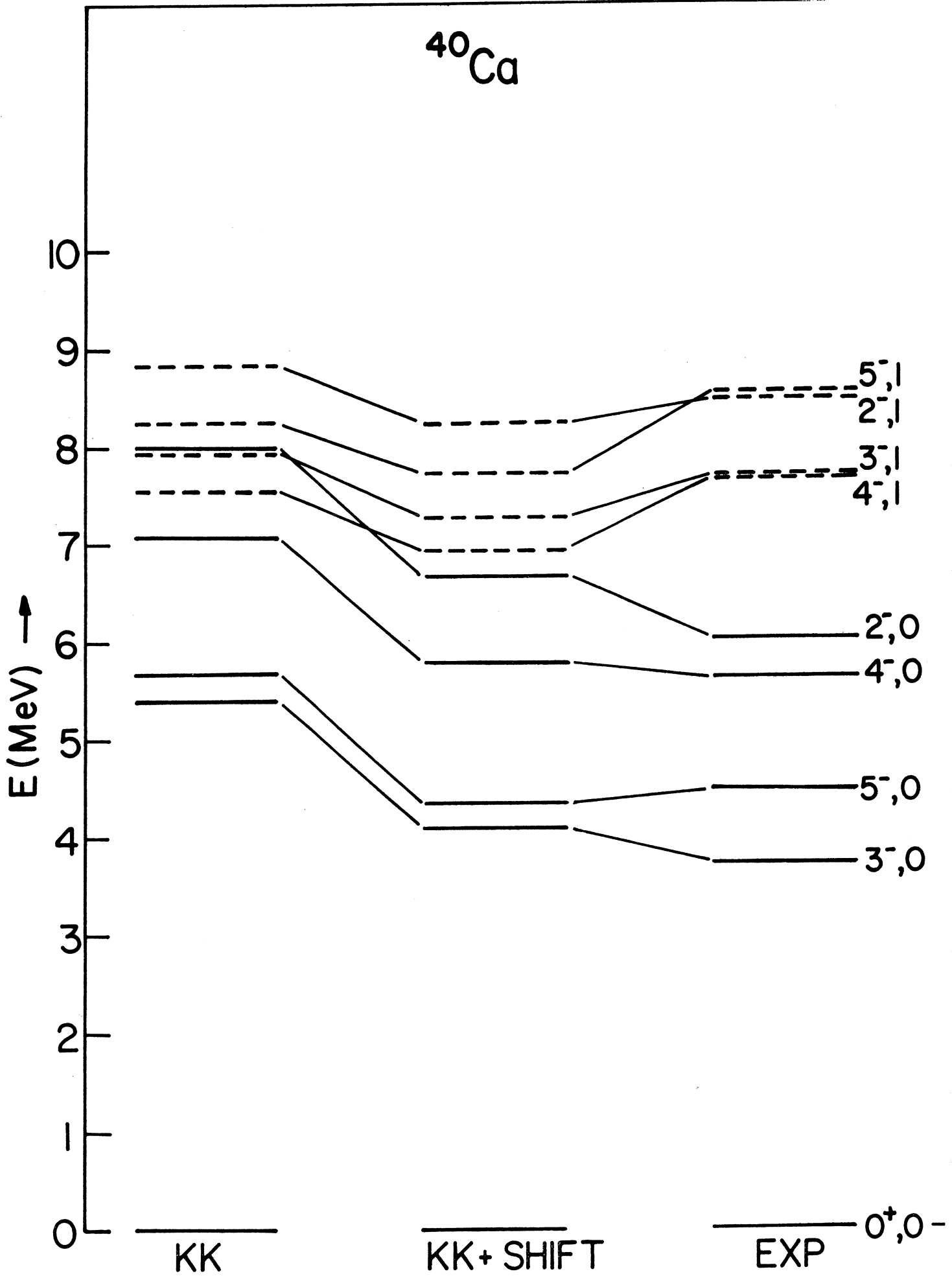


Fig. 1

The Coupling of Particle-Hole States to Vibrations\*

L. Zamick

Rutgers, The State University, New Brunswick, New Jersey

and

Brookhaven National Laboratory, Upton, New York

We wish to consider the two-particle-two hole states of a closed shell nucleus such as  $^{40}\text{Ca}$ , in a formalism in which the one-particle one hole vibrational states, e.g.,  $3^-$ ,  $5^-$  enter explicitly. The two particles are in the f-p shell (negative parity) the two holes in the s-d shell (positive parity).

Let  $\phi^{I_A T_A}$  be a one particle-one hole vibrational state which can be expanded as  $\phi^{I_A T_A} = \sum_{P_A H_A} (x_{P_A H_A} [a^{+P_A H_A} \alpha^{I_A T_A}] - y_{P_A H_A} [\alpha^{P_A H_A} a^{I_A T_A}]) |0\rangle$

$$H\phi^{I_A T_A} = \omega_{I_A T_A} \phi^{I_A T_A}$$

Let  $\psi^{JT}$  be the (2p-2h) wave function of the system

$$H\psi^{JT} = \omega\psi^{JT}$$

Define the amplitude  $A^{JT}((p_L h_L)_{L L}^{I_L T_L} \phi^{I_A T_A})$  as the overlap

---

\* Work supported, in part, by U.S. Atomic Energy Commission while a Summer Visitor to Brookhaven National Laboratory, 1971, and in part by National Science Foundation.



$$= \langle \psi^{JT} [ [P_L H_L]_{L L}^{I_L T_L} \phi_{A A}^{I_A T_A} ]^{JT} 0 \rangle .$$

The amplitudes obey the following equation

$$[\omega - \omega_{I_A T_A} - (\epsilon_{P_L} - \epsilon_{H_L})] A^{JT} ((P_L H_L)_{L L}^{I_L T_L} \phi_{A A}^{I_A T_A}) = \langle JT [V, (a_{L \alpha}^{+P_L H_L})_{L L}^{I_L T_L}] \phi_{A A}^{I_A T_A} \rangle$$

where  $V$  is the potential energy. By evaluating the commutator the following equation for the amplitudes can be derived, the solution of which will be obtained by matrix diagonalization, just as in the more conventional shell model calculations:

$$(\omega - \omega_{I_A T_A} - (\epsilon_{P_L} - \epsilon_{H_L})) A^{JT} ((P_L H_L)_{L L}^{I_L T_L} \phi_{A A}^{I_A T_A}) = \sum_{P_R H_R J R R I_B T_B} P_R H_R J R R I_B T_B \langle P_L H_L I_L T_L I_A T_A | \mathcal{M} | P_R H_R I_R T_R I_B T_B \rangle A^{JT} ((P_R H_R)_{R R}^{I_R T_R} \phi_{B B}^{I_B T_B}) .$$

Here  $\mathcal{M}$  is a symmetric matrix, which can be written in four parts

$$\begin{aligned} \mathcal{M} &= \mathcal{M}(\text{particle-hole}) + \mathcal{M}(\text{particle-vibration}) \\ &+ \mathcal{M}(\text{hole-vibration}) + \mathcal{M}(\text{backward}) \\ \langle L | \mathcal{M}(\text{p-h}) | R \rangle &= \langle (P_L H_L)^{-1} I_L T_L V (P_R H_R)^{-1} I_L T_L \rangle \\ &\delta_{I_L I_R} \delta_{T_L T_R} \delta_{I_A I_B} \delta_{T_A T_B} . \end{aligned}$$

Here we have written the particle-hole matrix element, which is equal to

$$- \sum_{I_X T_X} \begin{Bmatrix} P_R & H_L & I_X \\ P_L & H_R & I_L \end{Bmatrix} \begin{Bmatrix} \frac{1}{2} & \frac{1}{2} & T_X \\ \frac{1}{2} & \frac{1}{2} & T_L \end{Bmatrix} (-1)^{P_L + P_R + H_L + H_R} \langle (H_L P_R)_{L R}^{I_X T_X} V (H_R P_L)_{R L}^{I_X T_X} \rangle_A$$

where the subscript  $A$  always denotes an unnormalized (this is important because there will be cases where  $p_L$  and  $h_L$  are the same state) anti-symmetrized particle-particle matrix element

$$\langle L | \mathcal{M}(\text{particle-vibration}) | R \rangle$$

$$= \frac{1}{2} \delta_{H_L H_R} \sum_{st} ((2I_L+1)(2T_L+1)(2I_R+1)(2T_R+1)(2I_B+1)(2I_y+1)(2T_y+1))^{\frac{1}{2}}$$

$$(-1)^{I_A+T_A+J+T+H_L+p_L+1}$$

$$\begin{Bmatrix} I_R & I_y & I_L \\ P_L & H_L & P_R \end{Bmatrix} \begin{Bmatrix} I_R & I_y & I_L \\ I_A & J & I_B \end{Bmatrix} \begin{Bmatrix} T_R & T_y & T_L \\ \frac{1}{2} & \frac{1}{2} & \frac{1}{2} \end{Bmatrix} \begin{Bmatrix} T_R & T_y & T_L \\ T_L & T & T_B \end{Bmatrix}$$

$$\langle (P_L P_R)^{-1} \rangle_{I_y T_y} V(st^{-1})_{I_y T_y} \rangle$$

$$\times \Delta(s,p) \langle \phi_{I_B T_B}^{I_A T_A} [a^+ s t]_{I_y T_y} \phi_{I_A T_A}^{I_B T_B} \rangle$$

where  $\Delta(s,p) = 1$  if  $s$  (and hence  $t$ ) has the same parity as  $p_L$  (or  $p_R$ );  
 $\Delta(sp) = 2$  if  $s$  has the opposite parity as  $p_L$ .

The last matrix element is easy to evaluate if the coefficients  $x_{pH}^\alpha$  and  $y_{pH}^\alpha$  are known.

$$\langle L | \mathcal{M}(\text{hole-vibration}) | R \rangle$$

$$= -\frac{1}{2} \delta_{P_L, P_R} \sum_{st} ((2I_L+1)(2T_L+1)(2I_R+1)(2T_R+1)(2I_B+1)(2T_B+1)(2I_y+1)(2T_y+1))^{\frac{1}{2}}$$

$$(-1)^{P_L+H_L+I_L+I_R+I_A+J+I_y} (-1)^{I+T_L+T_R+T_A+T+T_y}$$

$$\begin{Bmatrix} I_R & I_y & I_L \\ H_L & P_L & H_R \end{Bmatrix} \begin{Bmatrix} I_R & I_y & I_L \\ I_A & J & I_B \end{Bmatrix} \begin{Bmatrix} T_R & T_y & T_L \\ \frac{1}{2} & \frac{1}{2} & \frac{1}{2} \end{Bmatrix} \begin{Bmatrix} T_R & T_y & T_L \\ T_A & T & T_B \end{Bmatrix}$$

$$\langle (H_R H_L)^{-1} \rangle_{I_y T_y} V(st^{-1})_{I_y T_y} \rangle$$

$$\Delta(s,H) \langle \phi_{I_B T_B}^{I_A T_A} [[a^+ s t]_{I_y T_y} \phi_{I_A T_A}^{I_B T_B} \rangle$$

$\mathcal{M}$  (backward) involves the amplitudes in which  $p_R$  is a positive parity state and  $H_R$  is a negative parity state. These will not be considered here - we restrict  $p_R$  to the f-p shell and  $H_R$  to the s-d shell.

The solution to these equations is obtained by matrix diagonalization just as in the more usual shell model calculations.

The representation used for the amplitude forms an overcomplete non-orthonormal set. Hence some of the eigenvalues of our matrix diagonalization will be associated with spurious states. (On the other hand we can avoid to a very large extent the spuriousity associated with centre of mass motion by simply not including the spurious  $J = 1^- T = 0$  state  $\vec{R}|0\rangle$ ).

Application: If the Effective Interaction method, in its simplest form, is applied to obtain the lowest 2p-2h energy levels with  $T = 0, 1$  and  $2$ , then a large discrepancy results. One really doesn't know where the  $T = 0$  state of this multiplet is because of the presence of 4p-4h states at a very low energy so we shall concentrate upon the  $T = 1$  and  $T = 2$  states.

In the effective interaction method one assigns the configuration

$[(f_{7/2}^{-2})_{J_0=0 T_0=1} (d_{3/2}^{-2})_{J_0=0 T_0=1}]^{0T}$  and one gets the particle-hole matrix elements from the negative parity spectrum of  $\text{Ca}^{40}$ . Assuming that  $\epsilon_{f_{7/2}^{-2}} - \epsilon_{d_{3/2}^{-2}} = 7.2$  MeV these are:

T=0		T=1	
J	V	J	V
$2^-$	-0.45	$2^-$	1.3
$3^-$	-3.5	$3^-$	0.5
$4^-$	-1.6	$4^-$	0.45
$5^-$	-2.7	$5^-$	1.35

One takes the particle-particle and hole-hole matrix elements from  $\text{Ca}^{42}$ ,

Sc<sup>42</sup> and A<sup>38</sup>, K<sup>38</sup>.

Experimentally, the  $T = 1$  state is at 9.3 MeV in Ca<sup>40</sup> (the analog of the 1.6 MeV state in <sup>40</sup>K) and the  $T = 2$  state is at 12.00 MeV. But the above technique leads to a much wider spacing between these states, the  $T = 2$  state is well predicted, but the  $T = 1$  is much lower, in <sup>40</sup>K it is predicted to be below the 4<sup>-</sup>  $T = 1$  ground state. This result is clearly seen if one uses the monopole force  $a + b t_1 t_2$  for a particle-hole interaction and one fits  $b$  to the difference in center of gravity of the  $T = 1$  and  $T = 0$  states. This leads to  $b \approx 2.5 \leftrightarrow 3$  and the  $T = 2, T = 1$  splitting is  $\frac{b}{2}[T_1(T_1+1) - T_2(T_2+1)] = 2b \approx 5 \leftrightarrow 6$  MeV. The experimental separation is only 2.7 MeV.

In order to get results that are better than this simple effective interaction method we must explicitly display the configuration mixing which causes the collective states to lie so low; this is done in our formalism.

We employ a surface delta interaction  $V = -4\pi A \delta(r_1 - R) \delta(r_2 - R) \delta(\Omega_{12})$ .

We compare three calculations which are as follows:

- 1)  $A_{T=0} = 1.07$   $A_{T=1} = 0.49$ . These are Glaudemans' parameters. All vibrations are assigned the configuration  $f_{7/2} d_{3/2}^{-1}$ . With the above force the energies of the  $T = 0$   $J = 2^-$ ,  $3^-$ ,  $4^-$  and  $5^-$  states are 7.54, 6.87, 7.28 and 5.93 MeV compared with the empirical values 6.75, 3.74, 5.60 and 4.49. For  $T = 1$  the calculated values 7.98, 7.52, 7.50 and 8.50 compare better with the empirical values 8.46, 7.70, 7.66 and 8.55.
- 2)  $A_{T=0} = 1.07$   $A_{T=1} = 0.49$  as before. The lowest  $3^-$   $T = 0$  vibration and only this one is made collective in the T.D.A. approximation with the above force. The calculated energy of the  $3^-$  vibration is now 2.99 MeV; its wave function is strongly mixed over many particle-hole states.

3) With the above force it was noted that the particle-particle and hole-hole effective matrix elements were too weak especially in  $T = 1$  states. For example the  $J = 0$   $T = 1$   $\langle f_{7/2}^2 V f_{7/2}^2 \rangle$  (normalized) matrix element is only -2 MeV whereas the effective value from experiments is 3.2 MeV. It is true that correlations such as particle-particle scattering and core polarization could increase this value but since in this calculation we have not put these correlations in we felt justified in making the  $T = 1$  particle-particle and hole-hole force stronger. Hence we have  $A_{T=0} = 1.07$   $A_{T=1} = 0.89$  for p-p and H-H; but as in cases 1) and 2) for p-H interaction. It should be emphasized that the parameter  $\omega_{I A T A}$  (see page 2) was always taken from experiment, i.e., lowest negative parity state (except for the  $2^-$   $T = 0$  which was chosen to be 6.75 MeV because the lower state is a 3p-3h state).

It was further decided that in some of the calculation the  $2^-$ ,  $4^-$  and  $5^-$   $T = 0$  matrix elements would be modified by adding a diagonal shift to the surface delta particle hole matrix elements of -0.79 MeV, -1.67 MeV and -1.44 MeV respectively; this shift is the difference between the surface delta results and experiment. We designate by SHIFT or NO SHIFT whether this was done or not.

ENERGIES of 2p-2h  $J = 0$  States in  $^{40}\text{Ca}$

	I NO COLLECTIVITY NO SHIFT	II 3 <sup>-</sup> COLLECTIVE NO SHIFT      SHIFT		III 3 <sup>-</sup> COLLECTIVE SHIFT
T=0	9.12 10.82	7.67 9.82	7.67 8.57	6.47 7.52
T=1	9.71 10.93	10.40 11.16	10.33 11.14	8.58 10.99
T=2	14.11 16.81	14.11 16.81	14.11 16.81	12.06 16.81

Note that there is not a great deal of difference between the shift and NO SHIFT calculations.

As a result of making the  $3^-$   $T = 0$  collective the 9.12 MeV mainly double-octopole  $T = 0$  state goes down from 9.12 MeV to 7.67 MeV. But for  $T = 1$  the 9.71 mainly double octopole states goes up in energy to 11.16 MeV so that another state (a mixture of double  $4^-$  and  $5^-$  vibrations) becomes the lowest state.

In calculations I and II the  $T = 2$  state is about 2.1 MeV too high because the particle-particle and hole-hole force was too weak. In calculation III in which we make this force more attractive it comes down to 12.06 MeV; note that the  $T = 0$  state does not come down so much as the  $T = 2$  state, because this double octopole state is less sensitive to the p-p, H-H correlations.

Finally, the results for the  $T = 2$ - $T = 1$  splitting are much better than was obtained in the simple effective interaction approach, although there is still a discrepancy of about 0.7 MeV. It was necessary to explicitly display the collectivity of the  $3^-$  vibration for this to be so. We predict the lowest  $T = 0$  2p-2h state at 6.47 MeV. We no longer obtain a  $T(T+1)$  spectrum as one would get from the configurational assignment  $(f_{7/2}^{2, J=0}) (d_{3/2}^{-2, J=0})$ .

## Monopole Polarization With a Surface Delta Interaction\*

L. Zamick

Rutgers, The State University, New Brunswick, New Jersey

and

Brookhaven National Laboratory, Upton, New York

We shall consider four problems where the consequence that the nucleon-nucleon force is density dependent might be important. All of these involve the coupling of particles to monopole phonons, both scalar and isoscalar. They are:

- i) Nolen Schiffer Anomaly, i.e., discrepancy in the mass difference of  $^{41}\text{Ca}$  and  $^{41}\text{Sc}$ .
- ii) Isotope Shift.
- iii) Effect of monopole exchange on the particle-particle interaction.
- iv) Effect of monopole exchange on the particle-hole interaction.

We shall employ the surface delta interaction

$$V = -4\pi G_T \delta(r_1 - R)\delta(r_2 - R) \delta(\Omega_{12}) \quad (T=0 \text{ or } 1)$$

perhaps the simplest of the density dependent interactions.

---

\* Work supported, in part, by U.S. Atomic Energy Commission while a summer visitor to Brookhaven National Laboratory, 1971, and in part by National Science Foundation.

To orient ourselves we note that with  $G_0 = 1$ , the (normalized) matrix element  $\langle (f_{7/2}^2)^{J=1 T=0} V (f_{7/2}^2)^{J=1 T=0} \rangle = -1.63$  MeV; with  $G_1 = +1$  the corresponding matrix element for  $J=0, T=1$  is  $-4$  MeV. The values  $G_0 = 1.07, G_1 = 0.49$  have been used by Glaudemans in structure calculations.

All the four above mentioned properties can be calculated, once the vertices  $\langle jV[j(\text{Ph})^{J''T''}]^{j\frac{1}{2}} \rangle$  with  $J''=0, T''=0$  or  $1$  are known. This vertex can be expressed in terms of a particle-hole matrix element

$$\begin{aligned} & \langle J_a V[J_b(\text{Ph})^{J''T''}]^{j_a\frac{1}{2}} \rangle \\ &= (-1)^{j_a+j_b+p+h} \left( \frac{2J''+1}{2(2j_a+1)} (2T''+1) \right)^{\frac{1}{2}} \langle (hp^{-1})^{J''T''} V(j_b j_a^{-1})^{J''T''} \rangle \end{aligned}$$

The resulting expressions are very simple

$$\begin{aligned} \langle jV[j(\text{ph})^{00}]^{j\frac{1}{2}} \rangle &= -(G_0+G_1) \frac{3}{2}(8)^{\frac{1}{2}} (2h+1)^{\frac{1}{2}} \\ \langle jV[j(\text{ph})^{01}]^{j\frac{1}{2}} \rangle &= (3G_0-G_1) \frac{1}{2}\left(\frac{3}{8}\right)^{\frac{1}{2}} (2h+1)^{\frac{1}{2}} \end{aligned}$$

The ordinary delta interaction yields the same expressions except that  $G$  gets replaced by an integral over four radial wave functions  $\int |R_{ej}|^2 R_p R_H r^2 dr$ . Since  $R_p R_H$  has a node near the maximum of  $|R_{ej}|^2$ , the ordinary delta vertices are negligibly small. The use of a surface delta means that only the value of the integrand at the surface is important and so the vertices become very large. It should also be noted that forces like the Kallio-Kolltveit or any other so called realistic forces which do not have density dependence behave in much the same way as the delta force.



The Auerbach, Kahana, Weneser mechanism for explaining the Nolen Schiffer effect involves the mixing via the Coulomb force of a monopole isovector state, which then interacts differently with the valence nucleon of  $^{41}\text{Sc}$  and  $^{41}\text{Ca}$ . This leads to the expression

$$-\frac{4}{(3)^{\frac{1}{2}}} \sum_{\text{ph}} \langle jV[j(\text{ph})^{01}]^j \rangle > \frac{\langle 0 V_{\text{COUL}}[\text{ph}]^{01} \rangle}{\Delta E_{\text{PH}}} \\ (3G_0 - G_1) \left( \frac{3(2h+1)}{32} \right)^{\frac{1}{2}}$$

With the choice  $G_0 = 1.07$   $G_1 = 0.49$   $\Delta E_{\text{PH}} = -30$  MeV one obtains + 882 keV, which agrees very well with the empirical 700 keV that is required.

For the isotope shift the expression

$$r^2(\text{Ca}^{41}) - r^2(\text{Ca}^{40}) = \sum_{\text{ph}} \frac{2}{\Delta E_Z} \left[ -\frac{1}{(2)^{\frac{1}{2}}} \langle jV[j(\text{ph})^{00}]^{j\frac{1}{2}} \rangle \right. \\ \left. + \frac{1}{(6)^{\frac{1}{2}}} \langle jV[j(\text{ph})^{01}]^{j\frac{1}{2}} \rangle \right] \times \langle [\text{ph}^{-1}]^{J=0} r^2_0 \rangle$$

where  $\langle [\text{ph}^{-1}]^{J=0} r^2_0 \rangle = -(2h+1)^{\frac{1}{2}} \langle pr^2_h \rangle$ .

The answer is proportional to  $(3G_0 + G_1)$ .

We find  $\delta \langle r^2 \rangle^{\frac{1}{2}} = +0.062$  Fermi. Of this the isovector part is  $\frac{3G_0 - G_1}{6G_0 + 2G_1} \times 0.062 = 0.022$  Fermi. This agrees with the reasoning of C.W. Wong and of G.E. Brown that the isovector change should go as  $\frac{1}{2} r_0 A^{1/3}$ . This yields " $r_0$ " = 1.54f. But, it is very doubtful that the isotope shift will be as large as 0.062 Fermi. This would imply that the charge radius of  $\text{Ca}^{41}$  was 1.8% larger than that of  $\text{Ca}^{40}$ . Of course,

the relevant experiment "has" not yet been done.

The shift in energy due to the exchange of a monopole isoscalar phonon between 2 nucleons in the  $j$  shell is  $\sum_{pH} \frac{2 \langle jV[j(pH)^{00}]^{j\frac{1}{2}} \rangle^2}{\Delta E}$ ; this is necessarily negative, and independent of  $J$ . The exchange of an isovector monopole phonon yields  $-\sum_{pH} \frac{2 \langle jV[j(pH)^{01}]^{j\frac{1}{2}} \rangle^2}{\Delta E}$  for  $T = 0$  (this is necessarily positive) and for  $T = 1$  one gets  $-\frac{1}{3}$  of the above value (this insures that the exchange of an isovector phonon does not shift the center of gravity of all ( $T=0 + T=1$ ) states).

The numerical results are:

$$T'' = 0 \quad -0.82 \text{ MeV}$$

$$T'' = 1 \quad T = 0 \quad 0.83 \text{ MeV}$$

$$T'' = 1 \quad T = 1 \quad -0.28 \text{ MeV}$$

This means that the  $T = 1$  states in  $Sc^{42}$  ( $J=0,2,4,6$ ) would get shifted down by 1.1 MeV and the  $T = 0$  states ( $J=1,3,5,7$ ) would be shifted up a minute amount, 0.01 MeV.

This result does not appear to be empirically desirable.

In considering monopole exchange between a particle and hole we have in mind the negative parity states of  $Ca^{40}$  which in the simplest shell model picture would be assumed the configuration  $f_{7/2}d_{3/2}^{-1}$ . This is not adequate for the  $T = 0$  natural parity states  $J = 3^-, 5^-$ , but may be all right for the others  $J = 2^-, 4^-$   $T=0$   $J = 2^-, 4^-, 5^-$   $T=1$ .

With most standard forces, the separation of the center of gravity of the  $T=1$  and  $T=0$  negative parity states - call it  $b$  - comes out to be too small. And Shaeffer has noted that the unnatural parity  $T = 0$  states with  $J = 2^-$  and  $4^-$  come too high in energy.

What does the monopole exchange do? With the surface delta force

we note that the vertices are independent of the valence nucleon. This means that the results that we obtained for the particle particle interaction will apply to the particle-hole interaction provided we change the sign of the contribution of the isoscalar phonon exchange. The results then are:

$$T'' = 0 \quad +0.82 \text{ MeV}$$

$$T'' = 1 \quad T = 0 \quad 0.83 \text{ MeV}$$

$$T'' = 1 \quad T = 1 \quad -0.28 \text{ MeV}$$

(This change of sign relative to the particle-particle case is in agreement with the known result that the monopole force,  $-a+b t_1 \cdot t_2$  between 2 particles, becomes  $a+b t_1 \cdot t_2$  when acting between particle and hole).

The signs of the three numbers above is, for a surface delta force, independent of the signs and magnitudes of  $G_0$  and  $G_1$ .

We see that the  $T = 0$  matrix elements get shifted up 1.65 MeV and the  $T = 1$  get shifted up 0.54 MeV. This is totally undesirable. Now  $b$ , which was too small, gets even smaller and the unnatural parity states, which were too high to begin with, get pushed up even higher.

The Distribution of Neutrons in the Nuclear Surface from Elastic Alpha-  
Particle Scattering\*

Aron M. Bernstein and W. A. Seidler II

Physics Department and Laboratory for Nuclear Science

Massachusetts Institute of Technology

Cambridge, Massachusetts

From electromagnetic measurements, we have a great deal of information about the distribution of protons in nuclei. Although several methods have been proposed to measure the neutron or the total density distributions,<sup>1-3</sup> these methods have not yet achieved accurate results. The purpose of this article is to present an accurate determination of the surface of nuclear density distributions. The measurement of the RMS radius relative to Ca<sup>40</sup> is achieved to an accuracy of approximately  $\pm 0.1$  fm.

Since  $\alpha$  particles are strongly absorbed by nuclei, the major contributions to the scattering in the diffraction region comes from grazing distances where the half density points of the  $\alpha$  particle and the nucleus do not overlap.<sup>4</sup> This means we need to know the effective  $\alpha$  particle, bound-nucleon interaction,  $V_{\text{eff}}(\bar{r} - \bar{r}_{\alpha})$ , at relatively long distances that are determined primarily from the range of nucleon-nucleon interaction and the size of the  $\alpha$  particle. An estimate using this idea gives  $V_{\text{eff}}$  as a Gaussian potential whose approximate strength and range are 37 MeV and 2.0 fm.<sup>4</sup> Although the range is the most important parameter, the results presented here are not sensitive to its exact value (10 percent changes would not

\* This work has been supported in part through funds provided by the U. S. Atomic Energy Commission under AEC Contract AT(30-1)-2098.

change our results appreciably).

In this model, we take the optical potential  $U(r_\alpha)$  as <sup>4,5</sup>

$$U(r_\alpha) = (\lambda_R + i\lambda_i) \int V_{\text{eff}}(\bar{r} - \bar{r}_\alpha) \rho(\bar{r}) d\bar{r} \quad (1)$$

where:  $\rho(r)$  is the density distribution of the nucleus whose volume integral is  $A$  particles; and  $\lambda_R$  and  $\lambda_i$  are empirically determined functions of  $E_\alpha$  (the  $\alpha$ -particle energy). Fortunately, the scattering is insensitive to the theoretically undefined imaginary potential; e.g., the derivative form for  $\text{Im } U(r_\alpha)$  would fit the data equally well.<sup>6</sup> The scattering, particularly the phasing of the differential cross sections, is quite sensitive to  $\text{Re } U(r_\alpha)$ , which contains the information about  $\rho(r)$ .

For  $T = 0$  nuclei, it can be assumed that  $\rho_n(r)$ , the neutron distribution, and  $\rho_p(r)$ , the proton distribution, are approximately equal and can be obtained from electromagnetic experiments. This was checked in detail using Hartree-Fock wave functions.<sup>7,8</sup> By fitting the elastic  $\alpha$ -particle scattering to  $\text{Ca}^{40}$ , the parameters  $\lambda_R$  and  $\lambda_i$  were obtained by varying them until a best fit was obtained.<sup>6</sup> In this paper we shall consider the scattering of 104-MeV  $\alpha$  particles,<sup>9</sup> for which the values  $\lambda_R = 0.815$  and  $\lambda_i = 0.46$  were previously obtained.<sup>6</sup> Using these values of the parameters, Eq. (1) was tested by successfully predicting the  $\alpha$ -particle scattering from the  $T = 0$  nuclei,  $\text{O}^{16}$  and  $\text{Si}^{28}$  (ref. 6). We conclude that in so far as it is possible we have tested the validity of Eq. (1). For  $N > Z$  nuclei, for which there is no accurate experimental evidence for the  $\rho_n(r)$ , we can therefore use Eq. (1) with fixed  $\lambda_R$  and  $\lambda_i$  to obtain information about  $\rho(r)$ .

The optical potential was calculated by assuming a Fermi shape,  $\rho(r) = \rho_0(1 + \exp(r - c)/a)^{-1}$ , for the density distribution. It can be shown that the scattering is not sensitive to the exact value of  $a$ . Approximately

$\pm 20$  percent variations in  $\underline{a}$  can be compensated for by appropriate changes in  $\underline{c}$ .

A typical example of the results is presented in Fig. 1 for  $\text{Zr}^{90}$ . The goodness of fit parameter  $\Delta$  (usually called  $\chi^2$ ) is plotted versus the RMS radius,  $R$ , and has a deep minimum for which the agreement with experiment is excellent. To estimate the error in  $R$ , we have plotted the theoretical cross sections for values of  $R$  other than the minimum value of  $\Delta$ . For  $\Delta \geq 2\Delta_{\min}$ , the fit is unacceptable, as is indicated in Fig. 1.

Table 1 summarizes the results we have obtained. The values of  $R_p$ , the RMS radius of the proton distribution, have been obtained from measured charge distributions after the finite size of the proton has been unfolded. The values of  $R_n$  are then obtained from the values of  $R$  and  $R_p$ . From Table 1, it can be seen that  $R_n - R_p$  tend to be slightly positive but generally not inconsistent with zero. For  $\text{Zr}^{90}$  these results are in agreement with Hartree-Fock predictions.<sup>8</sup>

Equation (1) has been previously used to obtain agreement with the scattering of 42-MeV<sup>5</sup> and 166-MeV<sup>10</sup>  $\alpha$  particles. In these papers, however, nuclear models were used to evaluate  $\rho(r)$ ; no systematic attempt was made to extract  $\rho(r)$  from the data. A new investigation is now under way to extract  $\rho(r)$  from the 166-MeV data using a method similar to the one presented here; the preliminary results are in reasonable agreement with the results presented herein.

At the present time we have not yet considered the same nuclei as have been treated by other methods.<sup>2,3</sup> We shall discuss the relative accuracies of these methods if time permits.

It appears that alpha-particle scattering is an accurate method of measuring the density distribution in the nuclear surface. This analysis is being extended to other isotopes and scattering energies. Further experimental work is needed to check that the extracted neutron distributions are independent of energy and to explore further neutron distributions. Theoretical work pertaining to the justification of the method used here and on its accuracy is highly desirable.

Table 1. Preliminary

Differences of Neutron and Proton RMS Radii

Element	$R_p$ (fm)	$R_n - R_p$ (fm)
$^{64}_{28}\text{Ni}$	$3.82 \pm 0.02^{\text{a}}$	$0.16 \pm 0.16$
$^{90}_{40}\text{Zr}$	$4.16 \pm 0.03^{\text{b}}$	$0.23 \pm 0.11$
$^{124}_{50}\text{Sn}$	$4.60 \pm 0.03^{\text{c}}$	$0.09 \pm 0.12$

a)  $^{64}_{28}\text{Ni}$ . J. R. Ficenel, W. P. Trower, J. Heisenberg, and I. Sick, Phys. Lett. 32B, 460 (1970).

b)  $^{90}_{40}\text{Zr}$ . J. Heisenberg, private communication.

c)  $^{124}_{50}\text{Sn}$ . P. Barreau and J. B. Bellicard, Phys. Lett. 258,470 (1967).

## References

1. Reviews of this subject have been presented by R. Wilson, Comments on Nuclear and Particle Physics, 4, 117 (1970); D. H. Wilkinson, *ibid*, 1, 80 (1967) and 1, 112 (1967).
2. J. A. Nolen, Jr. and J. P. Schiffer, Ann. Rev. of Nucl. 19, 471 (1969).
3. G. W. Greenlees et al., Phys. Rev. 2C, 1063 (1970) and 3C, 1560 (1971).

4. A. M. Bernstein, Advances in Nuclear Physics. New York: Plenum Press. M. Baranger and E. Vogt, editors, 3 (1969).
5. D. F. Jackson, Phys. Lett. 32B, 233 (1960); C. G. Morgan and D. F. Jackson, Phys. Rev. 188, 1758 (1969); D. F. Jackson and V. K. Kumbhavi, Phys. Rev. 178, 1626 (1969).
6. A. M. Bernstein and W. A. Seidler II, Phys. Lett. 34B, 569 (1971).
7. D. Vautherin and M. Veneroni, Phys. Lett. 25B, 175 (1967) and private communication.
8. J. W. Negele, Phys. Rev. 1C, 1260 (1970).
9. G. Hauser et al., Nucl. Phys. A128, 81 (1969); G. Schatz, private communication.
10. B. Tatischeff and I. Brissand, Nucl. Phys. A155, 89 (1970).
11. B. Tatischeff, I. Brissand, and L. Bimbot, private communication.



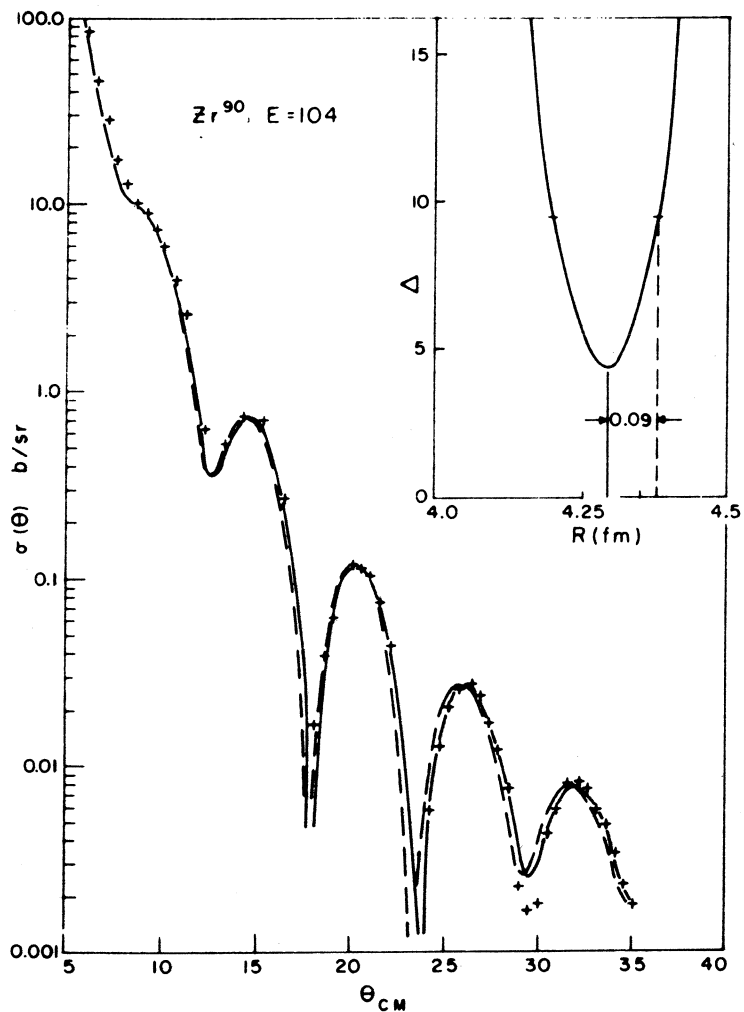


Fig. 1. The scattering of 104-MeV  $\alpha$  particles from  $Zr^{90}$ . The insert shows  $\Delta$ , the difference between theory and experiment versus the RMS radius  $R$ . The solid curve is calculated for  $\Delta = \Delta_{\min}$ . The dashed curve for  $\Delta = 2\Delta_{\min}$  when  $R$  is 0.09 fm larger than its value at  $\Delta_{\min}$ .

STRENGTH OF EFFECTIVE TWO BODY INTERACTION OBTAINED FROM A STUDY OF  
INELASTIC SCATTERING OF 50 MeV PROTONS BY  ${}^6,{}^7\text{Li}$ ,  ${}^9\text{Be}$ , AND  ${}^{42}\text{Ca}$

G. S. MANI

Schuster Laboratory, Manchester University, Manchester, U.K.

The proton linear accelerator at the Rutherford High Energy Laboratory has been used to measure the differential cross sections for the inelastic scattering of 50 MeV protons by various nuclei ranging from  ${}^6\text{Li}$  to  ${}^{208}\text{Pb}$ . In this paper the results of the analysis of the data in the case of  ${}^6\text{Li}$ ,  ${}^7\text{Li}$ ,  ${}^9\text{Be}$  and  ${}^{42}\text{Ca}$  are presented.

The inelastically scattered protons were detected using an  $n=\frac{1}{2}$  magnetic spectrometer with an acoustic spark chamber assembly mounted on its focal plane. Details of the experimental technique used have been discussed in earlier papers<sup>1)</sup>. Elastic scattering measurements were also obtained on these nuclei. An optical model analysis of the elastic scattering data was performed and the results are discussed by Mani et al.<sup>2)</sup>.

The angular distributions for inelastic scattering to the 2.184 MeV level in  ${}^6\text{Li}$  and to the levels at 0.478 MeV and 4.63 MeV in  ${}^7\text{Li}$  were measured from  $20^\circ$  to  $150^\circ$  in  $2.5^\circ$  interval. The 3.56 MeV level in  ${}^6\text{Li}$  occurs just at the onset of the three body continuum and hence the angular distribution for this state was obtained from  $5^\circ$  to  $25^\circ$  in  $2.0^\circ$  interval. Angular distributions for the 2.4 MeV and 6.4 MeV states in  ${}^9\text{Be}$  were measured to  $90^\circ$ . In the case of  ${}^{42}\text{Ca}$ , the angular distributions were obtained for all levels up to an excitation of 5 MeV. The energy levels obtained in  ${}^{42}\text{Ca}$  are shown in fig.1 and compared with the theoretical calculations of Flowers and Skouras<sup>3)</sup>.

Analysis of the p-shell data

The angular distributions were analysed using the DWBA

model with the form factors obtained from a microscopic description of the reaction. The two body interaction was taken to be

$$V(0,1) = \sum_{ST} V_{ST} f(r_{01}) (S_S(0) \cdot S_S(1)) (O_T(0) \cdot O_T(1)) \quad (1)$$

where  $S_S$  and  $O_T$  are spherical tensors of rank  $S$  and  $T$  in spin and isospin space of the two particles. The radial form factor  $f(r_{01})$  was assumed to be given by a single Yukawa,  $\text{Exp}(-\alpha r_{01}) / \alpha r_{01}$ , where the range  $\alpha^{-1}$  was fixed at 1.0 fm. Gaussian shape for the radial dependence was also tried but it was found to yield very similar results to the Yukawa shape.

The nuclear bound state wave functions were taken to be given by L-S coupled ( $1p^n$ ) configurations only. The radial part of the wave functions were obtained either from Harmonic Oscillator (H.O.) or Saxon-Wood (S.W.) potential. It was found that provided the rms radii were kept the same, both potentials yield similar results.

A typical fit to the experimental data for the  ${}^7\text{Li}(p,p_1){}^7\text{Li}(0.478 \text{ MeV})$  reaction is shown in fig.2. From the figure it is seen that, if the range  $\alpha$  of the interaction is fixed, then the radius  $R_N$  of the S.W. potential or the range  $\delta$  of the H.O. potential is determined from the shape of the angular distribution. The strengths of the effective two body interaction obtained from the analysis are given in table 1.

The  $V_{\infty}$  potential depth would be around 35 MeV if the effective interaction used by us is related to the Kallio - Koltveit (KK) force with is cut off below the separation distance<sup>4)</sup>. This then implies that an enhancement by a factor of 16 is needed to obtain the cross sections measured in this experiment. A part of this would be due to the neglect of exchange effects in our calculations. At this energy for  $L = 2$  transitions, the enhancement due to exchange effects

would be of the order of 30 - 50 %. Thus the major part of the enhancement should be due to excitation of the valence nucleons outside the Fermi sea and due to the polarisation of the  $^4\text{He}$  core. Two body correlations produced by the excitation of the valence nucleons outside the Fermi sea does explain part of the enhancement of the E2 transition in  $^6\text{Li}$ .<sup>5)</sup> Also such correlations have been considered by Lodhi<sup>6)</sup> in explaining electron scattering and electromagnetic transitions in  $^6\text{Li}$ . The enhancement in the cross section obtained in the present experiment is in agreement with the effective charge needed to explain E2 transitions in  $^6\text{Li}$ , if the expressions for enhancement derived by Atkinson<sup>7)</sup> are used. If we use a collective description for the reaction, then the deformation parameter  $\beta$  that we obtain has a value of around 1.4 indicating the highly collective nature of these levels.

#### Analysis of $^{42}\text{Ca}$

The low lying states of  $^{42}\text{Ca}$  has been successfully explained by the admixture of 4p-2h deformed states to the two particle spherical states in the f-p shell.<sup>3)</sup> The deformed states were constructed by placing four particles in the lowest available deformed orbital of the Nilsson model with  $k=\frac{1}{2}^-$  and the two holes are created in the highest available orbital with  $k=3/2^+$ .

The data on  $^{42}\text{Ca}$  was analysed in terms of the DWBA with the bound state wave functions being given by the deformed model as well as by pure  $(1f_{7/2}^2)$  configuration. The spin flip term in the interaction was neglected. Spin flip part of the interaction would yield no contribution for transitions of the type  $(j^n)^{0+} \rightarrow (j^n)^{J+}$ . The above assumption implies that even for shell model components in the wave function which are not  $j^n$  configurations the spin flip contribution is not negligible. This is partly justified since such components in the wave function are usually small. Also this approximation is

consistent with the conclusions of Satchler.

The radial part of the bound state wave functions were obtained from H.O. potential with the oscillator parameter given the value of 1.95 fm which is appropriate for nuclei in the mass region 42. Some typical form factors needed for the calculation of the deformed states are shown in fig. 3. The range of the Yukawa interaction was chosen to be 1.0 fm. The fits obtained to the experimental data are shown in fig.4 for both the cases of pure  $(1f_{7/2}^2)$  configuration as well as for the deformed configuration. The fits obtained in both cases are as good as those obtained when a collective model form factor was used. For the case of  $0_2^+$  level we were not able to obtain any reasonable fit at all and this we find hard to explain.

The results for the strength of the potential  $V_{00}$  as obtained from the various excited states are listed in table 2. It can be seen from the table that the introduction of the deformed  $4n-2h$  components in the wave function reduces the strength of the interaction considerably. The interaction can be further renormalised by taking into account core polarisation via the effective charge. The results of such calculations are listed under the heading '4p 2h + core' and ' $(1f_{7/2}^2) + core$ '. The effective charge used in either case was the appropriate one needed to reproduce the transition strengths for electromagnetic transitions. Also in the calculation, the ratio  $V_{00}/V_{01}$  was taken to be -2.5. One sees from the table that with the core polarisation renormalisation, the potential strengths agree with those derived from realistic interaction. The only discrepancy is the  $4_1^+$  level which yields twice the strength. This is certainly due to neglect of exchange which become more important for the higher L values.

REFERENCES

- 1) G. S. MANI, Nuc. Phys. A157 (1970) 471; Nucl. Phys. A165 (1971) 225  
D. T. Jones, Thesis, Manchester University 1970 (unpublished)  
D. Jacques, Thesis, Manchester University 1970 (unpublished)
- 2) G. S. MANI; D. JACQUES AND D. T. JONES; Nucl. Phys. A165 (1971) 384
- 3) L. D. SKOURAS, Thesis, Manchester University (1969) (unpublished)  
B. H. Flowers and L. D. Skouras, Nucl. Phys. A116 (1968) 529
- 4) F. PETROVICH; Thesis, University of Michigan (1970) (unpublished)
- 5) R. D. LAWSON; Nucl. Phys. A148 (1970) 401
- 6) M. A. K. LODHI, Nucl. Phys. 80 (1966) 125
- 7) J. ATKINSON AND V. A. MADSEN, Phys. Rev. 1 (1970) 1377

TABLE 1

Values of Effective Interaction Obtained from the Present Experiment

Nucleus	Transition	$V_{00}$ (MeV)	$V_{01}$ (MeV)	$V_{10}$ (MeV)	$V_{11}$ (MeV)
${}^6\text{Li}$	$1^+ \rightarrow 3^+$	$190 \pm 30$	$-50 \pm 15$		
${}^6\text{Li}$	$1^+ \rightarrow 0^+$				$7.5 \pm 3$
${}^7\text{Li}$	$3/2^- \rightarrow 1/2^-$	$165 \pm 25$	$-50 \pm 15$	$-30 \pm 10$	$7.5 \pm 3$
${}^7\text{Li}$	$3/2^- \rightarrow 7/2^-$	$160 \pm 30$	$-50 \pm 15$	$-30 \pm 10$	$7.5 \pm 3$
${}^9\text{Be}$	$3/2^- \rightarrow 5/2^-$	$150 \pm 25$	$-50 \pm 15$	$-30 \pm 10$	$7.5 \pm 3$
${}^9\text{Be}$	$3/2^- \rightarrow 7/2^-$	$155 \pm 25$	$-50 \pm 15$	$130 \pm 10$	$7.5 \pm 3$

TABLE 2

Strengths of the effective potential obtained from the present work

State	$V_{00}$ (MeV)			
	4p-2h	(4p-2h)+core	$(1f_{7/2}^2)$ $\frac{2}{2}$	$(1f_{7/2}^2)$ +core $\frac{2}{2}$
$2_1^+$	$140 \pm 20$	$46 \pm 8$	$190 \pm 28$	$50 \pm 10$
$2_2^+$	$120 \pm 17$	$40 \pm 8$		
$4_1^+$	$250 \pm 35$	$83 \pm 20$	$300 \pm 45$	$80 \pm 16$
$0_2^+$	$90 \pm 20$	$30 \pm 10$		

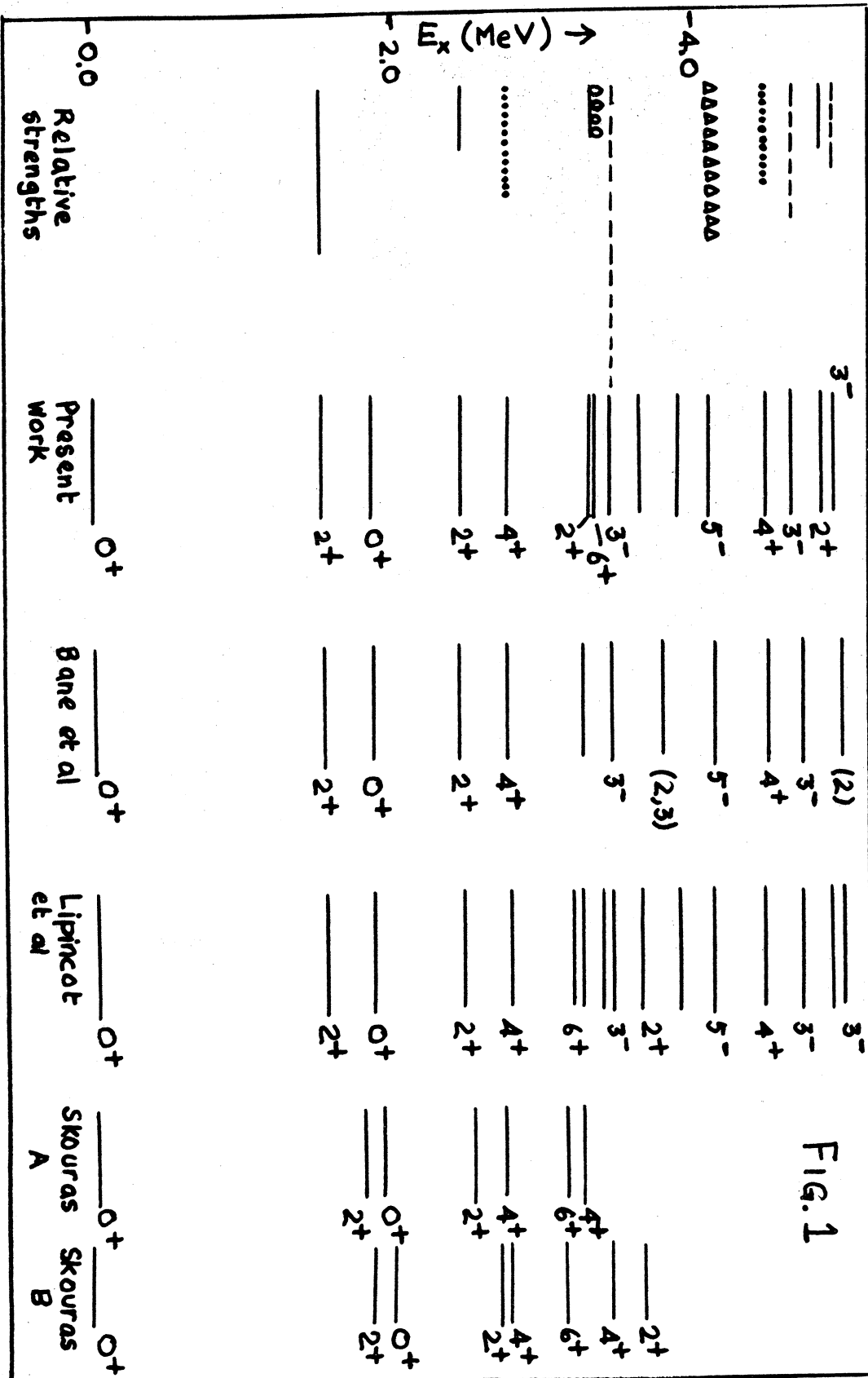
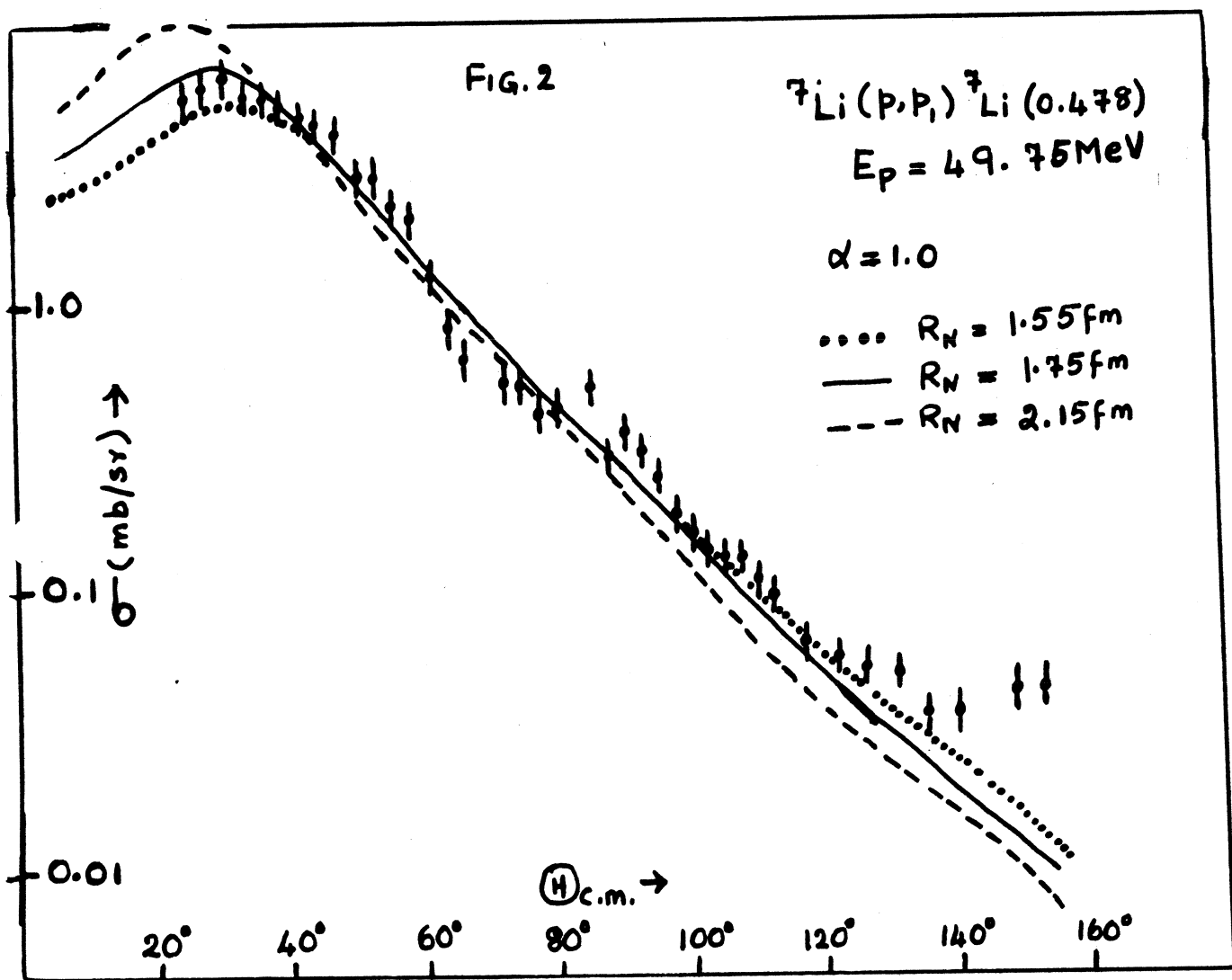
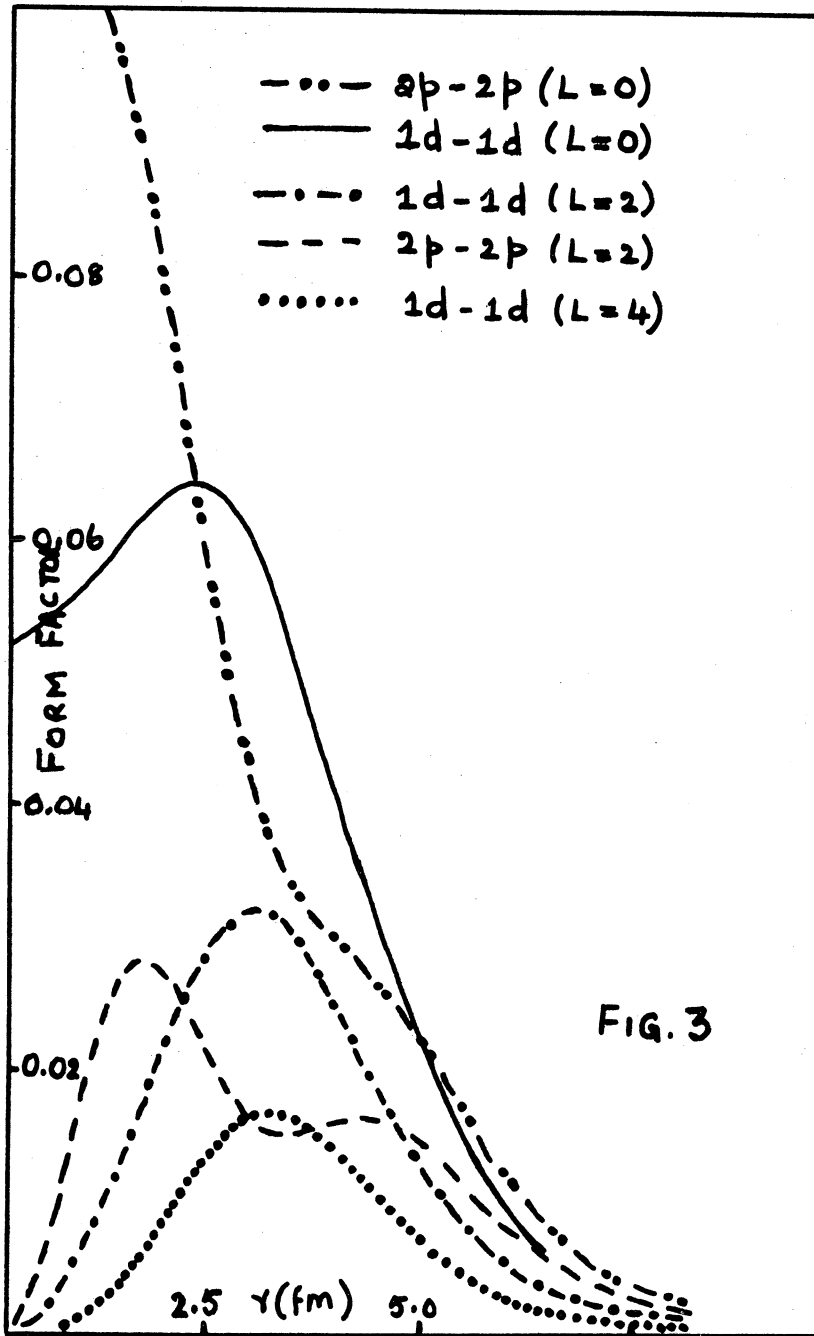
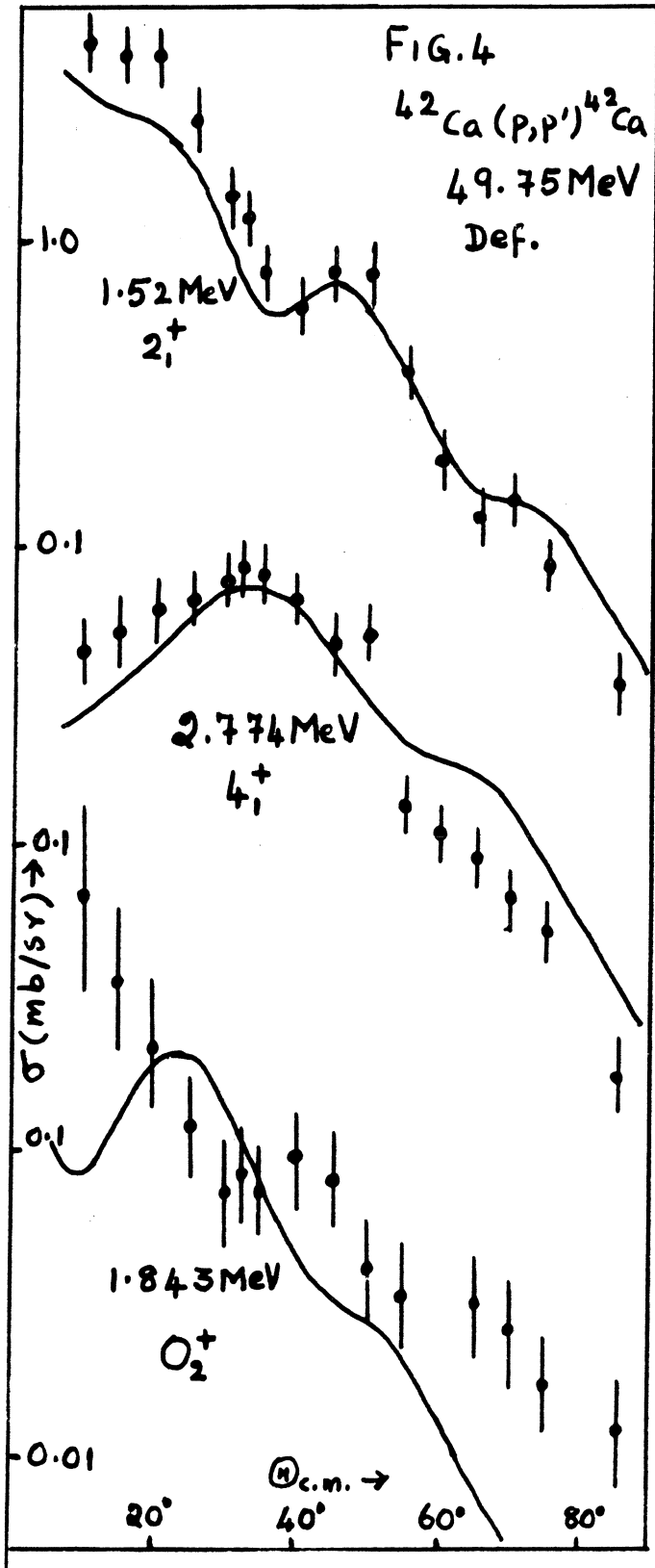


FIG. 1









Charge-Exchange and/or Knockout Spectator Poles  
in the  $D(^3\text{He}, tp)p$  Reaction

R.E. Warner\*†

Physics Department, Oberlin College

Oberlin, Ohio, 44074, U.S.A.

and

G.C. Ball, W.G. Davies, A.J. Ferguson and J.S. Forster

Chalk River Nuclear Laboratories

Atomic Energy of Canada Limited

Chalk River, Ontario, Canada

Abstract

Intense spectator-proton peaks were observed in the  $D(^3\text{He}, tp)p$  Reaction. Their shapes were well fitted by PWBA calculations assuming either knockout or  $^3\text{He}-n$  quasi-elastic scattering accompanied by charge exchange to be the mechanism. Their intensities relative to the quasi-elastic peaks from  $D(^3\text{He}, ^3\text{He} p)n$  were correctly predicted by CE calculations, but only when an unrealistic mixture of exchange forces was used. All direct knockout calculations gave relative intensities at least 10 times too small.

\* Research supported by the National Science Foundation through Grant No. GP-19269.

† Address during 1971-72: Department of Nuclear Physics, Oxford University, Oxford, England.

Charge-Exchange and/or Knockout Spectator Poles  
in the  $D(^3\text{He}, tp)p$  Reaction

R.E. Warner<sup>\*†</sup>  
Physics Department, Oberlin College  
Oberlin, Ohio, 44074, U.S.A.

and

G.C. Ball, W.G. Davies, A.J. Ferguson and J.S. Forster  
Chalk River Nuclear Laboratories  
Atomic Energy of Canada Limited  
Chalk River, Ontario, Canada

This paper reports, for the first time, intense spectator peaks from the reaction  $D(^3\text{He}, tp)p$ , which may result from quasi-elastic scattering (QES) accompanied by charge exchange (CE). Quasi-elastic scattering was first observed by Kuckes, Wilson and Cooper<sup>1</sup>, who found that large peaks (called spectator peaks) are observed in the p-p coincidence cross sections from the reaction  $D(p, 2p)n$  when momentum is transferred only between the two protons, and the neutron (called the spectator particle) remains nearly at rest in the laboratory. QES from the proton in the deuteron has also been studied<sup>2-4</sup> in the reactions  $D(d, dp)n$ ,  $D(^3\text{He}, ^3\text{He} p)n$ , and  $D(\alpha, \alpha p)n$ . In CEQES for  $D(^3\text{He}, tp)p$  reaction (see Fig.1a), the  $^3\text{He}$  and neutron would transfer momentum and exchange charge, emerging as triton and proton, and the proton from the deuteron would remain nearly at rest. Alternatively, a direct knockout (KO) process (see Fig.1b) might also produce spectator peaks.

A  $\text{CD}_2$  target was bombarded with 27 MeV  $^3\text{He}^{++}$  ions from the Chalk River MP Tandem accelerator. Coincidence events from two  $\Delta E$ -E counter telescopes, coplanar with and on opposite sides of the beam, were recorded on magnetic tape. Particle identification was achieved during analysis, using a triton range-energy

table<sup>5</sup>. Our absolute coincidence cross section data for two geometries appear in Figs. 2 and 3. In Fig.2a, for instance, the broad peak near  $E_t = 13$  MeV appears to be a spectator peak both because it is near the minimum spectator particle (undetected proton) energy and because of its large size, 30 mb/sr<sup>2</sup>-MeV; it is half as large as the ordinary QES peak from the  $D(^3\text{He}, ^3\text{He} p)n$  reaction which was observed simultaneously at this geometry (Fig.2b). Peaks observed in previous t-p coincidence studies<sup>6,7</sup> resulted from sequential decay of excited states in  $^4\text{He}$ , but their magnitudes<sup>7</sup> were only a few mb(sr<sup>-2</sup>)(MeV<sup>-1</sup>).

To interpret our data we performed a plane wave Born approximation (PWBA) calculation including both CE and KO processes; our development is similar to that of Henley et al. A Hulthen deuteron wave function<sup>9</sup> with  $\alpha = 0.232$  fm<sup>-1</sup> and  $\beta = 1.202$  fm<sup>-1</sup> and a Gaussian trion ( $^3\text{He}, t$ ) function<sup>8</sup> with  $\gamma = 0.36$  fm<sup>-1</sup> were used. The transition potential<sup>8</sup> was

$$V(r_{ij}) = V_0 [1 - B P_{\sigma,ij} P_{\tau,ij}] \exp(-\delta^2 r_{ij}^2) \quad (1)$$

which contains both ordinary and spin-isospin-exchange interactions, and causes the matrix elements to separate into spin-isospin and spatial factors. The range of the force was fixed with  $\delta = 0.656$  fm<sup>-1</sup>. The matrix elements for the two reactions are:

$$t+p+p: \overline{\sum (M_{fi})^2} = \frac{1}{12} (BM_{CE}^+ + M_{KO}^+)^2 + \frac{1}{4} (BM_{CE}^- + M_{KO}^-)^2 \quad (2)$$

$$\begin{aligned} ^3\text{He}+p+n: \overline{\sum (M_{fi})^2} &= \frac{1}{6} (BM_{CE}^- + M_{KO}^-)^2 + M_{KO}^+{}^2 (6B^2 - 3B + \frac{1}{2}) \\ &+ M_{CE}^+{}^2 (6 - 3B + \frac{1}{2}B^2) + M_{KO}^+ M_{CE}^+ (\frac{475}{72}B - \frac{3}{2} - \frac{3}{2}B^2) \end{aligned} \quad (3)$$

The +(-) superscripts on the M's denote even (odd) parity of the final nucleons.

The shapes of the spectra calculated from these matrix elements are insensitive to B and to whether CE and/or KO is

assumed to take place. Renormalized cross sections obtained for CE with  $B = 2.3$  appear in Figs. 2 and 3, and the peaks are generally well fitted by them.

Since we expect the PWBA to predict the ratio  $R = d^3\sigma(t+p+p)/d^3\sigma(^3\text{He}+p+n)$  more reliably than the magnitudes of the cross sections, equal but otherwise arbitrary normalization factors were used for the two reactions at each geometry. Acceptable values of  $R$ , close to the observed values of  $1/2$  to  $2/3$ , could be obtained only for pure CE with  $B = 2.3$ . Those predicted assuming both CE and KO, or KO alone, were only about 0.05 at  $B = 0$  and decreased monotonically with increasing  $B$ . For CE alone they were only 0.08 for  $B = 1.0$ , the Serber value<sup>10</sup>.

Henley et al.<sup>8</sup> deduced that both pickup and charge exchange are important in the  $D(^3\text{He}, tp)p$  reaction at the highest triton energies, where the  $p$ - $p$  final state interaction occurs. The present work provides additional evidence for the existence and strength of charge exchange, but underlines the need for a more sophisticated theoretical approach. The two most striking failures of our model are its inability to give a proper account of the strength of the KO process and, even assuming that only CE takes place, the unrealistic exchange force required to give the observed  $(t+p+p)/(^3\text{He}+p+n)$  cross section ratio. Perhaps these shortcomings could be rectified by straightforward changes within the PWBA framework, such as including tensor forces or other types of exchange forces, completely antisymmetrizing the wave functions for exchange of all 5 nucleons, or considering higher order processes. They may instead require a radically different and more sophisticated approach, such as a solution of the Fadeev equations.

\*Research supported by the National Science Foundation through Grant No. GP-19269.

†Address during 1971-72: Department of Nuclear Physics, Oxford University, Oxford, England.

It is a pleasure to thank Professor Robert Hofstadter and Dr. F.C. Khanna for their advice and encouragement.

## References

1. A.F. Kuckes, R. Wilson and P.F. Cooper, Jr., *Annals of Phys.* 15, 193 (1961).
2. P.F. Donovan, *Rev. Mod. Phys.* 37, 501 (1965); B.E. Corey, R.E. Warner, and R.W. Bercaw, *Nucl. Phys.* to be published.
3. P.A. Assimakopoulos, E. Beardsworth, D.P. Boyd and P.F. Donovan, *Nucl. Phys.* A144, 272 (1970).
4. R.E. Warner and R.W. Bercaw, *Nucl. Phys.* A109, 205 (1968).
5. B. Hird and R.W. Ollerhead, *Nucl. Instr and Meth.* 71, 231, (1969).
6. P.D. Parker, P.F. Donovan, J.V. Kane and J.F. Mollenauer, *Phys. Rev. Lett.* 14, 15 (1965).
7. R.E. Warner, B.E. Corey, E.L. Petersen, R.W. Bercaw and J.E. Poth, *Nucl. Phys.* A148, 503 (1970); G.C. Ball, W.G. Davies, A.J. Ferguson, J.S. Forster and R.E. Warner, to be published.
8. E.M. Henley, F.C. Richards and D.U.L. Yu, *Nucl. Phys.* A103, 361 (1967).
9. M.J. Moravcsik, *Nucl. Phys.* 7, 113 (1958).
10. J.M. Blatt and V.F. Weisskopf, Theoretical Nuclear Physics (John Wiley and Sons, New York, 1952) pp. 170-181.



3480-H

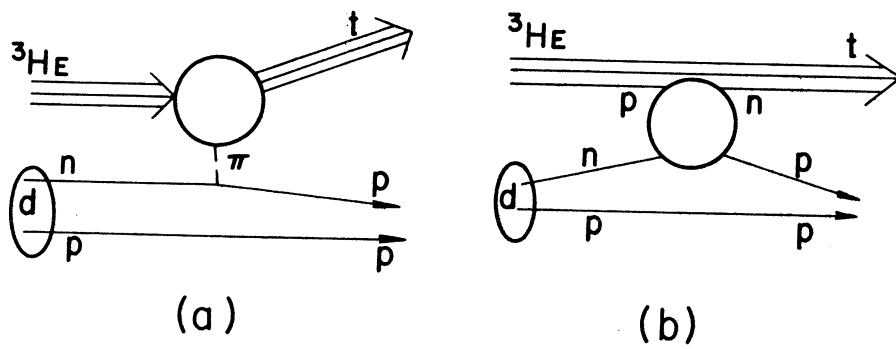


Fig 1 Feynman diagrams for charge-exchange quasi-elastic scattering (a) and knockout (b).

3481-D

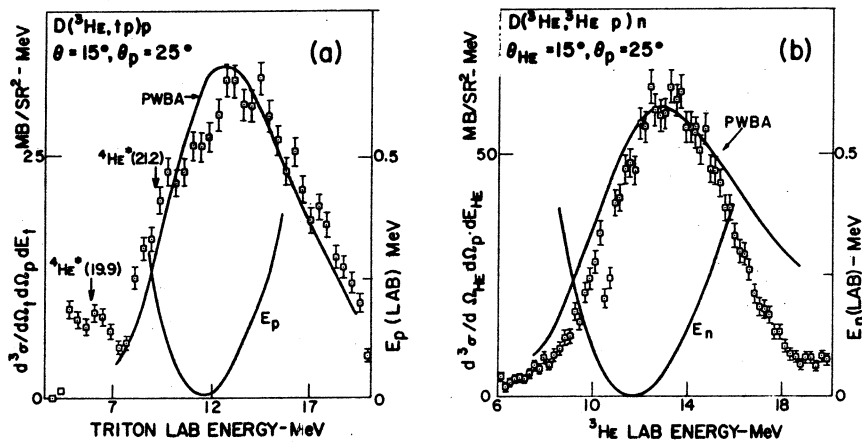


Fig. 2a  $D(^3\text{He}, tp)p$  absolute coincidence cross sections and PWBA predictions (left-hand scale) and spectator proton lab energy (right-hand scale) plotted vs triton lab energy at ( $\theta_t = 15^\circ, \theta_p = 25^\circ$ ). Arrows show where enhancements due to sequential decay of the  $^4\text{He}$  excited states at 19.9 and 21.2 MeV may occur.

Fig. 2b Similar to 2a except  $D(^3\text{He}, ^3\text{He} p)n$  data, predictions for the ordinary QES peak, and spectator neutron energy are plotted vs.  $^3\text{He}$  lab energy. Both PWBA predictions in Fig. 2 are multiplied by 0.02.

3481-C

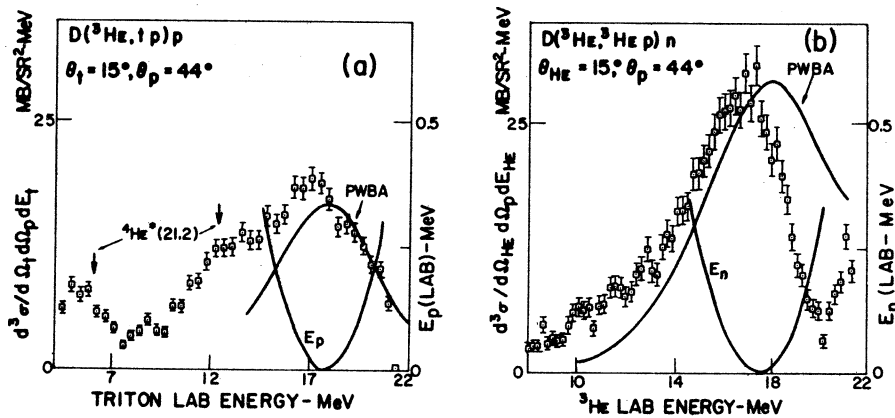


Fig. 3 Like Fig. 2, for the geometry ( $15^\circ, 44^\circ$ ). Both PWBA predictions are multiplied by 0.06. The rise in the  $^3\text{He}$  spectrum near 21 MeV is attributed to the singlet deuteron final state interaction.

## The Energy Dependence of the Isospin Part of the Optical Potential

T. J. Woods

School of Physics and Astronomy

University of Minnesota, Minneapolis, Minnesota 55455

The possible energy dependence of the isospin part of the optical potential was suggested by Thurlow<sup>1</sup> in her analysis of the (p,n) angular distributions obtained at a proton bombarding energy of 94 MeV by Langsford, et al..<sup>2</sup> She observed that the depth of the isospin potential at 94 MeV was significantly shallower than the depth obtained from analysis of (p,n) data at lower energies. She concluded that this discrepancy could be accounted for by an energy dependence of the isospin potential. However, it was pointed out later that the shallow isospin potential at 94 MeV could be due to the poor knowledge of the optical parameters at this energy.<sup>3</sup>

Recent analysis of (<sup>3</sup>He,t) reactions populating isobaric analog states (IAS) indicates that the isospin potential required to fit the data may be energy dependent.<sup>4,5</sup> The purpose of this paper is to show that the isospin part of the optical potential definitely possesses an energy dependence.

At UCLA we recently began a program to measure the (p,n)-IAS angular distributions utilizing the proton ( $\tilde{p}$ ) decay of the IAS to obtain neutron time-of-flight spectra. With this  $\tilde{p}$  timing technique we have measured angular distributions for the <sup>208</sup>Pb(p,n)<sup>208</sup>Bi(IAS) reaction at proton bombarding energies of 24.8, 30.5, and 38.6 MeV. Fits to these angular distributions as well as the one taken at 50 MeV at the Rutherford PLA<sup>6</sup> were obtained using the DWBA program DWUCK.<sup>7</sup>

The proton and neutron optical parameters were taken from the analytic expressions derived by Becchetti and Greenlees.<sup>8</sup> The analytic expressions

used were the ones labelled "best fit". The isospin form factor was complex, having a real volume and an imaginary surface component, and the isospin strength was taken to be four times the coefficients of the  $(N-Z)/A$  terms in the "best fit" expressions.

The fits from the DWUCK calculations were all obtained by normalizing the predicted cross sections to the data. The normalized predictions and the experimental data for the four bombarding energies are shown in fig. 1. The agreement between the normalized predictions and the data is quite good, particularly for the 24.8 and 30.5 MeV data.

The unnormalized predictions were smaller than the experimental data for all four energies. The interesting fact is that the ratio of the data to the unnormalized predictions tended to become smaller as the proton bombarding energy increased; but, due to the large uncertainties for the ratios, particularly for the 38.6 and 50 MeV data, only qualitative conclusions can be drawn as regards any possible decrease of the isospin potential depth with increasing proton bombarding energy. The point to be made here is that the "best fit" parameters adequately describe the shapes of the angular distributions for the (p,n)-IAS data, particularly the 24.8 and 30.5 MeV data. If any energy dependence is introduced into the isospin potential, it must be able to reproduce the angular distributions as well as the energy independent isospin potential did in fig. 1.

The observed differential cross section for the production of  $\tilde{p}$  events,  $\frac{d\sigma}{d\Omega}(\tilde{p})$ , is proportional to the total (p,n) cross section ( $\sigma_{\tau}$ ). The calculation of  $\sigma_{\tau}$  from such a measurement uses the relation

$$\sigma_{\tau} = 4\pi \frac{d\sigma}{d\Omega}(\tilde{p}) \frac{\Gamma}{\Gamma_{\tilde{p}}}$$

where the factor  $4\pi$  is based on the assumption that the  $\tilde{p}$  yield is isotropic and  $\Gamma/\Gamma_{\tilde{p}}$  is a correction for the fact that the IAS might decay through channels other than the observed  $\tilde{p}$  channels. Since this ratio is energy independent, the knowledge of its exact value is not necessary to obtain the energy dependence of  $\sigma_{\tau}$ . Such measurements of  $\sigma_{\tau}$  excitation functions using the  $\tilde{p}$  decay of the IAS have been made for various targets and energy ranges.

It should be pointed out that mere possession of the  $\sigma_{\tau}$  excitation function without any angular distributions allows only the most qualitative of conclusions as to the energy dependence of the isospin potential. Without knowing whether the form factor would also reproduce the (p,n)-IAS reaction angular distribution no real conclusions can be drawn.

The excitation function for the  $^{208}\text{Pb}(p,n)^{208}\text{Bi}(\text{IAS})$  reaction was measured over an energy range from 25.2 to 47.3 MeV.<sup>9</sup> The errors on the data were less than 10%. The same DWBA parameters which were used to obtain the unnormalized fits of fig. 1 were used to calculate the excitation function from threshold to 50 MeV. The data and the calculation (labelled A) are shown in fig. 2. The calculated curve A is normalized to the experimental data at 38.6 MeV.

It is readily apparent that the calculated excitation function A exhibits distinctly non-direct reaction characteristics, in contrast to the data. The data shows a definite decrease in the total (p,n)-IAS cross section over the observed energy range; whereas the curve A, using the energy independent isospin form factor, indicates that  $\sigma_{\tau}$  should still be rising at 50 MeV. It should also be pointed out that rather good fits to the (p,n)-IAS angular distributions were obtained using a purely real form factor, and the calculated excitation function for this form factor showed the same general features as did calculation

A of fig. 2. Furthermore, energy-independent complex isospin form factor predictions for the (p,n)-IAS reactions on  $^{91}\text{Zr}$ ,  $^{181}\text{Ta}$ , and  $^{197}\text{Au}$ , whose excitation functions have been measured at this laboratory, show similar disagreement with the data.

To investigate possible limits on the energy dependence of the isospin potential, two other DWBA excitation functions were calculated in which the isospin potential was assumed to have a linear energy dependence. These calculations are labelled B and C in fig. 2. The potentials themselves are listed below.

---

Table 1.  $V_{E.T} = V_R f(X_R) + i4a_I V_I \frac{d}{dX_I} f(X_I)$

	A	B	C
$V_R$	96	96-0.32E	120-E
$V_I$	48	48-0.25E	60-0.75E

---

The resulting excitation functions for these two energy-dependent isospin form factors were also normalized to the measured  $\sigma_T$  at 38.6 MeV (fig. 2). The form factor B, while slowing the increase of the calculated excitation function, still results in an increasing excitation function, albeit slower than A, at 50 MeV. The failure of B to reproduce the data indicates that a 0.3% rate of decrease per MeV of bombarding energy for the isospin potential is not fast enough.

The form factor C exhibits better agreement with the data than does B. For proton bombarding energies less than 28 MeV the calculated excitation function is still increasing, while the data is decreasing from 25 MeV on, thus indicating that a 0.8% decrease per MeV of bombarding energy is too slow.

At bombarding energies greater than 43 MeV the calculations decrease faster than the data, indicating that a 0.8% gradient is too large.

One can simply conclude that the energy dependence of the isospin potential is non-linear. There is nothing sacred about linearity, and optical potentials with quadratic energy dependence have been used before. A second conclusion, and at this stage of the game, a more reasonable one, is that the amount of data below 30 MeV is not sufficient to allow very definite conclusions as to whether the energy dependence of  $C$  is too large or too small. Lastly, one could conclude that the energy dependence in the region just above threshold could be quite different due to threshold effects, and so would have to be treated separately.

We submit that the energy dependence of the isospin potential is definitely indicated. Good quantitative results for the actual energy dependence as well as the  $E=0$  depth will require measurements of  $(p,n)$  angular distributions over a range of energies and targets as well as the excitation functions. At present there is a paucity of  $(p,n)$ -IAS data as regards to the number of targets and energy ranges investigated, particularly for  $A > 100$  nuclei.

#### BIBLIOGRAPHY

1. Nola Thurlow, Nucl. Phys. A109, 471 (1968).
2. A. Langsford, P. H. Bowen, G. C. Cox, and M. J. M. Saltmarsh, Nucl. Phys. A113, 433 (1968).
3. G. R. Satchler, Isospin Dependence of Optical Parameters. In: D. H. Wilkinson, ed. Isospin in Nuclear Physics (North Holland, Amsterdam) (1969).
4. W. L. Fadner, R. E. L. Green, S. I. Hayakawa, J. J. Kraushaar, and R. R. Johnson, Nucl. Phys. A163, 203 (1971).

5. F. D. Becchetti, Jr., W. F. Makofske, and G. W. Greenlees, to be published.
6. C. J. Batty, B. E. Bonner, E. Friedman, C. Tschalar, L. E. Williams, A. S. Clough, and J. B. Hunt, Nucl. Phys. A116, 643 (1968).
7. P. D. Kunz, University of Colorado, Boulder, private communication.
8. F. D. Becchetti, Jr. and G. W. Greenlees, Phys. Rev. 182, 1190 (1969).
9. G. J. Igo, C. A. Whitten, Jr., Jean-Luc Perrenoud, J. W. Verba, T. J. Woods, J. C. Young, and L. Welch, Phys. Rev. Letters 22, 724 (1969).



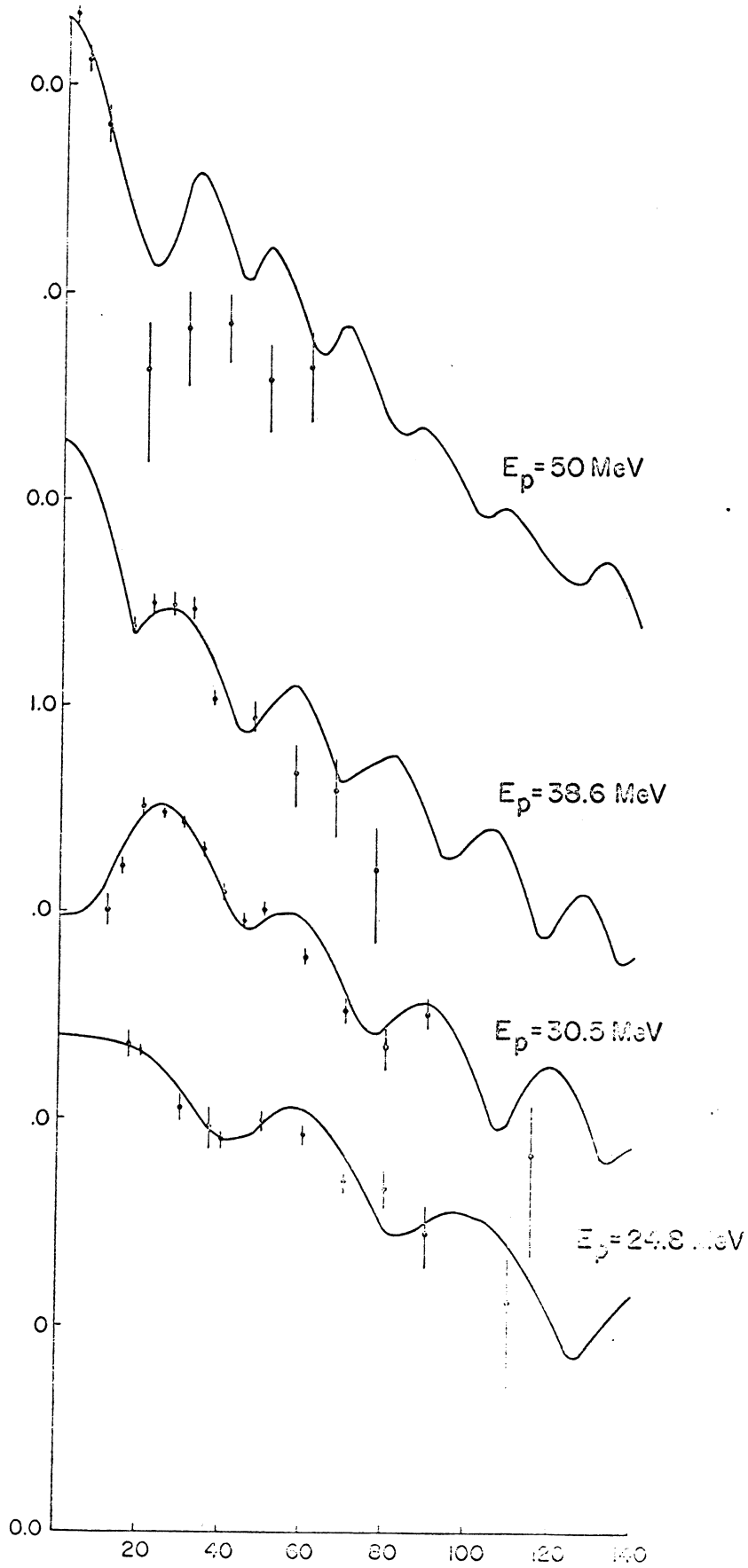


Figure 1. Normalized DWBA fits to the  $^{208}\text{Pb}(p,n)^{208}\text{Bi}(\text{IAS})$  data.

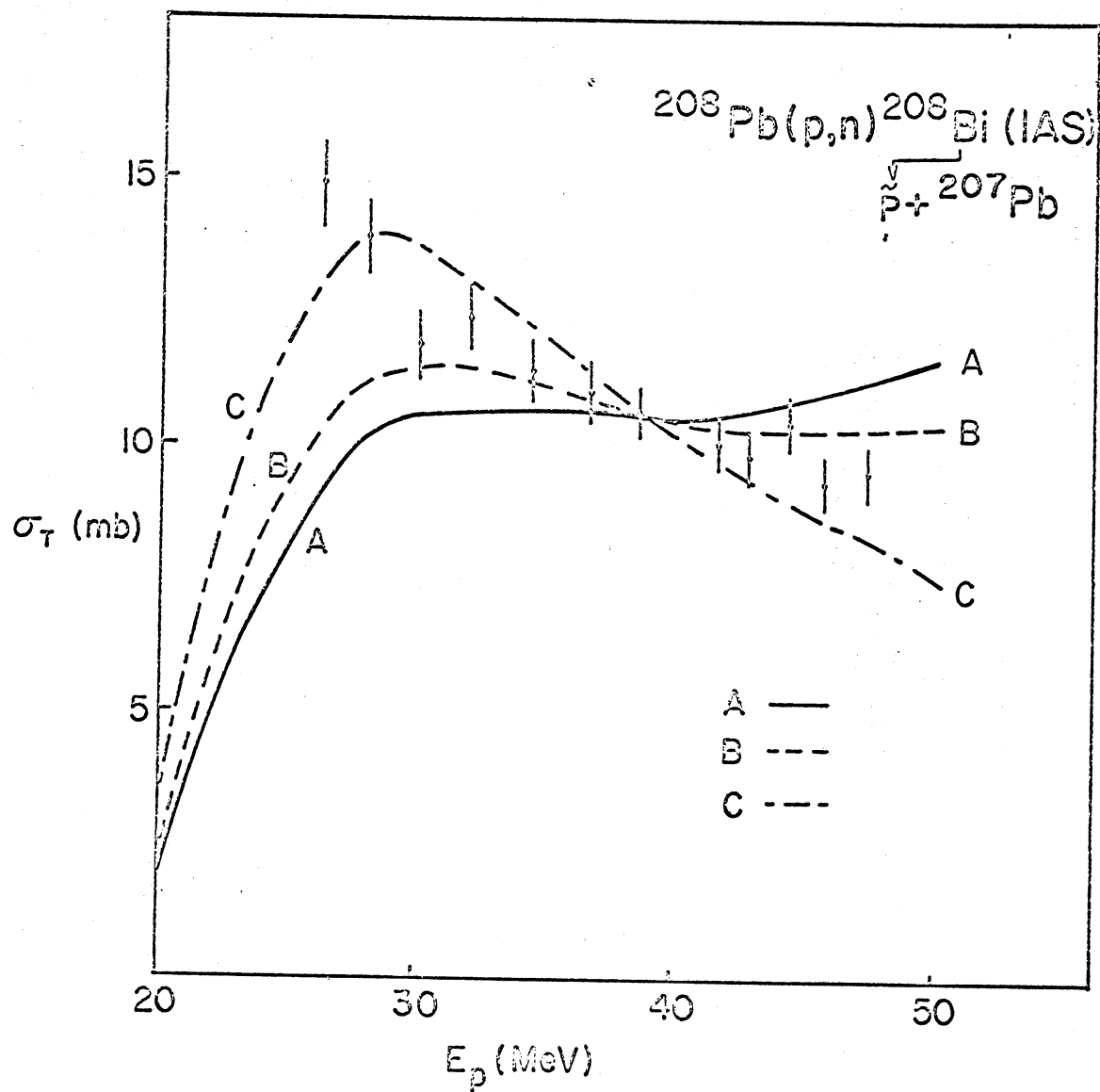


Figure 2. Total cross section excitation function for the  $^{208}\text{Pb}(p,n)^{208}\text{Bi}(\text{IAS})$  reaction. The DWBA predictions shown correspond to form factors which are energy independent (A) and energy dependent (B and C).

RENORMALIZED OPERATORS AND COLLECTIVE  
PARTICLE-HOLE EXCITATIONS IN  $\text{Ca}^{40}$

M. Dworzecka and H. McManus  
Michigan State University

Considerable success has been achieved by Gillet, et al., Nucl. Phys. 88(1966)321; 54(1964)472; 54(1964)321; 57(1964)698; in describing negative parity collective excitations in closed shell nuclei by means of a simple particle-hole model with ground state correlations taken into account via the R.P.A. The ground state correlations so treated consist of multiple excitations within the single particle and hole configurations originally picked for the description of the state (model space), and give, compared with the T.D.A. calculations in the original model space, a large energy shift and an increase in collectivity as measured, for instance, by the BE3 of a  $3^-$  state. However, the calculations used a force whose parameters were fixed by comparing calculation with experiment. Kuo, et al., Phys. Lett. 29B(1969)544, did a similar calculation using realistic forces, i.e. derived from the G-matrix. In this case the force between nucleons near the Fermi surface is altered by another type of correlation, core-polarization. This involves excitations, for instance, of positive parity particle-hole excitations, not included in the ground state correlations in the R.P.A. approximation. The results of the calculation were very sensitive to the way the core-polarization effects were taken into account, though some of the variations were due to an incorrect choice of backward going graphs in the R.P.A. Similar calculations were done by Dieperink, Nucl. Phys. A116(1968)556. This method treats one type of correlation--core polarization, by perturbation theory, and another,

ground state correlations, by a different approximation, the R.P.A. The present calculation compares the results of treating both effects by perturbation theory with the results of using R.P.A. taking the  $3^-$  states of  $^{40}\text{Ca}$  as an example. In perturbation theory both the effective interaction and the effective transition operator have to be calculated. The effective interaction is calculated from the diagrams of Fig. 2.  $V$  is the bare force, in this case Sussex matrix elements,  $V_{2p-2h} = V_{ph} + V_{pp} + V_{hh}$  the lowest order core polarization contributions involving energy denominators  $2h\omega$ .  $V_{\text{GSC}}$  gives the effect on the interaction of ground state correlations, via  $3p-3h$  intermediate states and hence should not be used in R.P.A. calculations. The effective operator is given by the diagrams of Fig. 3.  $t_{\text{DIR}}$  being the bare operator if all correlations are neglected and  $t_{\text{cp}}$  the addition to the bare operator from correlations. In the present case, the whole effect of  $t_{\text{cp}}$  comes from ground state correlations, so it corresponds to the effect of the Y parts of the vectors in R.P.A. For the perturbation calculation, vectors were calculated in the usual T.D.A. with an effective force and the transition operators BE3 calculated from these vectors with a corresponding effective operator. Thus if the bare force  $V$  was used, neglecting all correlations, then the bare operator  $t_{\text{DIR}}$  was used for calculating BE3. If ground state correlations were included then  $V = V + V_{\text{GSC}}$  and  $t = t_{\text{DIR}} + t_{\text{cp}}$ . The corresponding R.P.A. calculation used  $V$  in both A and B matrices. If core polarization was included  $V = V + V_{2p2h} + V_{\text{GSC}}$  then  $t = t_{\text{DIR}} + t_{\text{cp}}$  and the corresponding R.P.A. calculation used  $V = V + V_{2p2h}$  in the A matrix and  $V = V$  in the B matrix. The results for the lowest  $3^-$  state of  $^{40}\text{Ca}$  are shown in Table 1.

TABLE 1.

Interaction	TDA		Corresponding RPA		
	Transition Operator	E (MeV)	BE3 (WU) *	E	BE3
1 None pure $f_{7/2}d_{3/2}^{-1}$	$t_{\text{DIR}}$	7.1	0.72	* 1WU=	$665\text{fm}^6$
2 V	"	6.14	9.0	-	-
3 $V+V_{2p2h}$	"	6.34	6.75	-	-
4 $V+V_{\text{GSC}}$	$t_{\text{DIR}}+t_{\text{cp}}$	5.43	16.5	4.74	23.4
5 $V+V_{2p2h}+V_{\text{GSC}}$	"	5.68	14.2	5.16	19.6

The main configuration  $f_{7/2}d_{3/2}^{-1}$  lies originally at 7.1 MeV, and has a small BE3 of 0.72 W.U. Switching on the interaction (Col. 2) immediately creates a moderately collective state lowering the energy to 6.14 MeV and increasing the BE3 to 9.0 W.U. The overall effect of correlations is to decrease the energy further to 5.68 MeV and increase the transition rate to 14.2 W.U., most of the effect coming from core correlations, essentially similar to the R.P.A. results.

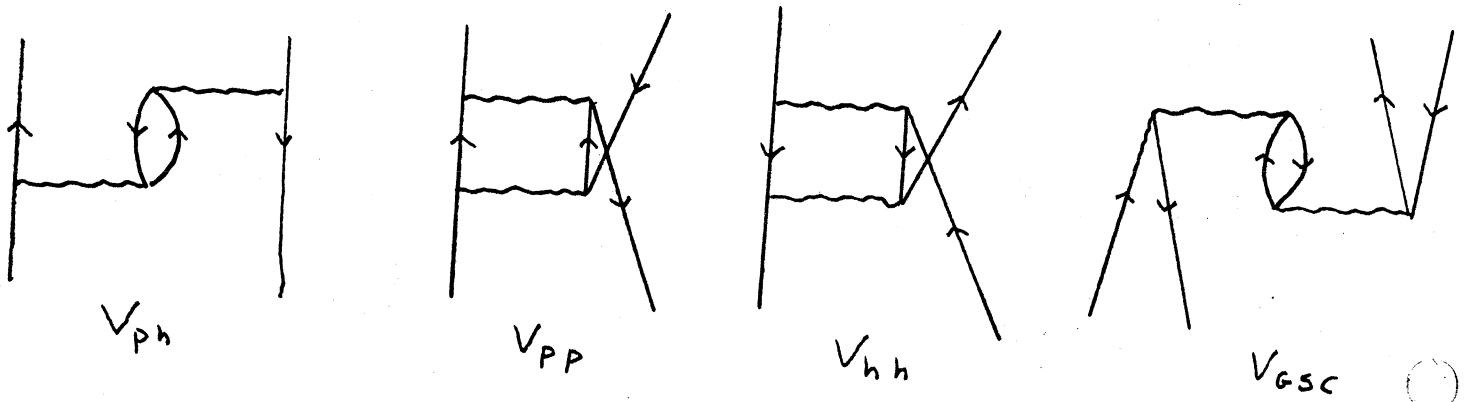
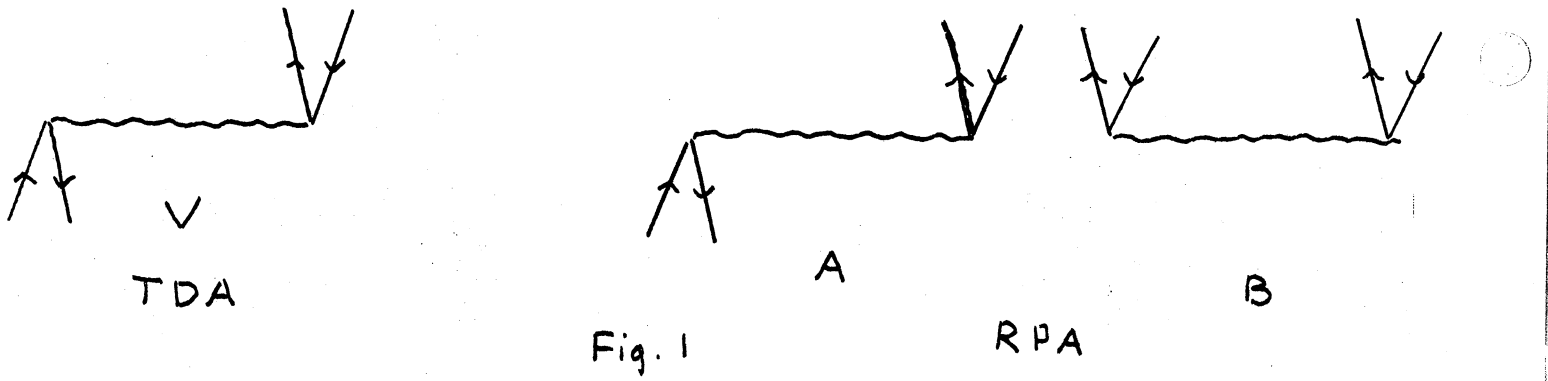


Fig. 2

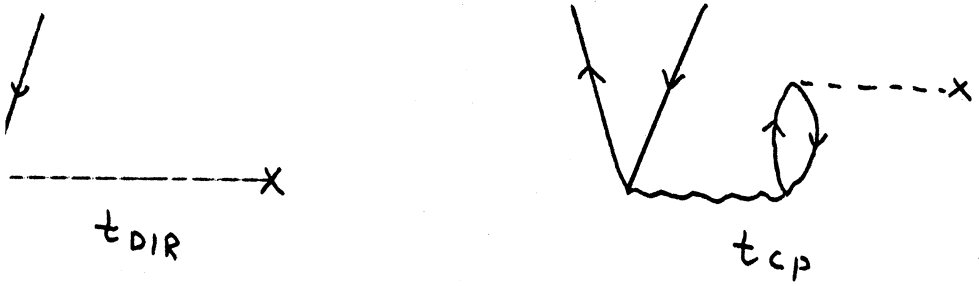


Fig. 3

LIST OF PARTICIPANTS

Alford, W. P.--University of Rochester  
Anantaraman, N.--Argonne National Laboratory  
Austin, S. M.--Michigan State University  
Banerjee, Manoj K.--University of Maryland  
Baranger, Michel--MIT  
Barrett, Bruce R.--University of Arizona  
Bernstein, Aron--MIT  
Bertsch, G.--Michigan State University  
Bethe, Hans A.--Cornell University  
Blair, J. S.--University of Washington  
Blosser, H.--Michigan State University  
Bodmer, Arnold R.--Oxford University/Argonne National Laboratory  
Borysowicz, J.--Michigan State University  
Breit, G.--State University of New York at Buffalo  
Brown, G. E.--Nordita/State University of New York at Stony Brook  
Brown, V.--LRL, Livermore  
Castel, B.--Queen's University  
Cline, Connie--University of Rochester  
Coester, Fritz--Argonne National Laboratory  
Crawley, G.--Michigan State University  
Davies, W.--Chalk River  
Doering, R.--Michigan State University  
Durso, John W.--Nordita/Mount Holyoke College  
Dworzecka, M.--Michigan State University  
Eisenstein, Robert A.--Carnegie-Mellon University  
Fox, S.--Michigan State University  
Galonsky, A.--Michigan State University  
Gammel, John L.--Los Alamos Scientific Laboratory  
Garvey, G.--Princeton University  
Gerace, W.--University of Massachusetts

Gilbert, K.--Michigan State University  
Glashausser, Charles--Rutgers University  
Goulard, Bernard--University of Laval  
Haftel, Michael I.--U. S. Naval Research Laboratory  
Halbert, M. L.--Oak Ridge National Laboratory  
Harris, Gale I.--Wright-Patterson AFB  
Heller, L.--Los Alamos Scientific Laboratory  
Hiebert, John C.--Texas A & M University  
Hinrichs, R.--Michigan State University  
Hodgson, Richard J. W.--University of Ottawa  
Holdeman, J.--Michigan State University  
Hyder, Anthony K.--Wright-Patterson AFB  
Iudice, Nicola Lo--University of Toronto  
Kashy, E.--Michigan State University  
Khanna, F. C.--Chalk River  
Kitching, J.--McGill University  
Lanford, William A.--University of Rochester  
Larson, D.--Michigan State University  
Larson, N.--Michigan State University  
Lawson, R. D.--Argonne National Laboratory  
Lee, Harry T. S.--University of Pittsburgh  
Lodhi, Mak--Texas Tech. University  
Love, William Gary--University of Georgia  
Ma, Chin W.--University of California, Davis  
Macfarlane, M. H.--Argonne National Laboratory  
McGrath, R.--State University of New York at Stony Brook  
McGrory, J.--Oak Ridge National Laboratory  
McKellar, Bruce H. J.--University of Sydney/Michigan State U.  
McManus, H.--Michigan State University  
Madsen, V. A.--Oregon State University  
Mani, G. S.--University of Manchester  
Maripuu, Sven--Wright-Patterson AFB  
Miller, P.--Michigan State University



Moszkoski, Steven--UCLA  
Müller-Arnke, Arnold--Darmstadt  
Noble, C. J.--Bartol Research Foundation  
Nolen, J.--Michigan State University  
Ophel, T.--Australian National University  
Parish, Leslie J.--University of Minnesota  
Petrovich, F.--Michigan State University  
Reid, Neal E.--University of Manitoba  
Reid, Roderick V., Jr.--University of California at Davis  
Richards, Keith--Bartol Research Foundation  
Robertson, R. G. H.--Michigan State University  
Roos, Philip G.--University of Maryland  
Schaeffer, R.--Saclay/Michigan State University  
Schiffer, J. P.--Argonne National Laboratory  
Scott, A.--University of Georgia  
Serduke, F.--Argonne National Laboratory  
Shamu, Robert--Western Michigan University  
Sher, M.--University of Illinois  
Signell, P.--Michigan State University  
Sprung, Donald--McMaster University/Orsay  
Svenne, Juris P.--University of Manitoba  
Tabakin, Frank--University of Pittsburgh  
True, William W.--University of California, Davis/LASL  
Vary, James--MIT  
Wagner, W.--Michigan State University  
Warner, R.--Michigan State University  
Wildenthal, B. H.--Michigan State University  
Woods, Thomas J.--University of Minnesota  
Zamick, L.--Rutgers University  
Kelly, W. H.--Michigan State University  
Benenson, W.--Michigan State University

